Jürgen Trzewik

Experimental analysis of biaxial mechanical tension in cell monolayers and cultured three-dimensional tissues

Experimental analysis of biaxial mechanical tension in cell monolayers and cultured three-dimensional tissues

- The CellDrum Technology -

Von Jürgen Trzewik

Universitätsverlag Ilmenau
2008

Impressum

Bibliografische Information der Deutschen Nationalbibliothek
Die Deutsche Nationalbibliothek verzeichnet diese Publikation in der Deutschen Nationalbibliografie; detaillierte bibliografische Angaben sind im Internet über http://dnb.d-nb.de abrufbar.

Diese Arbeit hat der Fakultät Informatik und Automatisierung als Dissertation vorgelegen

Tag der Einreichung:	25. Oktober 2006
1. Gutachter:	Prof. Dr.-Ing. habil. G. Henning
2. Gutachter:	Prof. Dr.-Ing. Dr. med. H. Witte
3. Gutachter:	Prof. Dr. rer. nat. habil. G.M. Artmann
Tag der Verteidigung:	23. November 2007

Technische Universität Ilmenau/Universitätsbibliothek
Universitätsverlag Ilmenau
Postfach 10 05 65
98684 Ilmenau
www.tu-ilmenau.de/universitaetsverlag

Herstellung und Auslieferung
Verlagshaus Monsenstein und Vannerdat OHG
Am Hawerkamp 31
48155 Münster
www.mv-verlag.de

ISBN 978-3-939473-26-8
urn:nbn:de:gbv:ilm1-2007000305

Meinen Eltern

1 Introduction and motivation

As compared to the tremendous efforts that have been made in the past to analyze biological samples for their biochemical cellular processes, only little is known on cellular processes related to mechanical properties of living cells and tissues. One reason for this situation was linked to the absence of suitable technologies analyzing mechanical properties of living cells in a natural environment (Trzewik et al. 2004).

In recent years, evidence has been growing about the important roles of mechanical forces in regulating the behavior of single cells and their communities (Chicurel et al., 1998; Galbraith and Sheetz, 1998; Geiger et al., 2001). Force on cells can be either external (e.g., resulting from blood flow or traction of other cells) or internal. In animal cells, internal forces are mostly generated by the actin cytoskeleton and transmitted to the extracellular matrix (ECM) through cell-matrix adhesion proteins. For stationary animal cells cultured on flat substrates, the most prominent type of cell-matrix interactions are focal adhesions (FAs) (Burridge and Chrzanowska-Wodnicka, 1996; Geiger and Bershadsky, 2001). FAs are large supramolecular protein assemblies, consisting of a submembrane plaque with more than 50 different proteins (including vinculin and paxillin) and a transmembrane part provided by receptors of the integrin family.

Cells sense changes in their mechanical environment and promote in return alterations and adaptations in tissue structure and function. In a feedback process, mechanical stimuli regulate fundamental processes such as cell division and differentiation and therefore play a crucial role in tissue growth and regulation. Addressing the loading conditions of test samples is important. Not only biomechanical engineers but also biologists must consider protein and gene expressions studies (Huang et al. 2002; Langholz et al. 1995) of tissue constructs and their relation to mechanical load conditions. The activity of a cell is regulated, in part, by changes in the mechanical environment in which it resides (Eastwood et al. 1998; Wakatsuki et al. 2000). The cellular impact on tissue tension plays an important role in numerous physiological and pathological processes like wound healing (Tejero-Trujeque 2001; Banes et al. 2001), connective tissue homeostasis (Banes et al. 2001; Brown et al. 1998; Tomasek et al. 2002), cardiac muscle contraction (Eschenhagen et al. 1997b; Langendorff 1895), morphogenesis (Benjamin & Hillen 2003). More obviously, mechanical loading is of substantial importance to the development, function and repair of all tissues in the musculoskeletal system (Henderson & Carter 2002; Payumo et al. 2002; Vandenburgh 1992), including bone, ligament, tendon, skeletal muscle, intervertebral disc and meniscus. Vice versa, information upon these cellular processes can be derived from the mechanical properties of living cells. In particular, measurements of mechanical properties of cell constructs would provide a

valuable insight into various cellular processes. It was our aim to develop a technology and corresponding analytical procedures analyzing mechanical properties of cell and tissue layers in their natural biaxial mechanical environment. A direct manipulation of mechanical properties of tissue constructs will be demonstrated in evaluation experiments. In the coming chapters we will discuss various influences of cellular constructs in tissues being involved in the mechanisms of tissue homeostasis and force generation.

2 Mechanical structures in cells and tissues

2.1 Molecular and cellular level

The cell's mechanical apparatus is build up by large structures consisting of many different protein molecules, which altogether form the intrinsic structure called the cytoskeleton, a cohesive meshwork of filaments formed by self-assembly of proteins. The cytoskeleton contains a network of actin filaments, microtubules and intermediate filaments. Actin filaments are thin flexible protein filaments with a diameter of about 8 nm. They are cross linked into a dense three-dimensional weave beneath the plasma membrane, or can be more regularly arranged into parallel bundles, forming microspikes cell-surface protrusions.
In the central region of the cytoplasm the dominant cytoskeletal components are microtubules, formed by long rods of tubulin sticking outwards because of their great thickness and inflexibility. Thin cross sections demonstrate their hollow cylindrical form with an outer diameter of 25 nm and a lumen of about 10 nm in diameter. Intermediate filaments often show a similar distribution pattern in cells like microtubules. Their filaments are significantly smaller in diameter, which is close to 10nm. They are irregular flexible ropes of proteins and composed of a large family of proteins that are often distinctive markers of a particular cell type.

Mechanical force transduction between intra- and extracellular structures

Many adult tissues are held together via cell-cell anchorages called adherens junctions. These connect actin filaments in adjacent cells. In non epithelial cells, they usually appear as small punctuate attachments. Whereas in epithelial cells they form a continuous adhesion belt around the apical end of the cell. The opposing faces of adherens junction are held together by membrane proteins capable of self-association. These adhesion proteins often show a Ca^{2+} dependency, and are called cadherins. They span the plasma membrane, having a cytoplasmic domain that becomes associated with the cytoskeleton through vinculin for example.

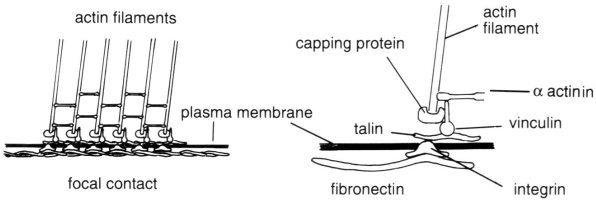

Figure 2-1 Schematic section through a focal contact showing the attachment of actin filaments to the plasma membrane and subsequently to fibronectin, a major component of the extracellular matrix (from (Bray 1992)

Focal adhesions

The attachment of cells to their substratum which may be a basement membrane in vivo or the culture dish in vitro is mediated by specialized proteins. The formation of these so called focal contacts is promoted by two proteins found in serum: fibronectin and vitronectin (Heath & Dunn 1978). These multidomain proteins adhere to the surface of the tissue culture dish and expose specific sequences that are recognized by cell-surface receptors. The cell-surface receptors involved in focal-contact formation belong to the integrin family. Integrins are noncovalently associated complexes of two distinct, high molecular weight polypeptides called α and β integrin acting as transmembrane linker in a variety of cells. Integrins span the plasma membrane in the region of focal contacts. Its cytoplasmic domain binds through a chain of various acting proteins like talin, vinculin and α actinin to actin filaments of the cortical cytoskeleton (Bray 1992).

Mechanical force generation and cytoskeletal action

Although all cytoskeletal proteins have an impact on the cell's mechanical properties, actin is the basis of movement in all known eukaryotic cells. Phagocytosis, cytokinesis, cell crawling and muscle contraction all depend on structures built from actin. Typically actin represents about 5-10% of total amount of proteins within a cell (20% of protein in muscle) (Pollard 1986). The primary function of actin is to make filaments. Each actin monomer, called gobular or G actin has binding sites that allow the association with two other actin monomers generating actin filaments (filamentous or F actin). Actin assembly and disassembly at either end of the polymer filament

follows a kinetic equation. The greater the concentration of actin filaments at the start of the polymerization, the faster they begin to form filaments, which are determined by a slow growing minus and a fast growing plus end (Korn et al. 1987). The kinetics of actin polymerization onset and depolymerisation can be manipulated by a number of actin-binding drugs, disrupting the normal polymerization kinetics. Cytochalasins for example, a group of closely related fungal metabolites are secreted by different species of molds. The effects of cytochalasins are specific to actin filaments, where they bind to the plus end of actin filaments (Bray 1979) resulting in an indirect depolarization of the actin fibers.

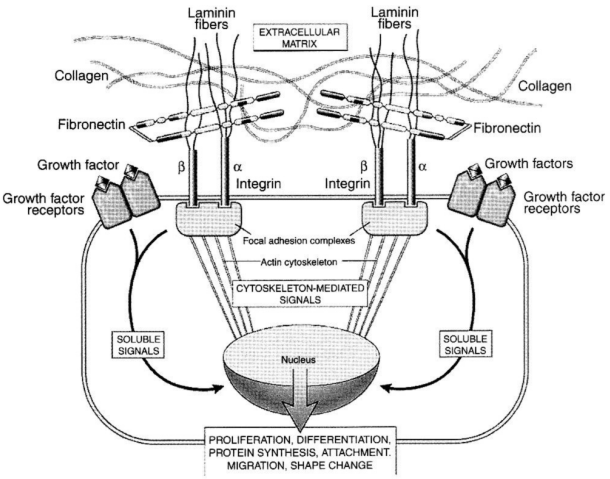

Figure 2-2 Cell-ECM Interaction from (Cotran et al. 1999). Schematic diagram showing the structures by which ECM and cell components, like integrins and cytoskeleton, are linked with each other. Integrins bind ECM and interact at focal adhesion complexes (protein aggregates that include vinculin, α-actinin and talin). This can initiate the production of intracellular messengers, or can directly mediate nuclear signals.

The transition between the non muscle cytoskeleton and the muscle cell is provided by myotube differentiation. Myotubes are composed of myofibrils which are self-assembled by the muscle specific myosin and the muscle α isoform of actin in contrast to the β and γ actin isoforms characteristic for nonmuscle cells. The myofibrillar apparatus is the dominating component of the cytoskeleton and the force generation unit in muscle cells. The contraction signal in the electrically coupled cardiac muscle cells is transmitted through low resistance gap junctions. Although the heart

is extensively innervated by sympathetic and parasympathetic axons, these are only regulatory in function and responsible for speeding up and slowing the heart rate (Bray 1992).

Extrinsic structures

Extrinsic structures determining the cells mechanical integrity are mainly formed by the extracellular matrix (ECM). The ECM is a molecular complex mainly consisting of fibers (collagen and elastin) and a largely amorphous interfibrillary matrix composed of components like glyco-proteins and proteoglycans. The ECM also contains molecules such as growth factors, cytokines, matrix-degrading enzymes and their inhibitors. The idea of a dynamic reciprocity between the ECM on the one hand and the cytoskeleton and nuclear matrix on the other hand is widely accepted. In this model, ECM molecules interact with cell surface receptors, which then transmit signals across the cell membrane to molecules in the cytoplasm; these signals initiate a cascade of events through the cytoskeleton into the nucleus, resulting in the expression of specific genes, whose products, in turn affect the ECM in various ways (Bissell et al. 1982). Basically all cell-ECM interactions participate directly in processes like cell migration, growth, differentiation, programmed cell death (known as apoptosis), cell adhesion, activating intracellular signaling and contractile response (Lanza et al. 2000). Matrix components and the mechanical forces that cells experience markedly influence the maintenance of cellular phenotypes and effect cell shape, polarity and differentiated function. In most tissues, the ECM is constantly being remodeled, in particular in processes like wound repair or tumor cell invasion. Some extracellular matrices are specialized for a particular function, such as strength (tendon, connective tissue) or adhesion (basement membrane of epithelia).

2.2 Tissue and organ level

Cells, organized as tissues or even organs, can be described in terms of biomechanics by multiple mechanical properties. They show differentiated reactions as a result of their physiological environment. To get an impression of this complicated matter, we should limit our focus on more or less clearly arranged structures like skin, tendon or muscle. Various biomechanical relationships have been proposed for soft tissue modeling, more than 30 models have been proposed only for skin under stretch for example (Skalak et al. 1986). But even for a clearly structured organ like skin, the mechanical properties of the tissue show many individual features. Skin is obviously not a homogeneous material because of the fibrous, cellular, vascular, granular and amorphous

components of which it consists. The skin contains collagen, elastin, reticulin, fibrocytes, blood and lymph vessels, nerve endings, hair and hair follicles, and glands together with their associated ducts. They are all embedded in a gelatinous matrix consisting of water, mucopolysaccharides (notably hyaluronic acid) and proteins (mostly soluble collagen). Furthermore, preconditioning effects like age, exposure, hydration, obesity, disease or the way of handling during experiments potentially change the material properties of test specimens.

Pseudoelasticity and non-linear relationship

Soft tissues are pseudoelastic; that is, they are not elastic, but under periodic loading and unloading each tissue will have a steady state stress-strain relationship which is not very sensitive to strain rate. For example, Figure 2-3 shows the load-strain relationship of rabbit abdominal skin subjected to biaxial loading. After a number of cycles, a repeatable stress-strain loop was obtained (Lanir & Fung 1974b). The loop shows, that the tissue is viscoelastic and not elastic, but since the loop is repeatable, we can treat the loading and unloading curves separately and borrow the method of the theory of elasticity to describe the mechanical properties. Further investigations (Vawter et al. 1978) on the stress-strain relationship at different strain rates and the hysteresis, defined as the ratio of area of the hysteresis loop divided by the area under the loading curve, is seen to be variable, but its variations with strain rate is not large. Records of skeletal and cardiac muscles, urethra, teniae coli, arteries, veins, pericardium, mesentery, bile duct, skin, tendon, elastin, cartilage, and other tissues show similar characteristics. Typically, in a 1000-fold change in the strain rate, the stress at a given strain-loading (or unloading) process does not change by more than factor of 2 (Fung 1986). Fung summarized the stress-strain relationship as nonlinear and the viscoelasticity as pseudoelastic. The simplest way to represent pseudoelasticity of a nonlinear material is to introduce a pseudoelastic potential (or strain energy function) $\rho_0 W$, which is a function of Green's strain components $E_{i,j}$. The partial derivates of $\rho_0 W$ with respect to $\rho_0 W$ gives the corresponding Kirchhoff stress components $S_{i,j}$. W is defined for a unit mass of tissue, and ρ_0 is the density of tissue in the initial state, hence $\rho_0 W$ is the strain energy per unit initial volume.

$$S_{ij} = \frac{\partial \rho_0 W}{\partial E_{ij}} \quad (I,j = 1,2,3) \qquad \text{Formula 2-1}$$

No general constitutive equation has been identified for living tissues and corresponding strain energy functions have to be developed specifically for each specimen.

Experimental data in uniaxial elongation experiments on rabbit mesentery (Fung 1967) revealed the nonlinear characteristics of the biological specimen which is described by Fung‘s Law for soft tissues:

$$\sigma = \beta[e^{\alpha(\lambda-1)} - 1] \qquad \text{Formula 2-2}$$

Here the Lagrangian stress (obtained by dividing the force by the original cross-sectional area of the specimen at zero stress) is taken for the true stress (Cauchy stress) in the resulting constitutive equation. It addresses the stiffening effect of tissue, leading to increased tissue tension σ levels due to extended elongation λ of the test specimen (α,β are constants). Other types of soft tissue, such as the skin, the muscles, the urethra, and lung tissues follow a similar relationship. For a body subjected to small changes in strains, the range of incremental strains may be chosen to be so small that the relationship between incremental stresses and strains is linear. The linear relationship is Hocks law, for which the familiar constants are the incremental Young’s module and incremental shear modulus (Fung 1986).

$$\sigma = \beta\alpha(\lambda - 1) = E\varepsilon \qquad \text{Formula 2-3}$$

It must be emphasized that this substitution is valid only for strains smaller than 2% of the resting length.

Anisotropic effects due to cellular orientation

Soft tissue is normally not isotropic. Directional effects of skin tension have been reported for long (Langer 1861). The soft tissue's anisotropy are evident from the different responses in different directions, both in vitro and in vivo, and under uniaxial as well as biaxial stretching (Lanir & Fung 1974b). The possible effects of cellular orientation and texture as demonstrated in Figure 2-3 will be further discussed for artificial tissue equivalents in chapter (9).

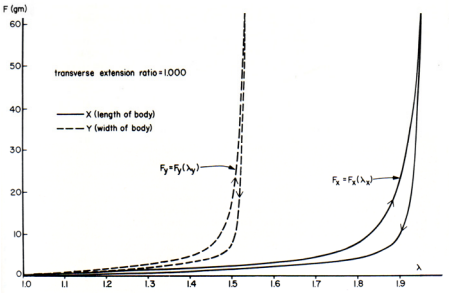

Figure 2-3 Load-strain relation of a square (3. 5 x 3. 5 cm) specimen of rabbit abdominal skin. The tissue is stretched in one direction while the transverse dimension is kept constant. Solid line: stretch along the body length. Dashed line: stretch across the body width (From (Lanir & Fung 1974b))

3 Experimental approaches to analyse the mechanical behaviours of tissues and organs

Information on cellular processes can be derived from the mechanical properties of living cells. In particular, elasticity measurements provide a valuable insight into various cellular processes. Prior to 1970, most observations of the mechanical behavior of tissues and organs were based on the behaviors of whole organs (e.g. pressure-volume relations of the heart). Subsequently, engineers and physiologists have attempted to describe the behavior of tissue as a material using uniaxial or biaxial stretch tests. A further breakdown started with the initial work of Harris et al. in 1980 (Harris et al. 1980). He visualized the traction forces of individual cells on flexible substrates, and therefore focusing on the impact of individual cells in contrast to the tissue approach. Other experimental approaches were developed focusing on individual cells. In the 90´s, however, researchers (Eastwood et al. 1994; Kolodney & Wysolmerski 1992) realized the impact of a 3 dimensional environment on individual cells and started analyzing mechanical properties of standardized cell seeded artificial tissues. The following section characterizes a subset of approaches which have been used to analyze the mechanical behavior of cellular structures and assemblies.

3.1 Tissue-stretch-technique

Many researchers have developed experimental systems for uniaxial and biaxial tests on animal or human based test specimen, patterned after that of Lanir and Fung (Lanir & Fung 1974b). Typically an optical-electromechanical system was used for measuring the force-deforming behavior of uniaxially or biaxially loaded slabs of soft tissue specimen as demonstrated in Figure 3-1.

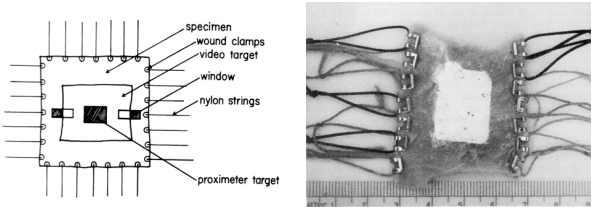

Figure 3-1 Schematic (left), parenchymal specimen (right) respectively with fixtures (Vawter et al. 1978)

The slabs were stretched in plane by two orthogonal mechanical drive systems, which allowed controlling parameters like stretch velocity, lateral displacement or load. The test specimens were

kept in an organ bath and the mechanical load was determined by force transducers. A major technical difficulty of nearly all tests on excised specimen is to reliable grip the tissue. There can be large differences between the spacing measurements and the specimen deformation if there is any slippage or tear-out near the clamps. But even the use of different kinds of clamps has an impact on the typical response curve.

3.2 Sheet-wrinkling-technique

One of the main techniques to measure cellular forces is the elastic substrate method introduced by Harris and coworkers in the early 1980s (Harris et al. 1980; Harris et al. 1981). Until today, there are few alternative methods to the elastic substrate method. In the seminal work by Harris and coworkers, the highly viscous, polymeric fluid polydimethylsiloxane (PDMS) was crosslinked at the surface by exposing it to heat. A thin elastic film over a fluid is obtained that under cell traction yields a wrinkled pattern, which is characteristic of the pattern of forces exerted. Major improvements of the wrinkling substrates method include the tuning of the elastic compliance (Burton & Taylor 1997). However, deformation data can be analyzed only semi quantitatively with this technique, because the buckling of thin polymer films is a nonlinear phenomenon that is very difficult to treat in the elasticity theory. Wrinkling can be suppressed by pre-stressing the film, thus allowing only for tangential deformation, which can be tracked by fluorescent latex beads (Lee et al. 1994).

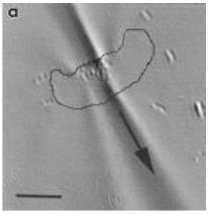

Figure 3-2 Micrograph of a single keratocyte locomoting on wrinkling substrata. Cell margins are outlined in black for clarity. Arrows indicate direction of cell locomotion. Bar, 25μm. (Oliver et al. 1999)

3.3 Microaspiration technique

The micropipette aspiration technique is widely used to quantify mechanical properties of single cells, especially suspended cells like neutrophils or erythrocytes (Artmann et al. 1998; Chien et al. 1978). Other researcher applied this method to determine the mechanical properties of single adherent cells like bovine aortic endothelia cells cultured on rigid substrates, that were scratched or enzymatically detached from the surface prior to the experiment(Sato et al. 1987). The basic idea of this technique is to optically analyze the deformation of a portion of a cell aspirated into a micropipette. The elastic shear modules can be derived from the relation between the aspirated length and the aspiration pressure.

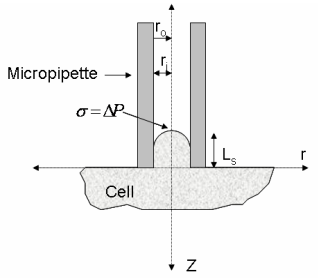

Figure 3-3 Diagram for the punch model micropipette aspiration technique in cylindrical coordinates. σ is the normal pressure stress applied parallel to the z-axis.

The endothelial "punch" model (Theret et al. 1988) differs from the erythrocyte–type model, which accounts no anchoring actin and microtubule network. The aspiration pressure in the pipette is treated as a tensile stress applied to a circular area on the cell surface. From the punch model it is possible to derive an equation to calculate the effective Young's modulus for the entire cell by compiling the characteristics of the membrane, actin filament apparatus, and cytoplasm within the tested cell:

$$E = \frac{3 r_i \Delta P}{2 \pi L_s} \Phi(r_i, r_o) \quad \text{Formula 3-1}$$

Where r_i and r_o are the inner and outer pipette radius, respectively. ΔP is the aspiration pressure, L_s is the equilibrium length of the aspired portion inside of the micropipette, and $\Phi(r_i, r_o)$ is the wall function which depends on r_i and r_o.

However, the micropipette aspiration technique does not reflect a normal in vivo or at least in vitro environment of adherent cells. Problems concerning the reproducibility of the micropipette fabrication process, especially with pipette tip diameter, variations in the fraction of µm´s are common. Furthermore the way of sample preparation (cell scratching) is quite doubtful and the total

experimental setup is complicated and time consuming. Thus, the usability of this system for evaluating mechanical properties of adherent cell monolayers or thin tissue constructs is quite limited.

3.4 Rectangular 3D-Gel and its variations

Non-contractile cells are able to exert 'tensional' forces on collagen substrates. One approach to quantify this behavior concerns the shrinkage of 3D cell-seeded collagen gels (Bell et al. 1979), (Elsdale & Bard 1972a) due to tensional forces exerted by individual cells. In this model, however, the cells are exposed to an undefined state of mechanical tension limiting the value of such experiments (Tomasek et al. 2002; Liu & Fung 1988). The contraction of tethered fibroblast populated collagen lattices floating in culture medium was analyzed directly by the application of strain gauges (Eastwood et al. 1994; Kasugai et al. 1990; Vandenburgh 1988; Vandenburgh & Karlisch 1989; Wakatsuki et al. 2000; Eastwood et al. 1994). In the system of Kasugai (Kasugai et al. 1990) a collagen matrix was attached between two stainless steel meshes, one fixed to the Petri dish and the other one supported by two fishing floats. Force measurements were carried out by a force transducer analogously logged to a chart recorder.

In a similar technique, the collagen gel was attached to glass rods via Velcro™ strips and the whole setup was placed in a mini-incubator (Delvoye et al. 1991). This system, however, was subject to high frictional losses in the transmission of strain into the strain gauges making it a relatively insensitive setup. These problems were solved by Kolodney and Wysolmerski (Kolodney & Wysolmerski 1992). A floating collagen matrix device attached to a force transducer was used transforming strain into an electronic capacitance signal. Since very small strains could be detected, the authors considered it an isometric measurement device. With the "culture force monitor" and its derivative, the "tension culture force monitor", respectively, quantitative investigations were performed with fibroblasts in a collagen lattice. These techniques focused on the application of adjustable, physiologically relevant mechanical load (Brown et al. 1998; Eastwood et al. 1998). Wakatsuki et al. used ring shaped fibroblast-populated gels and performed uniaxial stretch measurements. Samples were connected via a gold chain to an isometric force transducer and a stepper motor controlling tissue strain. The mechanical tension and the dynamic modulus of the sample were obtained (Wakatsuki et al. 2000).

In some methods published the mechanical tissue models suffered from necking of the uniaxially loaded collagen matrix and the biomechanical boundary conditions of the samples were not properly defined (Lanir & Fung 1974a). Also it should be mentioned that in living tissues a uniaxial tension distribution rarely is the case. Some methods were hard to handle which in some cases inhibited investigators from performing sufficiently high numbers of studies to satisfy basic statistical requirements.

3.5 Uncommon approaches

A comprehensive but rarely cited variety of experimental setups have been developed so far to monitor the mechanical properties of cellular components, individual cells and cellular aggregates. Some of these methods are briefly described here to give an impression of the range of research activity on this topic.

Using Atomic-Force-Microscopy (AFM), Young's module was derived from the deflection of the AFM tip while it approaches individual cells samples. Here, the Young's modulus was calculated according to the Sneddon's modification of the Hertzian model of elastic indentation (Rotsch & Radmacher 2000). Other approaches used microfabrication techniques to construct micromachined devices, that measure cellular forces acting on cantilevers etched into a solid substrate (Galbraith & Sheetz 1997). The use of centrifugal forces to induce rupture of adhesion on cells seeded on plastic substrata (Thoumine et al. 1996) was analyzed in terms of morphological variations and threshold values for the rupture of adhesion.

Mechanical effects of a volumetrically expanding tumor spheroid within a gel were analyzed in a microscopic setup by tracing the time lapse correlated displacement field of micrometer scaled glass beads embedded in the gel matrix (Gordon et al. 2003).

3.6 Evaluation of cardiomyocytes

Since the fundamental work accomplished more than 100 years ago by Langendorff (Langendorff 1895), the isolated perfused heart is one of the most popular experimental models in cardiovascular research. But from the moment an ex-vivo preparation was established, it began to deteriorate. Unphysiological situations like the formation of edemas may occur. Rate of deterioration depends on a large number of factors including the skill of the operator avoiding contusion injury, the species, the composition of the perfusion fluid, the presence or absence of various drugs, age, heart rate and work load and the temperature at which the studies are carried out. The rate at which a preparation deteriorates can be crucial in the design and interpretation of some studies where it may be necessary to use time-matched controls with corrections for baseline deterioration when comparing groups (Sutherland et al. 2003). Partial preparations from heart tissue like papillary or trabeculae preparations obviously have to cope with the same limitations.

Cultures of dissociated embryonic or neonatal cardiac myocytes cells have been used in studies on the pharmacology of cardiovascular physiology for more than 50 years (Cavanaugh 1957). Different approaches have been developed to use this cell type as a standard model to investigate myocyte related characteristics like ion channel function (Iijima et al. 1984; Morales et al. 1996), cardiac hypertrophy (Fink et al. 2000; RONA et al. 1959) or the contractility of cardiac structures (Brady et al. 1979; Lin et al. 2001b; Palmer et al. 1996; Tasche et al. 1999b).

The patch-clamp method (Hamill et al. 1981) is widely used to analyse electrical properties like action potential duration of single cardiac myocytes. Nevertheless, even in combination with microscopic observation techniques, almost no information could be derived regarding the mechanical properties like force or stiffness of individual, spontaneously contracting myocytes, or paced myocytes contraction, respectively. This limitation exists in any other approach, whenever cell contraction in unattached myocytes was measured.

The attachment to force-sensing system shows a different limitation: to resolve the small forces developed by isolated myocytes. The compliance of the force-sensing system may be appreciable relative to the shortening length of the cell. In order to measure myocyte forces or stiffness, respectively, we must form some attachment to the cell. This attachment may produce distorting strains or stresses influencing contractile responses. Many applications were developed in this regard. Mostly a polymer coating was used to accomplish the attachment of individual cells to a force transducer.

The isometric force related displacement of glass cantilevers (Tarr et al. 1979), microelectromechanical systems (MEMS), (Lin et al. 2001a), capacitive force transducers (Bluhm et al. 1995), and even ultra sensitive cantilever designs (Tasche et al. 1999a) with a low compliance all suffer from difficulties in preparation and handling of cell samples. Furthermore, in measurements on skinned or individual myocytes the physiological relevance of this model has not been fully evaluated. A major problem with attachments to highly sensitive force transducers is that in cases where the force-detection system is not submersible, some part of the force-sensing system must pass through a liquid-air interface. The surface tension of the meniscus around the connecting element through this interface can be in the order of ~10 μN, whereas the myocyte forces range one to two orders of magnitude below this level (Brady 1991).

3.7 Summary of the current status

Devices and methods reported previously were able to monitor mechanical properties of tissue constructs or individual cells, respectively. All so far proposed experimental approaches have very complicated setups in common. This limits the scientific benefit to the investigator's experimental skills and experience. Furthermore, since all related forces are very small, any variation of the physical environment during the experiment would cause erroneous data. The experiments described so far did not particularly account the influence of the environmental conditions like temperature, air humidity or surface tension between the interface of culture medium and surfaces. It would be unreasonable to assume that any of the described methods would have the potential to be upscaled for pharmaceutical relevant, high-throughput screening methods. Nevertheless, another profound reason for developing a new analysis device for cellular components is related to the absence of well defined and biologically relevant boundary conditions. Formerly adherent cell aspirated into a micropipette (Sato et al. 1987; Theret et al. 1988) do obviously not mimic any in vivo situation but provide complicated boundary conditions. Also, cells introducing wrinkles into stress free soft substrata (Harris et al. 1980) or the ability of cultured fibroblasts to reorganize and contract free floating three dimensional collagen I gels (Bell et al. 1979; Grinnell et al. 1999) is not related to any in vivo situation. However, such unstrained gels must be considered as mechanically completely different models to study mechanically regulated cellular processes.

Rectangular gels suffer from "necking" due to the stress variations imposed during uniaxial force measurements. The uniaxial loading also introduces a physiologically unknown parallel aligning in response to the applied force. It is reasonable to conclude, that the object to be investigated is

actively modified by the experimental setup. This problem will be analysed in detail in chapter 10. Another drawback of many concepts is that they do not consider the specific needs of a sterile and cell culture compatible experimental setup. However, this is quite essential since the interpretation of any experimental result is critically related to a long term observation (over weeks) of all relevant parameters. The cellular response is definitely determined by the time course of the cultivation. In addition, the impact of contamination by fungi, bacterial or other microorganism would also influence cellular responses of test specimen and may result in the misinterpretation of experimental data.

4 Objectives

4.1 Specification for a newly developed micromechanical experimental setup

General goals:

The major goal of this work was to introduce a new, precise but easy-to-handle technology to evaluate lateral mechanical tension in thin film soft tissues, cell monolayer structures or thin artificial tissue constructs, respectively. The thickness of the cell populated sample may range from a cell monolayer up to a couple of hundred microns. This range of thickness is of importance to avoid diffusion limitations of reagents used to activate cell contraction or to modify cells otherwise. Furthermore cells should have the opportunity, in particular in three dimensional (3D) tissue constructs, to model their environment freely (e.g. after gelation of the matrix they reside in). Additionally, they should not have to adapt to unphysiological, extrinsically applied experimental setups as for example rigid substrates which are rarely or never seen under vivo conditions (Pelham, Jr. & Wang 1997). In this technique, the separability of individual parameters (e.g. cell number, pre-stress, matrix composition) and the biomechanical boundary conditions are well defined. Direct microscopic observations of cells inside the cell-matrix composite are necessary for providing additional information on the cell number and spatial arrangement of cells. Furthermore, the developed system should be designed for a scale up towards a high-throughput systems for as many as hundreds of samples measured simultaneously.

Specific design criteria:

To analyse mechanical properties of cellular composites it was necessary to adapt special criteria meeting the requirements of cell culturing. Major considerations are listed below:

(a) Non contact, friction-free force measurement of flat, cell-populated collagen matrices or cell monolayers on membranes, respectively.
(b) Measuring mechanical tension in the range of 0.001 N/m) at high precision and reproducibility (for comparison: surface tension of water at 25°C is 0.072N/m)
(c) Cultivation of cells on ultra-thin (1-10µm) but highly elastic membranes.
(d) Cell growth at defined cell conditioning parameters.
(e) Possibility of microscopic observations during cell culturing.
(f) Long term culturing at 100% humidity, 37°C and 5% CO_2
(g) Optionally cell constructs should be cultured at cyclic mechanical stress conditions
(h) Use of autoclavable components.

(i) Handling at sterile conditions.
(j) Precise and automated control of experimental actuators.
(k) Precise, high speed data acquisitions of the spatial position of cell populated collagen matrices.
(l) Upgradeable to a high throughput system.

5 The CellDrum principle

The CellDrum principle was developed to assess biomechanical properties of various cell types at in vitro conditions. A CellDrum (Figure 5-1) consistsof a plastic cylinder which is sealed on one end with a thin, typically 1µm thick and biocompatible silicon membrane. A rubber ring is used to fix the CellDrum to the experimental setup. The membrane allows cell attachment and proliferation at in vitro cell culture conditions. Two different experimental setups based on the CellDrum principle had to be developed to meet the different needs of standard monolayer cell cultures on the one hand and of tissue equivalents on the other hand. Specific considerations concerning the CellDrum technology and impact of the cell-membrane interface will be discussed in chapter 8. Two slightly different CellDrum setups were used for cultivating cell monolayer (2D CellDrum) or thin tissue structures (3D CellDrum), respectively. During this work, it turened out that different measurement goal required different CellDrum setups. These are summerized on the following page in a respective scheme (**Table 1**). The following chapters will introduce into details.

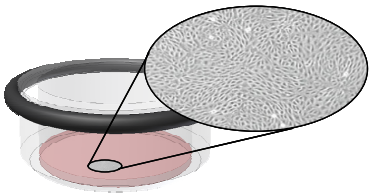

Figure 5-1 schematic of the standard CellDrum with a cell populated silicon membrane.

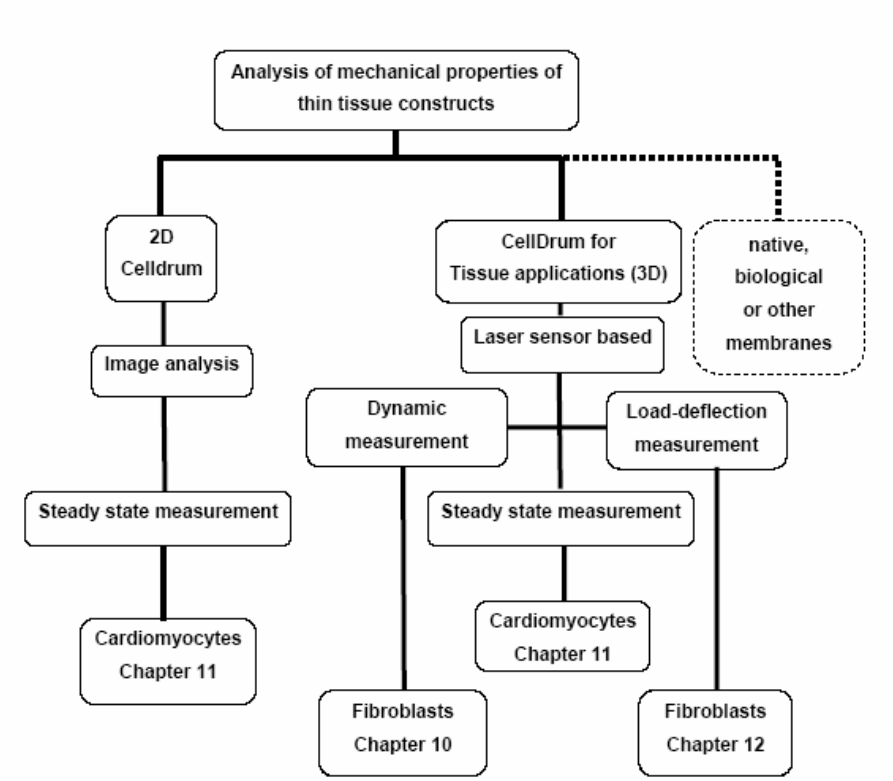

Table 1 Overview

5.1 2D CellDrum

Different cell types like endothelial cells, fibroblasts and cardiomyocyte were cultured on fibronectin precoated, custom made polydimethylsiloxane (i.e. Silicon) membranes. The membranes were produced in different membrane thicknesses, starting from ultra thin sub-micrometer levels up to 10 µm. The membranes were attached to the polycarbonate cylinder wall. The CellDrums were subsequently sterilized by autoclaving (121°C, 20 min.) prior to use. Individual CellDrum wells were arranged in sets of 7 units per custom made holder and placed into standard Petri-dish chambers.

5.2 Fiber and mesh supported CellDrums for tissue application (3D)

Cells do not necessarily express their diversity and natural behavior if cultivated under monolayer condition. Therefore the 2D setup had to be modified. Since in 3D tissue construct mechanical tension can be quite significant, it became necessary to provide an anchoring of the tissue construct to the cylinder wall. Adhesive, 1mm high Velcro® strips were glued concentrically to the CellDrum wall providing strong anchorage after gelation of cell seeded collagen matrices.

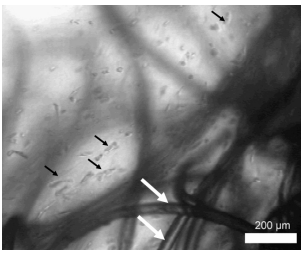

Figure 5-2 Velcro strip (white arrows) supported CellDrum. Individual cells within the gel are indicated with black arrows.

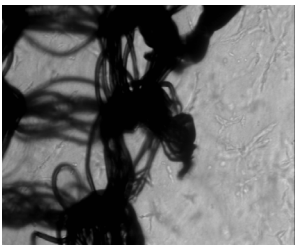

Figure 5-3 Polyamide mesh support

A glueless concept for sensitive cells was achieved using concentrical, 2mm wide Polyamide meshes which were thermically fused with the CellDrum wall. The CellDrum in both modifications was subsequently sealed with a silicon membrane similar to the 2D application described above. Again all wells were sterilized by an autoclaving process prior to cell seeding.

6 Basic concepts

The basic concept, for the validation of the biomechanical properties of cells, was to monitor the stress-strain relationship of the cell-membrane composites. This basic System was applied for endothelial and fibroblast cells proliferated on CellDrum membranes. Furthermore the basic concept was also applied to self-contracting cardiomyocytes in monolayer culture and cardiomyocytes embedded in a collagen I matrix, reassembling a heart tissue equivalent. The concept of tissue equivalents was also realized for fibroblast populated collagen I matrices.

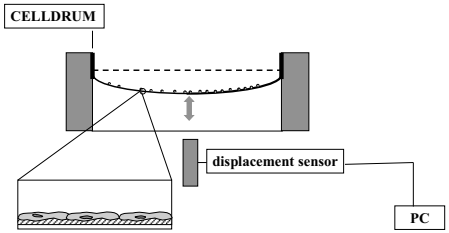

Figure 6-1 The basic measurement setup is arranged by the cell populated CellDrum membrane, displacement sensor and a data acquisition device (PC).

The relative displacement of silicon membranes attached to cylindrical wells (∅ 16 mm), termed CellDrum, was measured with non-contact displacement sensors at a resolution in the µm range (Figure 6-1). The CellDrum membrane is populated with cells grown as monolayer structures or the membrane served as a sealing boundary for thin film cell-matrix constructs anchored to the Cell Drum's wall. A high sensitive laser triangulation sensor and a custom made image oriented CCD sensor (CMS) were used in various experimental setups. All measurements were automated and controlled by a DAQ-board 6025E (National Instruments, Munich), custom made electronic compounds and software designed in Labview 6.0 (National Instruments, Munich). The relative membrane-cell composite displacement is the experimental setup variants described in this work. Figure 6-2,3 depicts the two principal roads of obtaining biomechanical data from the CellDrum: Mechanical properties of cell populated CellDrums are obtained either.

1) Load deflection concept (steady state) to obtain stress strain curves (Figure 6-2) and,

2) Oscillating membrane-tissue-compound (Figure 6-3).

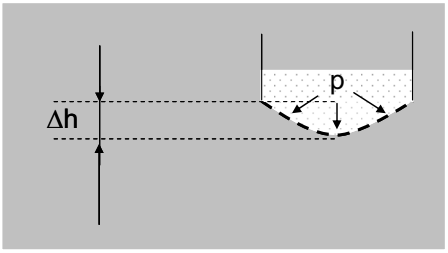

Figure 6-2 Load deflection concept: The deflection-pressure relation is obtained. Stepwise increment of pressure results in corresponding membrane deflections. From the resulting curve, mechanical properties of the cell populated CellDrum are calculated

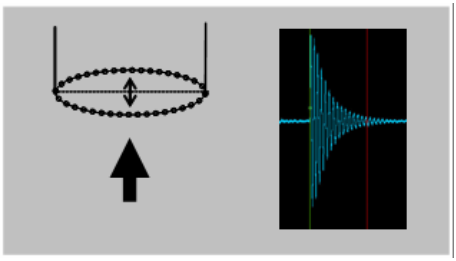

Figure 6-3 Oscillating membrane-tissue-compound: The resonance frequency and damping of the oscillating membrane tissue compound contain information on the tissue's mechanical properties, which are calculated according to mechanical models..

The mechanical properties of cell-membrane composites are derived by calculations based on the membrane displacement in relation to other boundary conditions like pressure load, etc., appropriate models were developed for that purpose (chapter 10, 11 and 12).

6.1 The Load-deflection concept

A number of different techniques such as beam buckling are used for measuring thin films under compressive stress (Guckel et al. 1985) or wafer curvature methods to measure both tensile and compressive stress (Madou 1997) of thin membranes. The concept of a membrane load-deflection technique (also referred to as bulge test (Bromely et al. 1983) has been employed to measure the properties of thin films under tensile residual stress in microelectronic film deposition procedures. This measurement concept allows evaluating residual stress in the specimen to be analyzed. This is quite desirable, since adherent cells are known for generating residual stress (σ_0) while proliferating on rigid substrates (Boswell et al. 1992; Bray 1992). Furthermore, the load-strain concept offers the quantitative determination of material properties such as Elastic module (E) and Poisson's ratio (ν).
We adapted the basic principle for the evaluation of thin film tissue construct for composites of cellmonolayers grown on silicon membranes (CellDrum) as well as for thin film tissue equivalents, respectively.
This load deflection concept works as follows: The blank and flat CellDrum membrane is manually focused by the displacement sensor. This defines the zero position before membrane bending. Separated cells either immerged in culture medium or collagen gel are pipetted into the CellDrum. The weight of the solution would bend the membrane slightly downwards. This bending is compensated by a computer controlled precision syringe, which aspirates air into the airtight

measurement chamber (Figure 6-5) until the zero position is reached again. The cells proliferate under precisely defined conditions (flat membrane) for a desired period of time. An optical sensor senses the membranes position and is in focus with it. In a next step, the sensor is moved downwards by 100µm. From the airtight measurement chamber, air is aspirated until the optical sensor and the membrane are in focus again. The pressure needed to achieve this indentation is monitored. Stepwise increase of membrane indentations together with the corresponding pressure needed for refocusing results in experimental aspiration pressure-deflection curves which can be transformed in the stress strain curves (Formula 11-4) of the membrane-tissue compound.

With this approach the tissue's residual tension and its elastic modulus can be calculated as separate parameters in just one stress-strain cycle. This offers new opportunities in assessing and optimizing reconstituted tissue in tissue engineering. New technology for quality assessment of culture tissues seems to be possible. The approach is easier to handle than common rectangular setups. However, experiments have to be carried out by remote control inside a temperature controlled incubator. Any variation in temperature has a direct impact on the pressure in the airtight chamber. This is due to the high sensitivity of the system and at the same time the low signal to noise (electrical and mechanical) ratio.

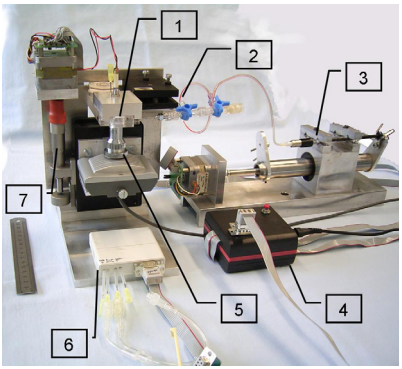

Figure 6-4 Image of the load-deflection setup measuring the membrane centre deflection as a function of aspiration pressure. The deflection is measured by a custom-made micrometer stage driven optical sensor.

Legend: Measurement chamber (1), t-adapter for pressure sensor fitting (2), step motor controlled syringe pump (3), microprocessor based controller unit (4), modified CCD camera with Leitz objective (5), accessory valve unit (6) and step motor driven micrometer stage (7)

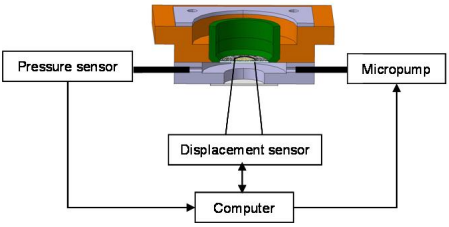

Figure 6-5 Schematic of the system with the measurement chamber (orange) and an embedded CellDrum (green). The appropriate computer controlled sensors and actuators are indicated schematically.

6.2 Steady state measurements

Steady state measurements function was especially adapted for the measurement of synchronously contracting cardiomyocytes. The concentrical contraction of circular cardiomyocyte seeded specimen (either monolayer or thin cell-collagen composite) did not result in an optically detectable vertical displacement of the CellDrum. But this contraction causes pressure variation in a pressure range of several Pa, which is detectable by a high sensitive pressure sensor. This pressure signal can be separated from mechanical and electrical noise due to the repetitive nature of the cell contraction. This separation is accomplished after the application of a software integrated filter algorithm. The steady state measurement system was similar to the load strain setup, but the membrane displacement was kept constant during the experiment and pressure variations were analyzed.
But this method can not be used to analyze stress variations introduced by the slow contraction processes of non-muscle cells. Due to the slow and non repetitive nature of the related pressure changes it is not possible to subtract cell signals from signals related to electrical and mechanical background noise.

6.3 Dynamic measurements

The dynamic measurement is the strongest diversification of the basic CellDrum concept. Complete membranes consisting of tissue equivalent cell-collagen structures were analyzed by exciting the membrane tissue compound with a brief air pressure pulse. The resulting resonance oscillation was monitored by a laser-based deflection sensor. Frequency and damping were analyzed revealing information on mechanical properties of the tissue construct. This system is very tolerant against most effects causing errors in all other described systems. Furthermore it offers the opportunity to perform a high number of measurements in short period of time. The system is perfectly suited for high throughput screening evaluations.

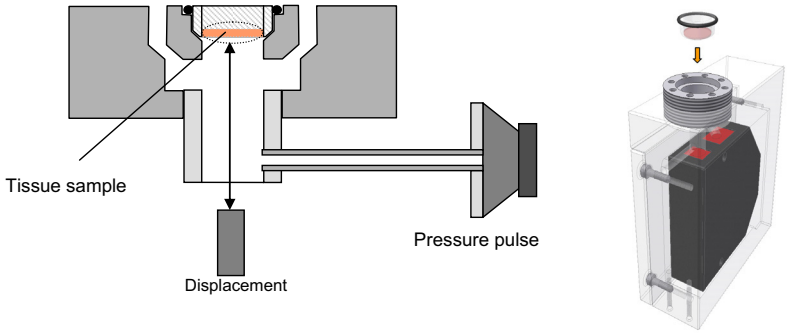

Figure 6-6 Dynamic measurement setup: Schematic (left); dynamic tissue tension analyzer device (right)

7 Displacement Sensor concept

7.1 CCD Laser displacement Sensor

Previous systems designed for non contact position detection within biological tissues were affected by variations within the objects surface color and roughness (Haut et al. 1998). Therefore appropriate precaution had to be made since tissue equivalents or cell seeded CellDrums have glistening white or transparent white surfaces. A CCD laser displacement sensor based on a triangulation algorithm is suitable, because its accuracy is not compromised by surface conditions characteristic for our specimens such as color and reflectivity. Therefore a CCD laser displacement sensor (Model LK-031, KEYENCE GmbH Neu-lsenburg, Germany) with a measurement range of 5mm and an accuracy of 1µm was chosen. The sensor accuracy was tested, in spite of its theoretical eligibility not to be affected by the objects surface color.

7.2 Sensor properties -custom made optical sensor

The concept discussed in the previous section has its limitations as soon as disturbances occur, such as temperature gradient related condensation and morphological changes within the cell monolayer. The possibility of condensation (Figure 7-1a) on the rear surface of the membrane is a result of cell culture handling during the initial cell deposition procedure under a sterile laminar flow outside the temperature controlled incubator. This condensation may cause a malfunction of the closed –loop displacement control algorithm leading to membrane displacement and curvature which may turn out to an inhomogeneous distribution of the seeded cells.

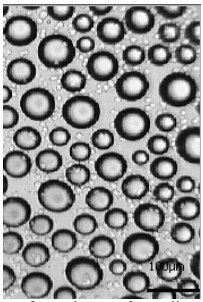

a) Rear of membrane after cell seeding. Cells (5-10 µm, white objects) are not spread yet and condensation (20-80µm, circular black edged objects) occur.

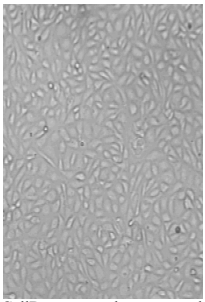

b) CellDrum membrane populated with a confluent cell monolayer.

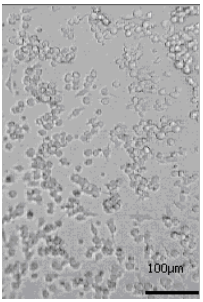

c) Situation after strain variations in the membrane. Cells appear rounded up and dead.

Figure 7-1 Cell proliferation on a CellDrum membrane under different mechanical conditions.

Furthermore, strain and stress alteration due to temperature or evaporation compensation processes may occur during the cultivation period. The impact of these events will be discussed in chapter 8.3. Briefly, intense cellular changes, finally causing processes like cell death, occurred within cells grown under special conditions in monolayer structures as soon as they were affected by strain variations within their underlying substrate. The optical monitoring opportunity of the custom-made sensor approach was necessary to detect morphological changes related to the variation of boundary conditions during the experiment.

7.3 Software properties and function

Software concept

The data acquisition software was written in Labview 6.0. Labview (National Instruments, Austin, TX). The main feature that distinguishes Labview from other software development tools is the graphical programming language, “G”, and a large library of mathematical and statistical functions. The advantage of graphical programming is that the code is flexible, reusable, and self-documenting (Kalkman 1995).
The software enabled automatic control of all relevant actuators and sensors. In contrast to the CCD laser triangulation displacement measurement approach, the custom made optical (CMS) sensor offered at the same time a visualization feature.

Autofocus based control loop system

The displacement measurement concept is based on an autofocus algorithm. The optical sensor concept was only used for load-deflection or steady-state experiments. In this application, the membrane displacement was kept constant at a preset value using an autofocus sensor algorithm. The membrane displacement was adjusted at maximum focus. Any changes in the focal plane either desired or introduced by the linear actuator driven change of the CCD camera focus or variations of the membrane displacement due to pressure changes (caused by temperature changes, evaporation of media) were sensed. As soon as these changes reached the preset tolerance limit, the autofocus subroutine was called by the main program. The focus itself was adjusted by an incremental, computer controlled syringe actuator, with a typical 0.125 µl volume incremental (within the air tight chamber) per motor step. This extremely small control variable led to a smooth refocusing procedure. This was extremely important since pressure variation introduce a variation of strain within the cell populated CellDrum membrane. Repetitive membrane straining has a direct impact on cellular processes and may alter cellular properties to a great extend (chapter 8.3). Therefore it was necessary to keep the time periods of auto focus interventions at a minimum while maintaining reasonable threshold values to compensate for evaporation related membrane displacement drifts
The control variable of the autofocus subroutine was obtained via an edge detection procedure using a Sobel operator algorithm to find the focal plane. The focal plane was given when the image showed maximum clarity as detected by the optical system. This was in contrast to the method of Schneider developed for red blood cell shape detection (Schneider 1996). The Sobel operator is

insensitive to artifacts caused by inhomogeneous illuminations (Ernst 1991). This is in particular important when condensed water changed the optical conditions. The Sobel operator is therefore well suited for the difficult cell culture environment.

Edge detection using the Sobel operator

The Sobel operator performs a 2-D spatial gradient measurement on an image and emphasizes regions of high spatial frequency that correspond with edges. Typically it is used to find the approximate absolute gradient magnitude at each point in an input grayscale image.

These kernels are designed to respond maximally to edges running vertically and horizontally relative to the pixel grid, one kernel for each of the two perpendicular orientations. The kernels can be applied separately to the input image, to produce separate measurements of the gradient component in each orientation (Gx and Gy). These can then be combined together to find the absolute magnitude of the gradient at each point and the orientation of that gradient.(Gonzalez & Woods 1992)

The gradient magnitude is given by $|G|=\sqrt{Gx^2+Gy^2}$ Formula 7-1

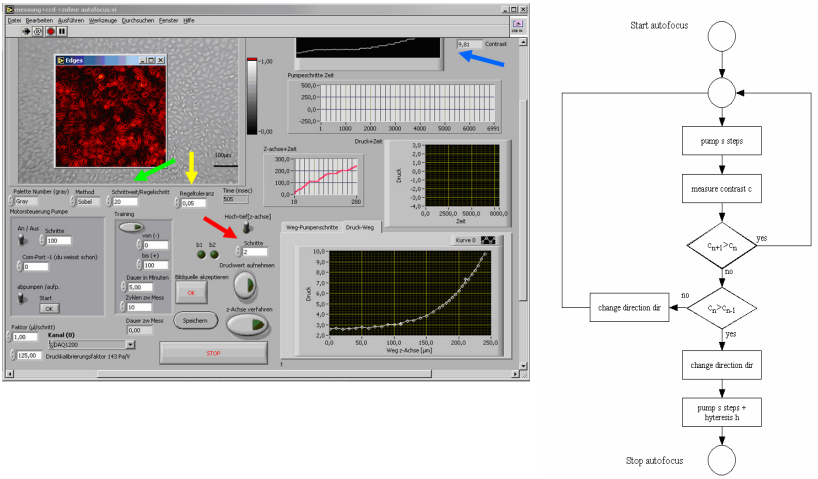

Figure 7-2 Left: Image showing the graphical user interface (GUI) of the vision based optical analysis approach. The arrows are indicating input settings related with the autofocus algorithm. Increment [individual pump step] per control cycle (green arrow), contrast value c (blue arrow), tolerance limit [in terms of % change in contrast] (yellow arrow) and incremental displacement of focus (red arrow). Right: Schematic flowchart of autofocus algorithm program structure.

The autofocus concept

Individual images of the lower CellDrum membrane part were grabbed by the custom made microscopy sensor (CMS) and further processed by custom made analysis software. The autofocus quality (control variable) was derived in terms of relative contrast (Figure 7-2 left blue arrow), calculated by the average of all grayscale pixel intensities (0-255) in the 2D array of the Sobel kernel processed image. After the call up of the autofocus subprogram (Figure 7-2 right) by the main program, the equivalent procedure executed preset pump steps (Figure 7-2 left green arrow) until the contrast value did not change within a preset tolerance limit (Figure 7-2 left yellow arrow).

Autofocus process evaluation

Relative contrast levels depend on surface properties, in particular the total width of detectable edges. Additionally, multiple relative focuses may occur. This problem was evaluated in more detail as follows.

We used a rectangular grid and µm-talcum particles as model samples. The maximum contrast level for the rectangular grid etched to a transparent glass surface (Figure 7-3) and the one for µm-talcum particle (Figure 7-4) differed by factor three in their maximum contrast value. This was related to the custom made auto focus algorithm, which accounts for the over all grayscale pixel intensities (0-255) in the 2D array of the Sobel operator processed image (Figures a´-j´). In this respect, the µm-talcum particles exhibited a high level of detectable edges leading to a high relative contrast level as compared to other structures with few edges (etched grid) at the same qualitative objective focus quality.

Another problem affecting the relevant control loop settings were due to object depended multiple focal planes. This is in particular relevant in investigations on cell-monolayer structures grown on transparent CellDrum membranes. Due to the optical properties of the cells, there were two relative maxima detectable in contrast (Figure 7-5). The global maximum was associated with a brightfield focus (i,i´) contrast maximum. However, the local maxima could be assumed to be darkfield maxima (j,j´). This was important to know to set the auto focus control loop settings correctly in order to achieve acceptable tolerance limits. The accuracy of the CMS sensor depended on the target. For cell cultures the typical accuracy was ± 2µm (Figure 7-5).

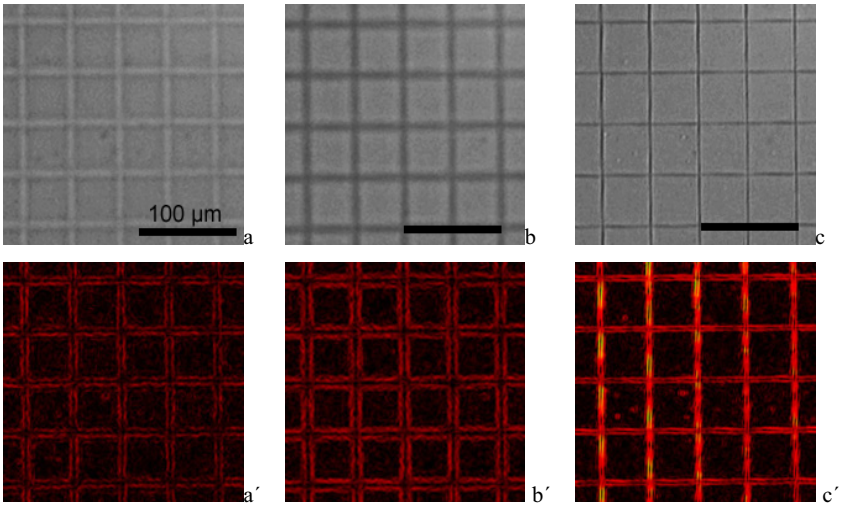

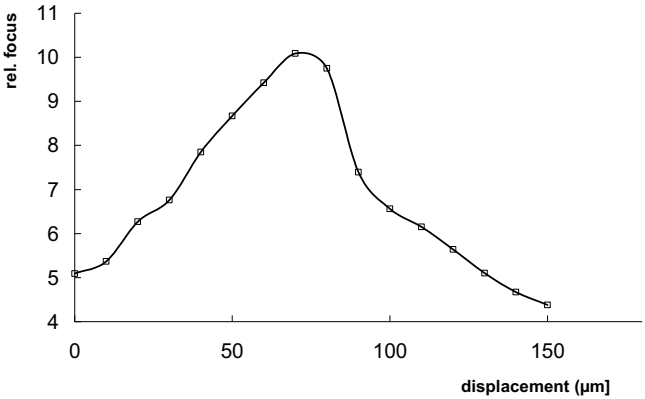

Figure 7-3 Top row: Brightfield micrographs (a,b,c) of a 50 µm grid, etched on a glass slide in which the focal plane was set to different levels. Pseudocolor micrographs (a´,b´,c´) show the same grid at the same focus setting after image processing with an edge detection Sobel-algorithm. The relative focus quality values were derived by image histogram analysis, calculating the average over all pixel intensities (0-255) in the 2D array of the Sobel kernel processed image. Bottom: Relative focus values as function of the focus displacement. The best focus quality was reached at a distance of approximately 75 µm.

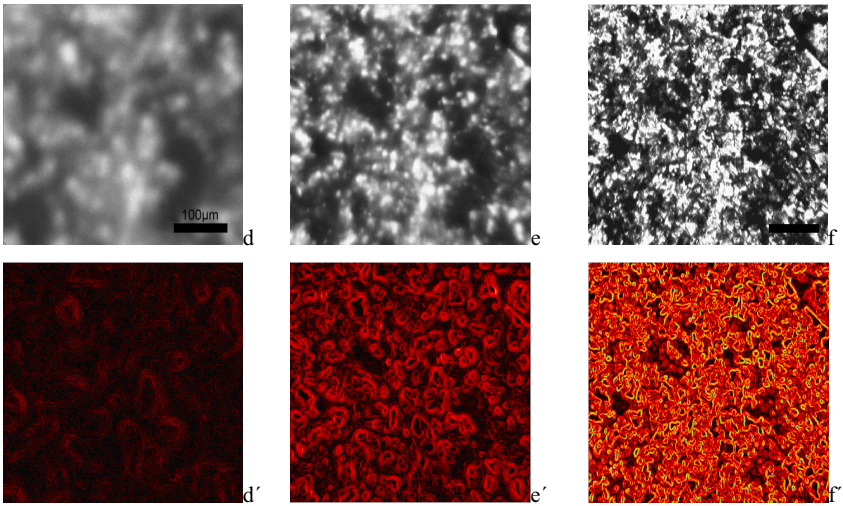

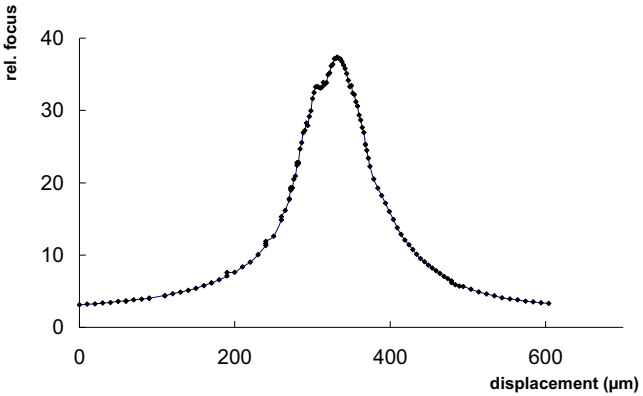

Figure 7-4 Top row: Brightfield micrographs (d,e,f) of a talcum powder coated CellDrum membranes in which the focal plane was set to different levels. Pseudocolor micrographs (d´,e´,f´) show the same setup after applying an image processing with an edge detection Sobel-algorithm. The relative focus quality values were derived as in figure 7-3 Bottom: Relative focus values as function of the focus displacement.

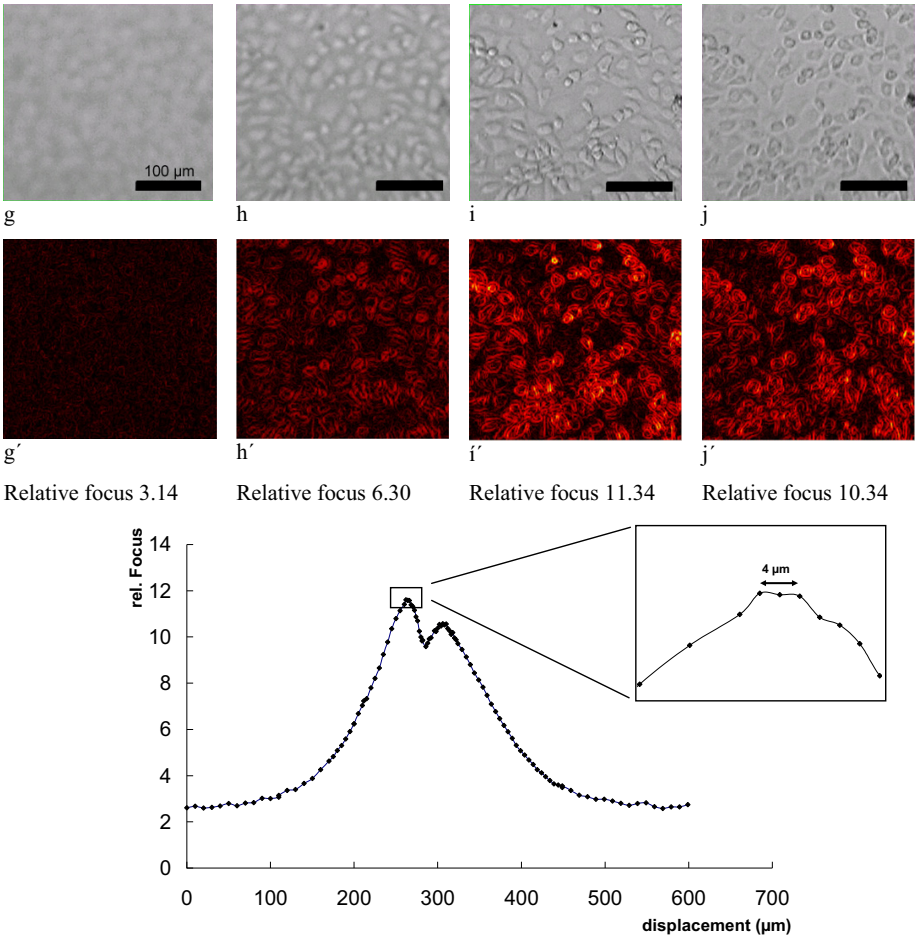

Figure 7-5 Top row: Brightfield micrographs (g-j) of a confluent BAEC (bovine aortic endothelia cells) layer grown on a fibronectin coated CellDrum. The plane of focus was diversified in all images. Pseudocolor micrographs (g´-j´) show the same setup after applying an image processing with an edge detection Sobel-algorithm. The relative focus quality values were derived as in figure 7-3. Bottom: Relative focus as function of the focus displacement. The displacement curve shows two focal planes for a BAEC monolayer, one global maximum was related to image i and the second local maximum was related to image j.

Conclusion-Optimal autofocus controls loop setting

The major conclusion of the previous chapter was that individual control loop settings were necessary for a specific specimen. The software based control function had to serve both possible control modes. One was the steady state mode during cell culture where major disturbances were mainly caused by evaporation (slow process). The second was the load-strain analysis mode with a fast disturbance caused by the applied shift of focus. The control settings had a direct impact on the following process functions: 1) total processing speed, 2) autofocus sensitivity for contrast changes, and 3) resolution.

Another important factor to be considered was the mechanical "training" effect of the cells. When cells are exposed to mechanical load, as during the autofocus procedure, they adopt their mechanical properties to the loading conditions. Popular control system algorithms like the PID were not applicable, because their oscillating compensation mechanism would cause the described cellular training effects. Therefore procedures potentially causing mechanical training effects had to be avoided in particular during long term cell culturing. The settings had to be balanced because of the defocusing effect of media evaporation (Figure 7-6). The tolerance limit of contrast change as well as the pump step increment had to be adjusted to a minimum of control cycles. At the same time the membrane focus had to be kept within the tolerance limit which was in the order of a micrometer.

	Processing speed	**Sensitivity**	**Resolution**	**Mechanical impact on cells**
Increment: Low	-	**±**	+	+
Increment: high	+	**±**	-	**-**
Tolerance limit: low	+	-	**-**	+
Tolerance limit: high	**-**	+	+	**-**

Table 2 Impact of different settings to the autofocus process: (+) positive effect, (**±**) no influence, (-) negative effect.

Table 2 shows that each individual process parameter setting had an opposite impact on most of the other autofocus processing results. The parameters were optimized for each individual specimen and experimental procedure. Typical settings accomplished a tolerance limit (calculated by the contrast difference) of 0.05 and an increment of pump steps s = 20 (equivalent to 3µl of volume

change). This resulted in a typical resolution of ±2 µm and a step response processing time of approximately 5s.

7.4 Steady-state system: properties and limitations

In particular for long term experiments media evaporation had to be accounted for. Although the measurement device was placed into a humidified incubator at 37°C, there was still a significant drift in the relative (differential) pressure signal due to evaporation of media from the monitored CellDrum.

Variations of differential pressure during cell cultivation do not change the deflection of the CellDrum membrane, since its position was actively monitored and pressure was compensated by the measurement software driven experimental setup. Compensation of evaporation as illustrated in Figure 7-6 turned out to be extremely important since typical pressure regimes for membrane deflection were in the pressure range of 0-100 Pa (1Pa~100µm water column). The sensitivity of the system and the effect of surface tension on the load-deflection curve are demonstrated for the CMS sensor setup in Figure 7-7. The load-deflection curves were reproducible after an initial wetting (Figure 7-7 open circles) of the CellDrum wall above the initial media level by membrane deflection and at the same time the liquid level rise into this direction (black squares Figure 7-7). After this initial wetting repeated pressure-deflection cycles turned out to be very reproducible (black squares and circles Figure 7-7).

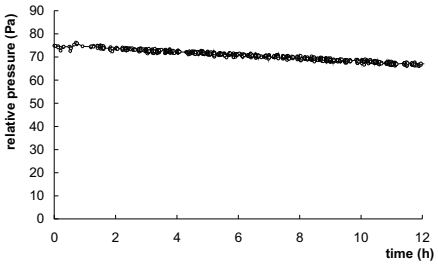

Figure 7-6 Pressure drift due to evaporation

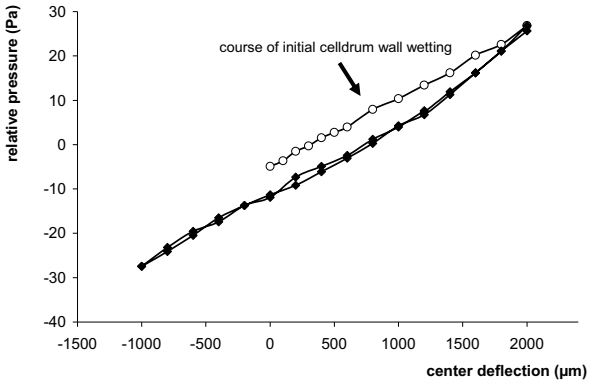

Figure 7-7 Effect of surface-liquid interaction on the load –deflection curve

The strong effect of liquid-surface interactions made it reasonable to evaluate the effects of different, evaporation related liquid columns on the load-deflection curve of a typical CellDrum setting. The dependency of these curves on the media level is shown in Figure 7-8a (the linear part of the curve is displayed in Figure 7-8c) for the high sensitive laser sensor setup. Variations of liquid level based on the typical CellDrum media volume of 500µl were found to cause a liquid level related error of only 0.47 % in the slope of curve compared to the 400µl filing quantity. The 400µl filling quantity describes the maximum loss of liquid for a typical observation period without media change. The variations in the slope of the curve for other filling quantities was typically in the range of 3%-8%, but a significant error of 18% occurred for the 300µl filling. This is related to the incomplete coverage of the CellDrum membrane with media at high central deflection at low liquid levels.

The reproducibility of the measurement was not affected by the media filling quantity, except for the low-level 300µl filling with a visible hysteresis between two successive measurements. The accuracy of repeated measurements was further addressed in Figure 7-8b. The accuracy of measurement at standard conditions was ±0.15Pa within the linear slope of the curve. This equals a pressure change of a 15µm high water column.

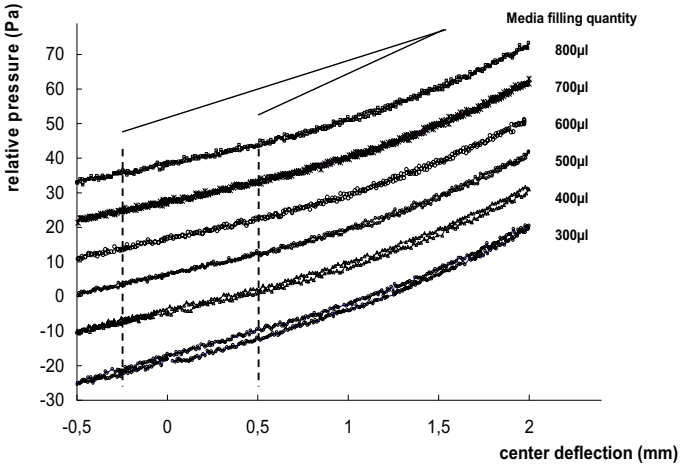

Figure 7-8a Typical load-deflection curves for a bare CellDrum membrane at various liquid levels. The linear part (dotted line) of the curve is displayed in figure 7-8c

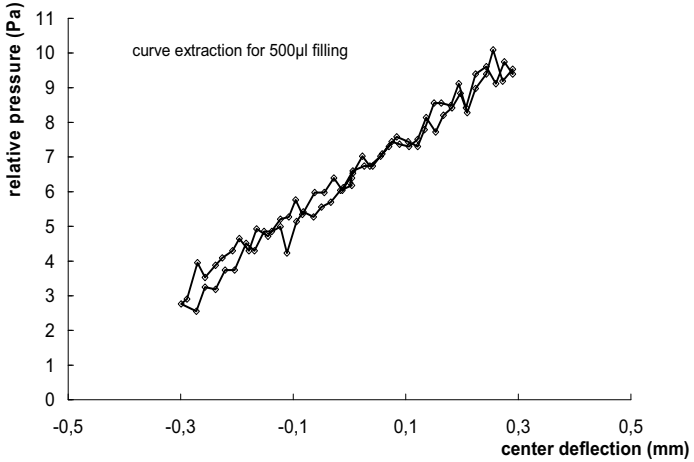

Figure 7-8b represents the linear part of the load-deflection curve at 500µl filling

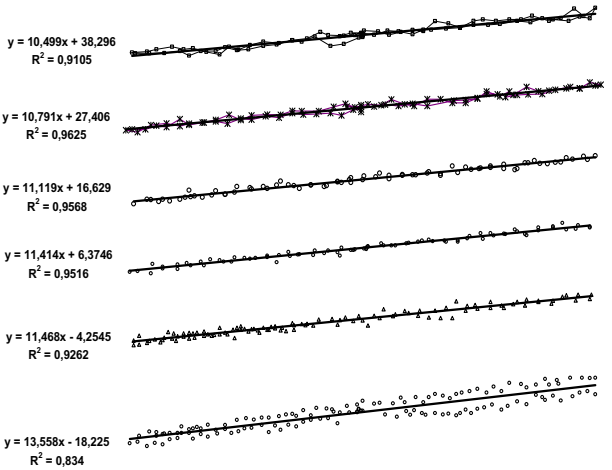
y = 10,499x + 38,296
R2 = 0,9105
y = 10,791x + 27,406
R2 = 0,9625
y = 11,119x + 16,629
R2 = 0,9568
y = 11,414x + 6,3746
R2 = 0,9516
y = 11,468x - 4,2545
R2 = 0,9262
y = 13,558x - 18,225
R2 = 0,834

Figure 7-8 c

7.5 Laser sensor dynamic system: Sensor properties

Dynamic sensor evaluation and precautions

The dynamic system was developed because of its prospective usefulness in a high-throughput system for tissue tension analysis. This is a complementary approach to the highly sensitive load-deflection system.

The dynamic system's fast measurement cycles (typically 200ms) allow multiple measurements per sample without consideration of variation of the experimental boundary conditions. Any sudden or unanticipated interference within the environment, which might affect the signal, can be easily detected by FFT analysis of the signal (custom made software). For testing the instrumental setup in terms of accuracy and reproducibility, oscillations of pure silicone membranes of the CellDrum were excited. The frequency of the first fundamental oscillation was at 57 Hz+/-0.044 (ten repeats), representing a coefficient of variation of 0.0035% and showed an almost ideal pattern of a harmonic oscillation. The frequency did not vary with the amplitude of the initial indentation of the membrane up to 1 mm.

Major attention was paid to the characteristics of the excitation pulse, to avoid any intrinsic errors caused by the device itself. An asymmetrical excitation pulse (air pressure pulse) could affect the membranes vibrational mode and would shift the resonance frequency of the oscillating membrane from the fundamental frequency to higher frequencies leading to misinterpretation of the experimental data. The nature of the excitation pulse was analyzed in a separate setup (Figure 7-9). As the Figure 7-9 shows there were no turbulences detectable within the relevant dimensions of the dynamic system and the pressure pulse was symmetrical. The impact of an asymmetrical excitation pulse will be discussed theoretically in chapter 10.4 .

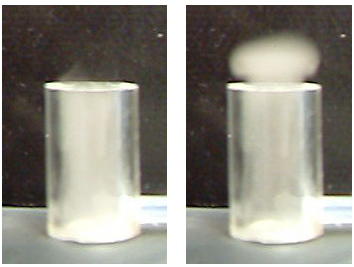

Figure 7-9 Time series of the excitation pressure puls visualized using NH_4Cl dust. There were no detectable turbulences within in the system's relevant dimensions.

Data acquisition- adapted measurement software

The custom made data acquisition software enables dynamic, automated periodical data acquisition with a typical scan rate of 100 kHz. Energy and incidence of the excitation pulse is determined by the software. There is a delay of 50 µs between the activation of the measurement and excitation of the pressure pulse to avoid any misinterpretation of the signal. An automated periodical data acquisition can be executed with the desired repetition and measurement period.

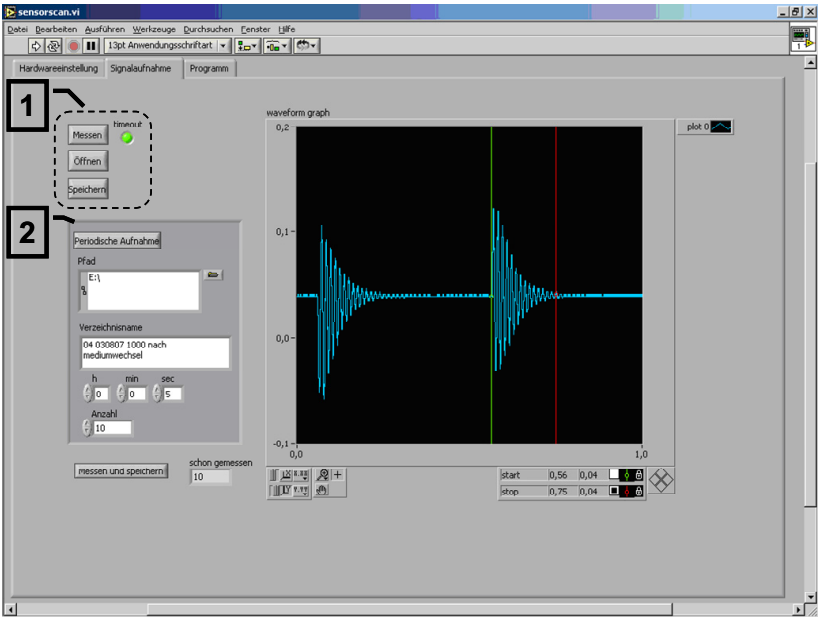

Figure 7-10 GUI front panel –dynamic data acquisition for single mode (1) and automated mode (2)

Data analysis- the analyzing software

All acquired oscillation curves were analyzed by the custom made analyzing software based on procedures like peak detection, Fast Fourier Analysis, etc. The software determines the main oscillating frequency and the damping coefficient of the excited membrane. The relevant data were extracted from the whole signal, zero-padded, and processed by the FFT with Hanning window. FFT detects any overtones in the signal which could allude to errors in the experimental setup. All frequency maxima are listed in an array and transferred to a spreadsheet format.

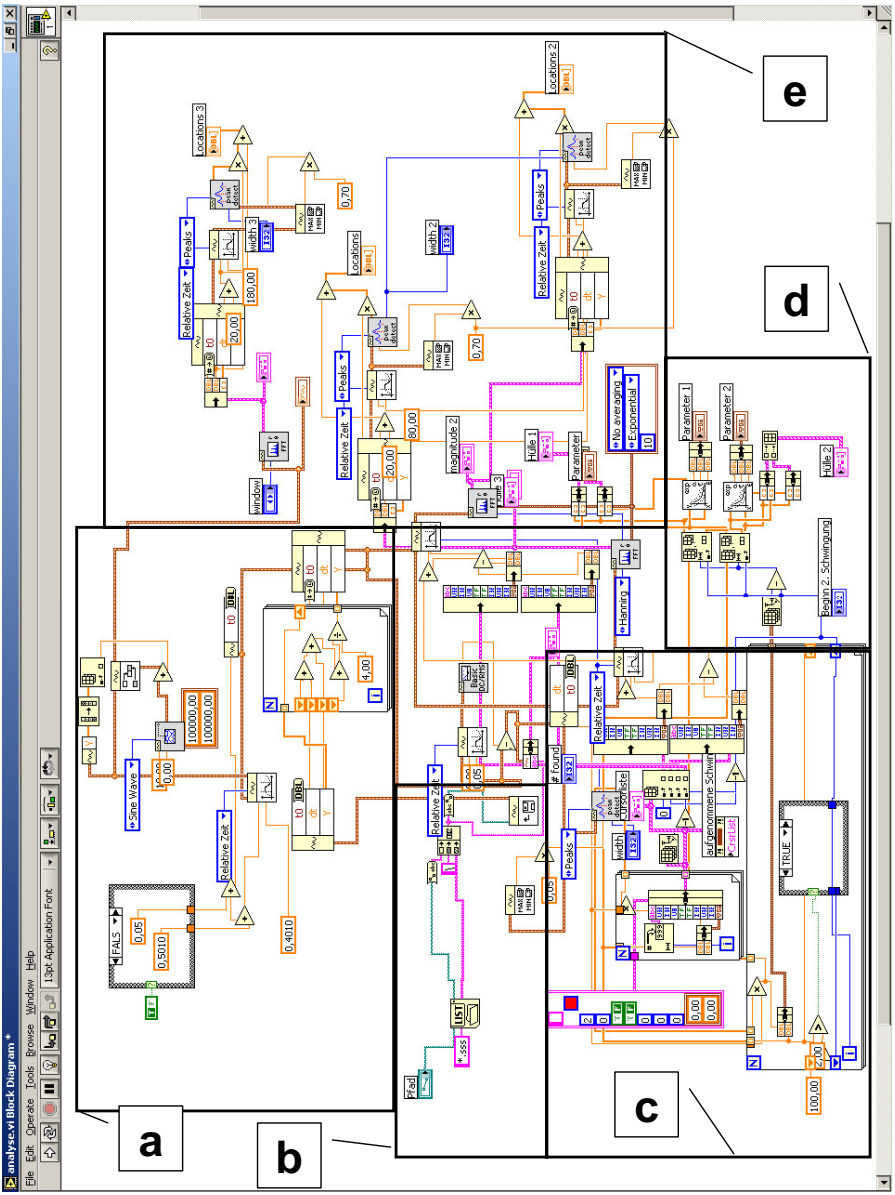

Figure 7-11: Example of a single sequence in the data analysis software. Signal preparation for FFT (a), data import (b), detection of beginning and end of oscillation (c), calculation of damping coefficients (d),

8 CellDrum technologies

8.1 Membrane fabrication technology

CellDrum membranes were manufactured using 184 Sylgard™ polydimethylsiloxane (Dow Corning, Michigan, USA) known as a silicon rubber. Individual batches were manufactured for typical membrane thickness varying from 1µm to 10µm. The CellDrum is now commercially available at Cell&Tissue Technology Corporation (Juelich, Germany).

8.2 Biocompatibility

Unfortunately there are no precise definitions nor commonly accepted measurements of biocompatibility available (Ratner et al. 1996). However, biocompatibility is defined in terms of performance or success at a specific task. In our experiments, biocompatibility was defined in terms of providing a viable environment for cell growth, attachment and proliferation on the CellDrum membrane.

The polydimethylsiloxane (PDMS) based CellDrum membranes show different, but more adequate properties to the biological environment as compared to surfaces and substrates usually used in cell culture technologies. The CellDrum membranes are permeable for gases, flexible (soft) and coatable with ECM proteins. The control of extra cellular matrix (ECM) organization and cell adhesion are critical for the attachment of cells. Adequate procedures were therefore developed to exhibit relevant matrix proteins at the CellDrum surface. Other aspects of biocompatibility are related to the segregation of harmful molecules (i.e. monomers) from the materials, leading to necrotic or apoptotic cell death, respectively. Various investigations were accomplished to exactly reveal these features and properties.

Surface tension

Cell adhesion and spreading are influenced by the physico-chemical and mechanical characteristics of the underlying solid surface (Harris 1973). Substratum surface free energy is related to cell spreading, as illustrated in Figure 8-1 (Schakenraad et al. 1988). Poor spreading on hydrophobic substrata can be observed in both absence and presence of preadsorbed serum proteins like fibronectin.

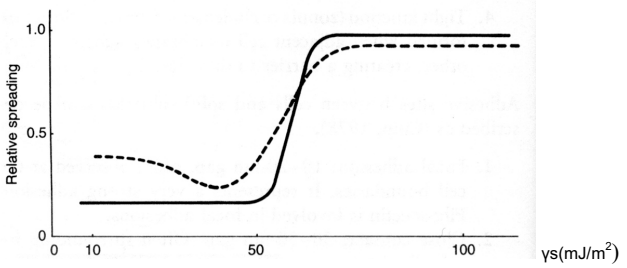

Figure 8-1 Cell spreading as function of substratum free energy (γ_s=γ_2) (Schakenraad et al. 1988). Dotted line: Cell spreading in the absence of proteins; Solid line. Cell spreading in the presence of serum proteins.

The free surface energy characterizes the wettability of a surface which is quantitatively described by the angle θ between the surface of a liquid drop and the surface of the substrate in the contact point. The angle θ depends on the surface energies of the liquid γ_1, the substrate γ_2 and the energy γ_{12} of the boundary surface between liquid and substrate, respectively. The relationship is known as **Young's equation** for dry wetting:

$$\cos\theta = (\gamma_2 - \gamma_{12})/\gamma_1 \qquad \text{Formula 8-1}$$

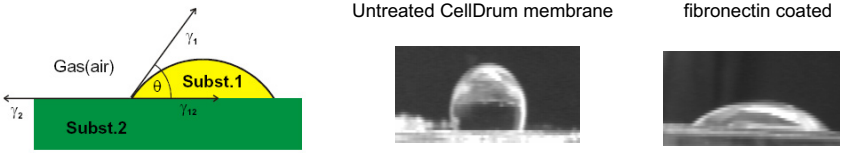

Figure 8-2 Scheme of a substrate-liquid interface (left). Distilled water drop on top of an untreated (middle) and a fibronectin coated (right) polydimethylsiloxane substrate (CellDrum membrane).

Contact angle measurements provide a useful "first line" characterization and insight into how the surface interacts with the environment in general and the cell in particular. For practical reasons, (γ_2- γ_{12}) becomes summarized to the critical surface energy γ_c, which can be easily determined by test inks according to DIN 53 364. According to this procedure a typical γ_c value for the untreated

CellDrum membrane (polydimethylsiloxane) would be approximately 14.1 mJ/m^2. To enhance cell spreading and adhesion, the CellDrum membranes were modified by a fibronectin adsorption method (Eckl & Gruler 1988; Horbett & Schway 1988) and the air dried surfaces were evaluated using distilled Water ($\gamma_{liquid} = \gamma_l = 73$ mJ/m^2) as a test ink. The treatment of the CellDrum membranes by surface energy modification methods like protein adsorption (Eckl & Gruler 1988; Horbett & Schway 1988) or plasma etching (Ratner 1992) enhances the bioactive features of the polydimethylsiloxane material used. Although plasma etched membranes featured useful properties for cell attachment and proliferation (Ratner 1992) the method was not applicable because the thin membranes became brittle and lost their elastic properties after treatment. In contrast, the treatment with fibronectin did not alter the elastic properties of the CellDrum membrane but shifted the substrates surface free energy (Figure 8-3) towards the energy plateau for enhanced cell spreading (Figure 8-1) and adhesion. A fibronectin coating was established for all 2D CellDrum applications by the administration of a 30µg/ml fibronectin solution on top of the spreading area for at least 30 min. prior to CellDrum usage. Besides physical considerations, fibronectin, as many other proteins exhibit specific binding sites called RGD domains for the attachment of cell membrane proteins. Thus, besides the fact that plasma etching was not suitable a protein coating is the condition sina qua non for CellDrum usage. Fibronectin for example is a protein naturally present in the extracellular environment of most cells. Cells can bind to the RGD sequence of fibronectin, which in turn can bind to solid substrates (Figure 2-1, Figure 2-2).

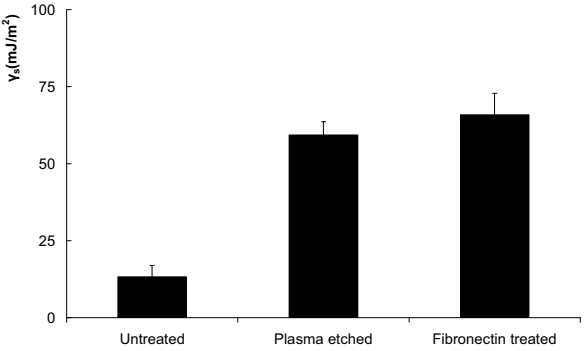

Figure 8-3 Effects of different treatment methods on the CellDrum surface free energy.

Protein adsorption related cell proliferation and adhesion

In a physiological environment, protein adsorption always precedes cellular adhesion (Ratner et al. 1996). Preadsorbed proteins, in combination with proteins produced by the cell, and depending on the substratum properties, determine the strength and type of adhesion.

As mentioned in the previous paragraph, the Cell Drum's silicon elastomer surface itself is not suitable for cell culture applications without specific coating. This is on the one hand related to the hydrophobic characteristics of the silicon membrane and on the other hand to the lack of RGD binding sites on the artificial CellDrum membrane.

In order to demonstrate the effects of coating, we patterned the surface of the CellDrum (Figure 8-4). In this method, protein was absorbed from the protein solution on top. By doing so, the protein concentration on the surface becomes about a 1000 times more concentrated than it was in solution. (Eckl & Gruler 1988). The adsorption of proteins from the liquid phase to the solid surface is largely irreversible and leads to an immobilization of protein species on the surface. Various protein coatings were tested for their usability enhancing cell spreading and proliferation on the CellDrum membrane. Figure 8-5 shows some of the results. Membranes which were incubated with a 30µg/ml fibronectin or 10µg/ml Cell-tak™ (BD Biosciences, Heidelberg) solutions for more than 30 min, respectively, showed an enhanced proliferation of Bovine Aortic Endothelial Cells (BAEC) within 4 days of almost 400%. Correspondingly, the fraction of unattached cells after this cultivation period was negligibly low at around 0.5%. In contrast, untreated surfaces showed no increased proliferation after four days. Most of the initially seeded cells were found in suspension while only 0.7% of BAEC cells adhered to the surface. The usage of a 200µg/ml Gelatin solution did not alter adhesion and proliferation rates efficiently. The results reflect earlier findings for fibronectin (Eckl & Gruler 1988; Horbett & Schway 1988; Akiyama et al. 1985) and for cell-tak™ (Jiang et al. 2001; Miyazaki et al. 2000).

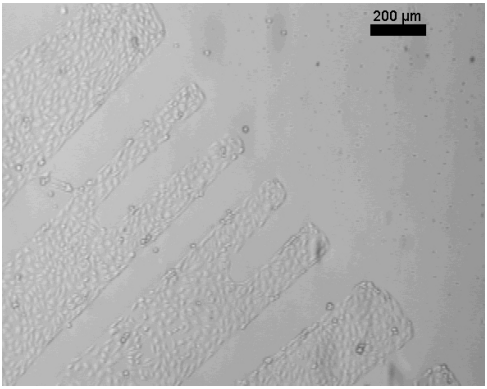

Figure 8-4 Micrograph of Endothelial cells on a protein patterned ("finger" patterning) silicone substrate. BAEC cells did not adhere to uncoated CellDrum surface.

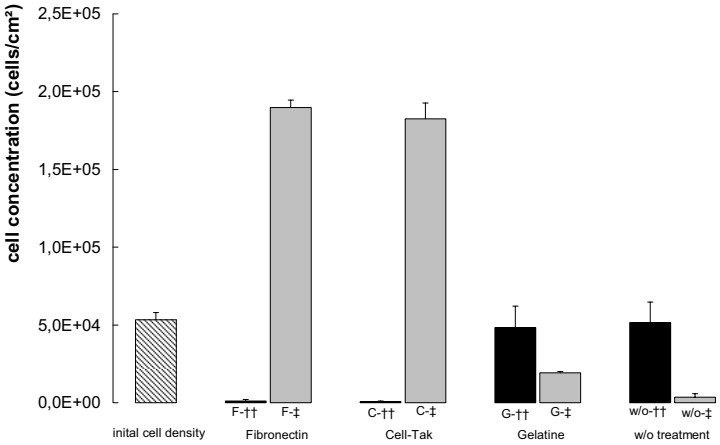

Figure 8-5 BAEC density after 4 days of culturing. Various coatings were tested (grey bars). The fraction of unattached, dead cells (††) and proliferated cells (‡) (black bars) strongly depended on theemployed surface coating.

8.3 Force transduction between the silicon membrane and an individual cell?

Duval et al. (Duval et al. 1988) have clearly demonstrated on a series of substrata that strength of adhesion and spreading are indeed two separate phenomena. In other words, the strength of adhesion to a substratum is not necessarily correlated to the area of contact. For this reason, the type of adhesion sites and force transduction between the cell layer and the CellDrum membrane are essential for a successful and reliable analysis of cellular mechanical properties.

Direct microscopic evidence

The effect of traction patterns on the CellDrum membrane curvature was shown with LSM microscopy (Figure 8-6a) prior to SEM investigation.

A Scanning Electron Microscopic (SEM) visualization of individual 3T3 fibroblasts grown on fibronectin coated CellDrum membranes was performed. As figure 8-6b and 8-6c show, traction patterns were visible after post-processing of the original SEM image by height encoded pseudocolor illustration. This experimental approach was a modification of the first cell induced sheet wrinkling experiment of Harris et al. (Harris et al. 1980). With reference to that publication, it was reasonable to relate wrinkles or traction patters to a force transduction between cell and substrate. This study was carried out on fibronectin coated silicon membranes.

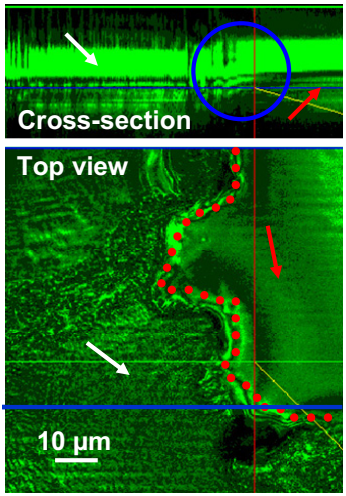

a

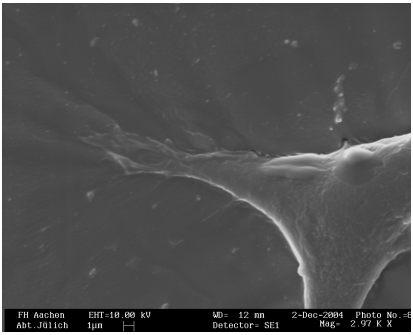

b

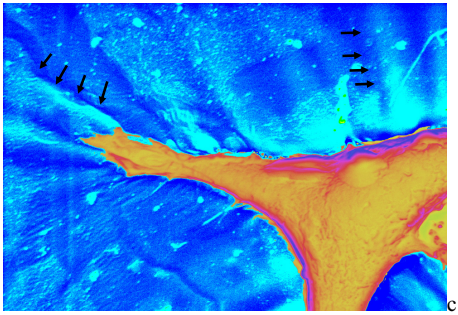

c

Figure 8-6

a) Autofluorescence image of a CellDrum membrane (white arrow) acquired by Laser Scanning Microscopy (LSM) with two different views, cross-section and top view. The upper part shows the cross-section along the blue line of the top view. Air dried ink (red arrow) on top of the membrane introduced a traction related curvature change at the border (red dots) between CellDrum and ink. The area of curvature change is indicated by a blue circle in crossection of the membrane.

b) SEM micrograph of an individual 3t3-fibroblast cultivated on a cell-tak™ coated CellDrum membrane.

c) Pseudocolor height- encoded illustration of the same fibroblast. Traction pattern are visible within the CellDrum membrane (partially marked with arrows).

Indirect mechanical evidence

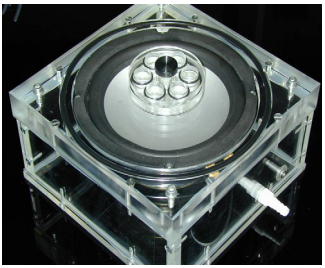

Figure 8-7 cell trainer (left); individual CellDrums (right)

The detection of wrinkle formation is not possible for complete cell monolayers. Other evaluation procedures had to be accomplished in order to prove force transaction form a cell monolayer to its supporting substrate. We addressed the question whether a cell monolayer of 3T3 fibroblasts would react to cyclic mechanical load via restructuring their cytoskeletons. It is known, that cyclic mechanical load leads to various intracellular responses (Cohen et al. 1997). Thus, if the cells were attached to the membrane, those responses must be observable. The CellDrum technology, although not developed for that purpose is ideally suited to expose cells to cyclic load. A custom made device was constructed for that purpose (Figure 8-7). Several procedures were applied to evaluate the above question.

Visualization of cytoskeletal reconstruction:

3T3-fibroblasts subjected to cyclic sinusoidal strain at 0.25 Hz for 2 h at a maximum strain of 0.26 % and unstrained control groups were microscopically inspected for development of Actin stress fibers. Actin stress fibers are known to be generated in cells, subjected to extrinsic stress conditions (Franke et al. 1984). The cytoskeletal Actin components were specifically visualized by fluorescent labeled Phalloidin (Alexa488-Phalloidin, Molecular Probes, Karlsruhe). The occurrence of pronounced fibres in the mechanically stimulated group (Figure 8-9) compared to the absence or only weak appearance in the control group (Figure 8-8) proved indirectly an active force transduction between the CellDrum membrane and the cells. The lack of strong stress fibres revealed another very interesting aspect for using flexible CellDrum membranes for cell culture instead of solid substrates. The prevalence of large actin-containing stress fibers, which are commonly studied in vitro, are rarely if ever seen in vivo. One well-recognized and well studied reason for such differences is, that many cell types in vivo function within a flexible three-dimensional matrix, in contrast to their culturing in vitro on a solid/liquid interface (Bard & Hay 1975). Cell growth on flexible CellDrum membranes seems to mimic the in vivo environment much better than the commonly used stiff substrates.

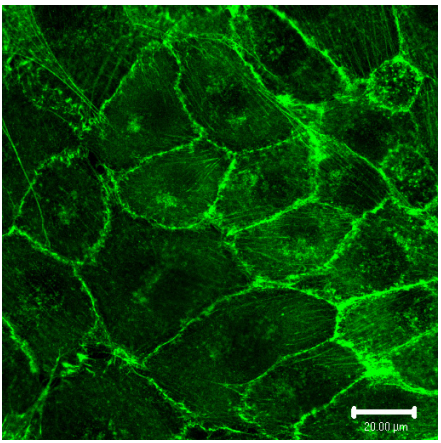

Figure 8-8 3T3 fibroblasts grown on a CellDrum membrane with no cyclic strain. Actin components are labelled in green.

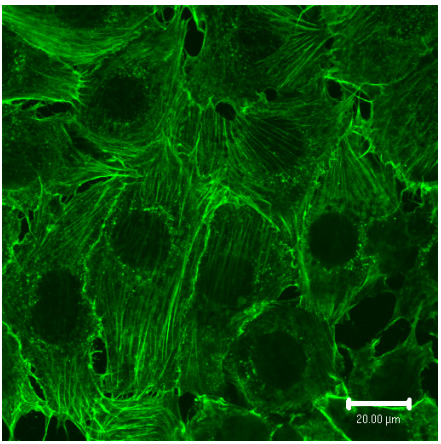

Figure 8-9 3T3 fibroblast subjected to cyclic sinusoidal strain at 0.25 Hz for 2 h at a maximum strain of 0.26 %. The occurrence of Actin stress fibres (green) is notable under these conditions.

Proteome approach

Our next hypothesis was that if there is a force transduction between membrane and cells on top, then there must be some proteomic and metabolic response visible within the cells cytoplasm. Proteomic and metabolic techniques are believed to be ideally suited for the quantitative evaluation of protein and metabolite changes at physiological and non physiological conditions (Loscalzo 2003; McGregor & Dunn 2003). Mechanical stretching is known to activate multiple cellular responses (Cohen et al. 1997). However, it is widely unknown, which molecules are directly activated by mechanical stretching and which molecules are indirectly activated by further upstream modulators. The aim of the experiment was, thus, to develop a proteome-based approach to examine metabolic changes in fibroblasts induced by controlled mechanical stress using the novel CellDrum technology.

Mechanical strain application

3T3 fibroblasts were seeded on the silicone membrane inside the CellDrum (well) at 1.5×10^5 cells per well. Six CellDrums at a time were placed in a holder and cultured simultaneously at same conditions for 48h in medium. Afterwards they were subjected to cyclic sinusoidal strain at 0.25 Hz for 2 h at a maximum strain of 0.26 %. Strain experiments were carried out in a humidified incubator with 5% CO_2 at 37°C. The cells were washed twice with cold PBS. Cellular extracts were harvested according to the protocol described below. All experiments were performed in sterile conditions.

Results: SDS PAGE analysis of protein extracts derived from the same amount of mechanically stressed vs. control cells revealed substantial difference in total protein content. According to the Bradford assay, it was approximately 19.3±4.3 % higher for strained cells as compared to controls (Figure 8-10).

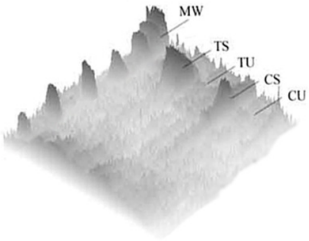

Legend:

MW-molecular weight marker,
TS-cells mechanically stressed, soluble protein fraction,
TU-cells mechanically stressed, hardly soluble proteins,
CS-control cells, soluble protein fraction,
CU-control cells, hardly soluble protein fraction.

Figure 8-10 Comparison of the major protein amounts in mechanically stressed vs. control cells as detected in SDS PAGE.

For more detailed observations, the protein extracts were subjected first to isoelectrofocusing (pH 3-10) and then SDS PAGE was applied as a second separation technique (Figure 8-11). Differences in protein content were clearly visible, in particular in the low-molecular weight area.

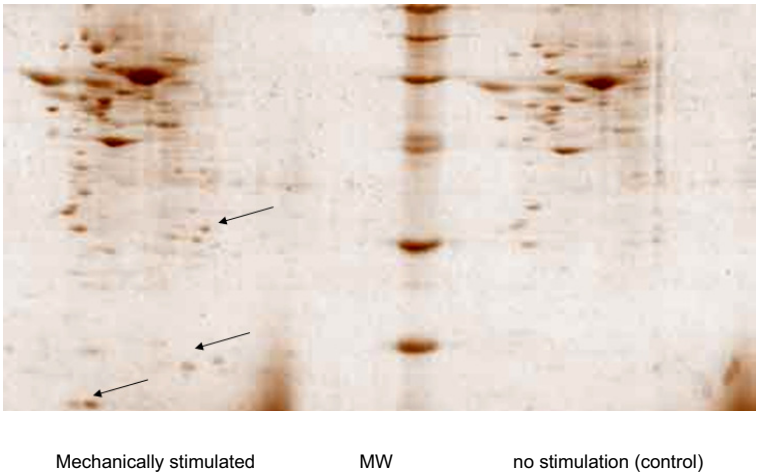

Figure 8-11 Changes in the protein composition of fibroblasts induced by mechanical stress. Middle: molecular weight marker; left: cells were subjected to mechanical stress for 2 hours; right: intact cells. Differences are indicated by arrows.

The applicability of two-dimensional SDS PAGE for monitoring the response of fibroblasts to mechanical stress was shown. Such a “proteome-based” approach appears to be a helpful tool in the

future for examining cellular responses at various mechanical conditions. It revealed useful semi-quantitative information about relative protein amounts of major cellular proteins and proved the microscopically revealed hypothesis of a force transduction between cells cultured on CellDrum membranes. Gene expression real-time-PCR investigations (Demirici et al. 2004) on BAEC and 3T3 fibroblasts gave further evidence that cells are efficiently connected with their substrate.

8.4 Force transduction and surface coatings

Cell-Tak™ is described to promote an extremely strong binding between cell and substrata (Miyazaki et al. 2000). A strong force transmission between cell and CellDrum membrane was desired in our monolayer experiments, and therefore Cell-Tak™ was seen to be the best choice for membrane coating. Cell-Tak™ Cell adhesive is a formulation of polyphenolic proteins extracted from Mytilus edulis (marine mussel). The adhesive is described to be biocompatible. Cell proliferation and viability tests (chapter 8.2) for BAEC cells grown on precoated CellDrum membranes which were not exposed to strain variations during culturing supported that assertion.
However, the replacement of fibronectin with Cell-Tak™ as a membrane coating led to ablation and destruction of cells after mechanical stretching. The response was completely different from identical experiments carried out with fibronectin coated membranes. After exposure to mechanical stress adherent cells (in particular BAECs) grown on Cell-Tak™ coated surfaces, lost contact to their environment and rounded up. This is an indicator of cell death. The underlying mechanism of this phenomenon was unclear, but nevertheless important to identify. This phenomen had to be considered for the experimental setup.
The apoptosis analysis of BAEC's grown on fibronectin or Cell-Tak™ coated CellDrum membranes did not show any differences in the appearance of apoptotic cells. The same situation occurs for cells which were exposed to oscillating mechanical strain (0.5 %) for a period of 2 h (Figure 8-12,-13). It seemed that the ablation of cells due to mechanical impact at different surface adhesion sites was not due to an apoptosis inducing process, at least not at our specific experimental protocol.

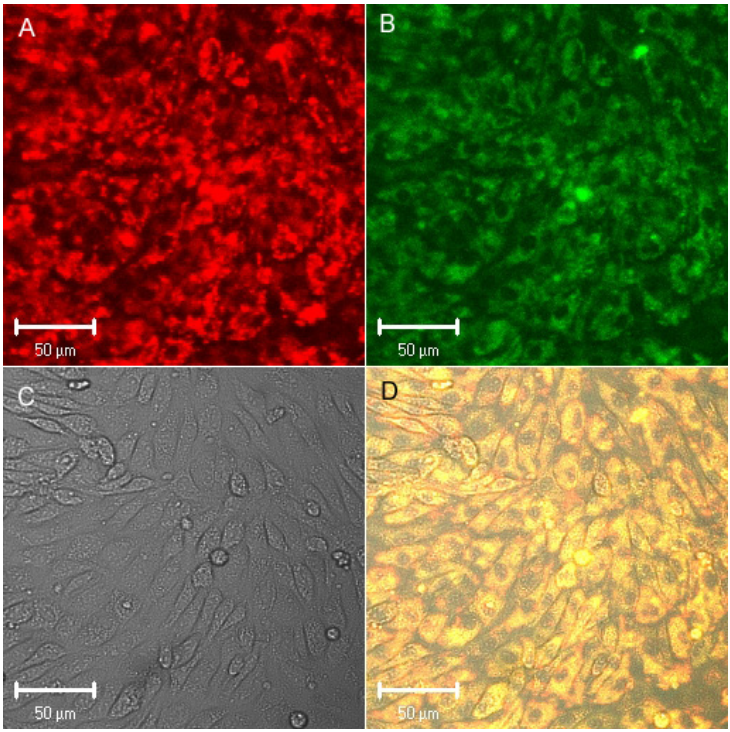

Figure 8-12 Mitocaputre™ stained BAEC`s cultivated on a fibronectin coated CellDrum after exposition to mechanical strain (ε=0.5%) for 2 h: Nonapoptotic cells display a red staining (A) indicating a active metabolism within their mitochondria. Green staining (B) displays the control image for a successful total staining. The superimposed control image (D) indicates untruthful areas in red, but apoptotic cells in green and nonapoptotic cells in yellow. Image (C) in brightfield mode displays the intact BAEC monolayer on top of the CellDrum.

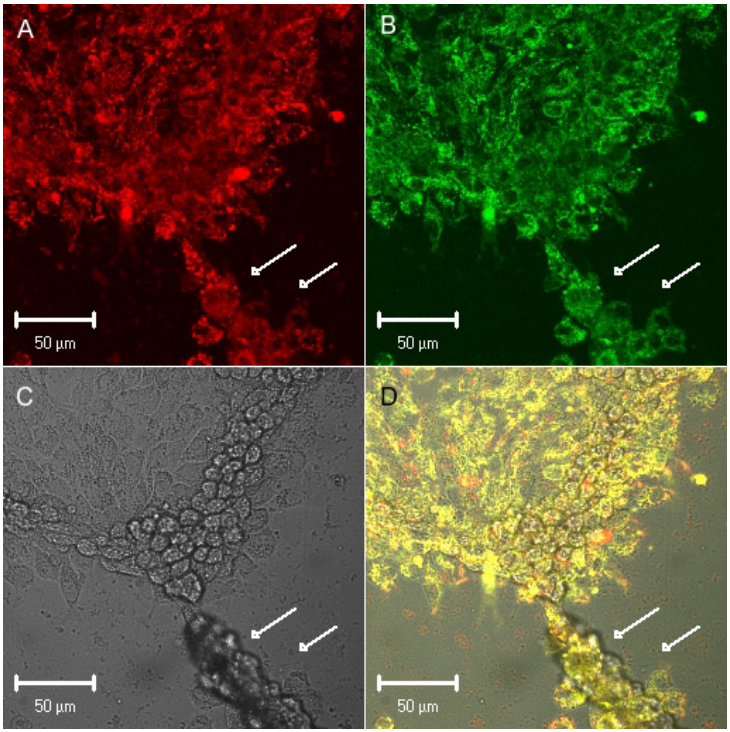

Figure 8-13 Mitocaputre stained BAEC's cultivated on a Cell-tak coated CellDrum after exposition to mechanical strain (ε=0.5%) for 2 h: Clusters of cells separated (white arrows) from the monolayer and remained only in lose contact with the monolayer. Nonapoptotic cells display a red staining (A) indicating an active metabolism within their mitochondria. Green staining (B) displays the control image for a successful total staining. The superimposed control image (D) indicates untruthful image areas in red, but apoptotic cells in green and nonapoptotic cells in yellow. Image (C) in brightfield mode displays the disrupted BAEC monolayer on top of the CellDrum.

Nevertheless, a potential ablation of cells from the CellDrum membrane is critical for all experiments made on cell monolayer structures grown on flexible membranes. Possible reasons for such results are differences both in elasticity of coating molecules and in their specificity to cellular receptors. Cell-Tak™ is a mixture of mechanically strong proteins capable of introducing strong but unspecific adhesive binding due to presence of poly-phenolic amino acids (Deacon et al. 1998). In contrast, fibronectin binds specially to the cellular cortex and is an elastic molecule rearranged by cellular action into a complex network with high elasticity (Wierzbicka-Patynowski & Schwarzbauer 2003). Thus, we assumed that tension generated in the membrane is transmitted

elastically to the cells when fibronectin was coated. It was inelastically transmitted when Celltak was used which then caused irreversible damage to the cells.

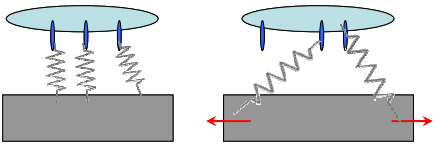

Figure 8-14 Schematic for fibronectin coating. Mechano tranduction between a stretched substrate and the cell is transmitted trough the elastic and specifically bound fibronectin structures.

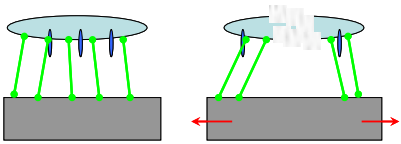

Figure 8-15 Schematic for Cell-Tak coating. Unspecific, non elastic cell-tak mediated force transduction between substrate and cell that may lead to cell disruption.

Despite the so far unknown effect described above, force transduction between cell and substrate is a critical issue. Not only the quality of the cell-substrate interaction is a limiting factor, but also the nature and number of adhesion points. Other researchers (Balaban et al. 2001) identified that large focal adhesions characteristic of adherent cells did not form on stiff surfaces.

8.5 Mechanical properties

Surface integrity and microstructure

Scanning electron microscopy showed that CellDrum membranes were smooth, homogeneous, and had no pores (Figure 8-17). The wrinkles in the upper part of the figure were of sub micrometer size and were correlated with the membrane mounting process. These wrinkles served as a control for a focused image under optimal SEM settings. The gas permeability of the membranes is therefore not associated with any pore formation during the membrane fabrication process.

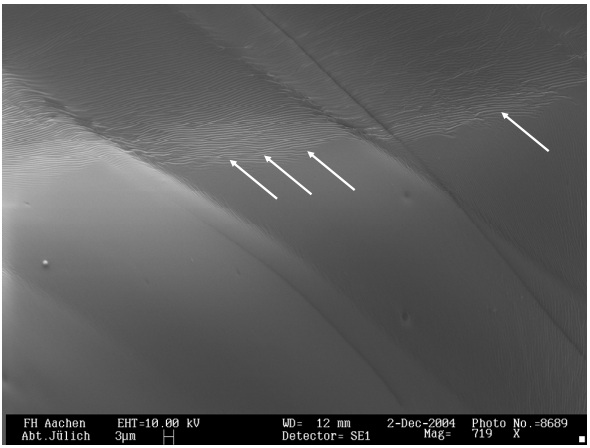

Figure 8-16 Scanning electron micrograph of the membrane surface. The wrinkles in the upper part (arrows) were related to the mounting process of the membrane.

Gas permeability

Gas permeability is of big physiological importance for some applications. As for example in vivo, the smooth muscle cell relaxation and related vasodilatation are mediated through basal delivered Nitrogen monoxide (NO). It diffuses from the interstitium (from below) into the smooth muscle cell layer surrounding the vessel. Mediators for vascularization like vascular endothelial growth factor (VEGF) and pigment epithelium derived factor (PEDF), are both regulated by tissue oxygenation (King & Suzuma 2000). Expression of VEGF is induced by hypoxia, thus promoting neovascularization. Granulocytes for example are known to be attracted by a negative oxygen gradient after the implantation of a biomaterial (Ratner et al. 1996). These and many other in vivo effects, requiring substratum permeability for gasses, are not yet sufficiently considered in the literature. In contrast, the impact of the gas delivered with the cell culture medium was clearly demonstrated (Rasmussen 1984). In conclusion, offering a gas permeable substrate to adherent cells in vitro mimics to a great extend the in vivo situation where there are gas permeable basal membrane adhesion sites. In contrast to surfaces commonly used in in-vitro cell cultures, the CellDrum system implies the feature of gas permeability.

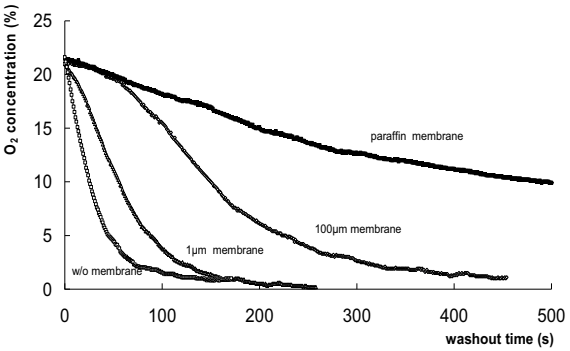

Figure 8-18 gas permeability for different membranes

The gas permeability of the CellDrum was proven indirectly in terms of the CO_2-passage through the CellDrum membrane between a CO_2 saturated reservoir and a significantly smaller reservoir, filled with media at an atmospheric O_2 composition of 21%. The CO_2 diffused through the membrane and had a washout effect on the O_2 composition in the measurement chamber. This effect was rather fast. For 1µm CellDrum membranes $T_{1/2}$ was 55s) and for the much thicker 100 µm membranes $T_{1/2}$ was 150s (Figure 8-18). Therefore it is reasonable to assume cells grown on a CellDrum membrane are exposed to the same gas composition at their adhesion side as administered at the media site.

9 Orientation of cells in a mechanically anisotropic environment

9.1 Effects of mechanical loading to tissue behaviour

The mechanical environment of cells inside a tissue determines the distribution of the cells and their orientation (Brown et al. 1998) and vice versa. As discussed in section 2.2, the mechanical response of soft tissue depends on texture and cellular orientation. Most of the mechanical testing on cell seeded collagen matrices found in the literature has been performed uniaxially on rectangular strips and were thus one-dimensional stretching approaches. As a result, most phenomenological constitutive models are based on uniaxial data (Bell et al. 1979; Brown et al. 1998; Delvoye et al. 1991; Eastwood et al. 1994). Prior to our developments of mechanical tissue models we studied macroscopic and microscopic aspects at multiaxial loading conditions in vitro. In order to monitor the material's state of transformation in terms of cell orientation, an appropriate optical analysis method was developed. Since cell orientation has a profound effect on the mechanical response of cell seeded matrices texture studies were conducted in these structures. It will be demonstrated that cell orientation is guided by the distribution of the mechanical tension in the tissue.

9.2 Experimental setup

We used a fibroblast seeded collagen matrix as model (Bell et al. 1979; Trzewik et al. 2004b) studying the ability of fibroblasts to reorganize and contract collagen matrices in vitro. Appropriate biological protocols and engineering tools to monitor cell orientation were developed. This chapter describes an in vitro method for quantitative analysis of the orientation of live 3T3 NIH fibroblasts within a collagen based tissue construct (at difficult optical conditions) based on confocal microscopy.

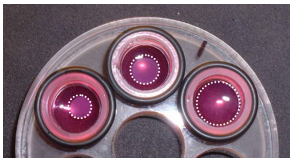

Figure 9-1 Freely floating fibroblast seeded collagen matrices (FCM) inside CellDrums consisting of 16mm in diameter cylinders and a 1µm membrane. The border of the tissue construct was marked with white dots. Matrix shrinkage due the cellular remodelling and force development is clearly visible in the reduction in diameter of the construct.. The figure shows the same construct at day 4 (far left), day 2 (middle), and right after gelation and cell seeding (initial cell density 1 x 10^5 cells/ml) (right).

Figure 9-2 Uniaxial loading device. The FCM (pink) is connected to parallel walls via Velcro® rods (white arrow), where the left wall was fixed and the right wall can be pulled to the right. The FCM was strained by at maximum 5% after gelation (3T3 fibroblasts were labelled with cytoplasmic fluorescent dye and added to the gel at a final concentration of 1 x 10^5 cells/ml).

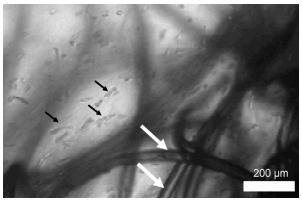

Figure 9-3 Brightfield micrograph of a randomly chosen x-y plane within the matrix right at the border of a Velcro® rod fixed FCM. The Velcro® rods binds to the collagen matrix after gelation, providing a strong and reliable connection. Clusters of fibroblasts (black arrows) were distributed within the collagen in the vicinity of the Velcro® rods (white arrows). Velcro® rods out of focus can be seen as blurred structures in the background. Individual cells were undetectable in this setup.

The tissue constructs were prepared as described in capter14.2. After gelation, this resulted in a laterally fixed (Velcro® enhanced CellDrum) or freely floating (Figure 9-1; normal CellDrum) circular gel, respectively, approximately 1mm in thickness. A uniaxial mechanical loading chamber (Figure 9-2) was used to prepare freely floating but uniaxially strained collagen gels. After adding culture medium, all samples were incubated at 37° C and 5% CO_2 in humidified incubator. Culture media were changed daily.

9.3 Microscopic analysis

The cell orientation was determined with a confocal laser scanning microscope (LSM 510, Zeiss, Oberkochen, Germany), 10x objective lens (LD-Achroplan, Zeiss) using integrated data processing software (LSM 3.0, Zeiss) in fluorescence mode.

Analysis was performed on multiple collagen matrices seeded with 3T3 fibroblasts labeled by fluorescent cytoplasmic dye (Celltracker Green CMFDA, Molecular Probes, Leiden, Netherlands).

These dyes are fluorescent chloromethyl derivatives that freely diffuse through the cell membranes of live cells. Once inside the cell, these mildly thiol-reactive probes react with intracellular components producing cells that are both fluorescent and viable for at least 24 hours. A series of images with a stack size of typically 200 slices (each 1-4 µm thick) dissecting the collagen matrix along the z-axis (perpendicular x-y-plane) was obtained providing information on the cellular spatial orientation.

9.4 Isotropicity and anisotropicity of cell distribution

After gelation, cells adhere to the collagen fibers and start to reorganize within the matrix. The gel's plane surface represents the x-y-plane. In order to visualize location and orientation of the cells inside the gel, a new procedure based on confocal imaging was introduced (Trzewik et al. 2004a). 3D confocal images were taken 48 h after gelation and cells were coded in pseudo colors according to their depth inside the gel. The colors encode the location of the cells in z-direction (depth) below the gel's surface. Dark red marks top cell, and dark blue bottom cells. If a cell is uniformly colored, then its orientation is stretched out solely in the x-y-plane and does not extend into the z-direction.

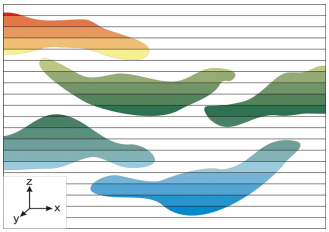

Figure 9-4 : Schematic cut through a cell seeded collagen gel with depth encoded cells using pseudo colours.

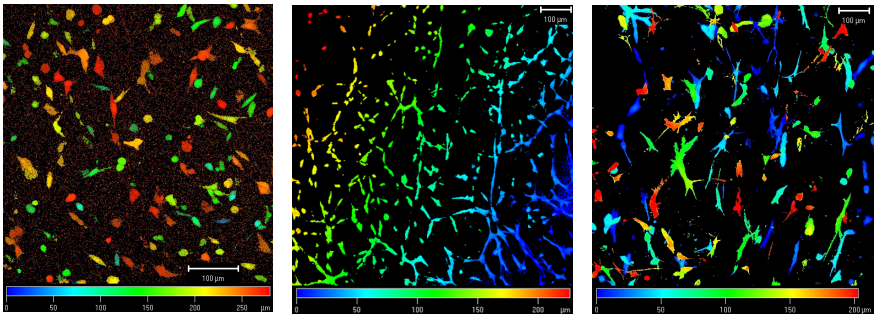

Figure 9-5 Depth encoded 3-dimensional distribution of 3T3 fibroblasts dyed with Cell-Tracker™. The gel's surface represents the x-y-plane. The colours encode the location of the cells in z-direction (depth). Dark Red represents top cells and dark blue bottom cells, respectively (see color bar). Left: Center portion of a freely floating, circular collagen gel with randomly distributed cells in different planes. Middle: Same gel but at the edges of the collagen matrix. Due to the color encoding a curvature in the gel becomes visible, which is as well seen on a macroscopic scale at zero magnification (gel bending). The right Image displays a biaxially fixed gel with random cell orientation.

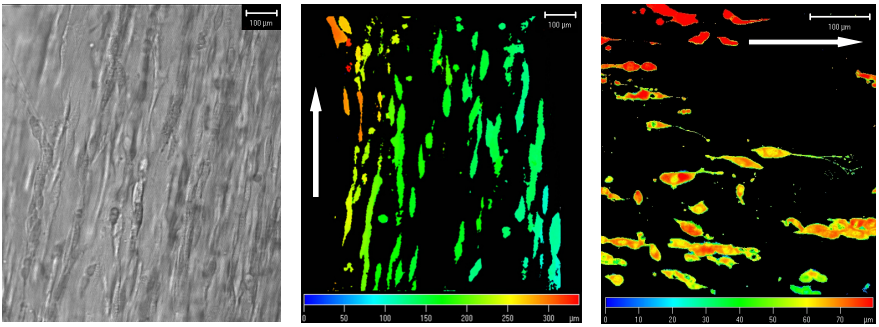

Figure 9-6 Depth encoded 3-dimensional distribution of Celltracker™ dyed 3T3 cells in a uniaxially strained matrix (middle), compared to a brightfield image of cells in the setting (left). The right image displays an uniaxially strained gel at higher magnification and higher dissection resolution. Individual protrusions became visible, growing in parallel to the principal strain directions. The direction of strain is indicated by white arrows.

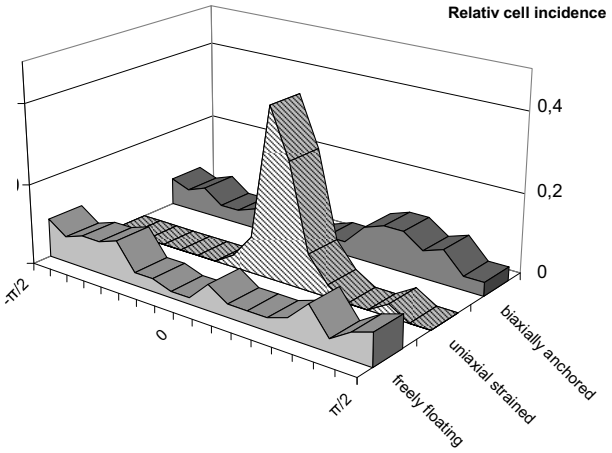

Figure 9-7 Angular cell orientation distribution at different boundary conditions. The orientation was analysed in the plane parallel to the gels's surface. Zero degree describes cells stretched out in the direction of the major strain at uniaxial loading. Zero degree at biaxial loading describes cells in the direction of a freely chosen orientation vector. It is clearly visible that in freely floating as well as in biaxially anchored situations the cell orientation is isotropic. Whereas uniaxial loading leads to cell orientation into the direction of the y-axis, e.g. the direction of strain. Only minor angular aberrations were observed.

Our observations indicated that fibroblasts in freely-floating gels were randomly distributed. However, the major plane of growth must not be necessarily parallel to the x-y plane as displayed in Figure 9-5 (left and middle). The orientation of biaxially fixed cells (Figure 9-5 right) was

randomly distributed in the x-y-plane, but there was no tendency to grow perpendicularly along the z-direction, out of the plane of tension. A different situation occurs in collagen gels which were strained by 5% after gelation. The cells were elongated and oriented in the direction of the externally applied stress (Figure 9-6), but did not spread out of the x-y-plane, which is again parallel to the plane of tension. The use of fluorescent stained live cells in combination with a confocal microscope enabled acquiring depth encoded information on the orientation of cells in three dimensions. As an application of this method, we showed some effects of mechanical stress on cell orientation. The experimental approach of uniaxially strained, rectangular cell seeded collagen gels has a direct influence on the distribution and orientation of cells within the collagen matrix. It must be noted that uniaxial test devices exhibit active remodeling impact on the test specimen. Uniaxial stress conditions are rarely seen in vivo, except for structures like tendons, whereas biaxial stress conditions are highly frequent in the body as for example in skin. In biaxially cell seeded collagen matrices attached to the CellDrum wall, which will be used in further investigations, it appeared reasonable assuming an isotropic distribution of cell orientation in the x-y plane. Since there were no measurable cellular protrusions into z-directions and therefore there exist no major traction forces which would thin out the membrane, we assumed an almost constant collagen thickness during the time of cultivation. This assumption was proven by additional measurements on the cell seeded collagen matrix thickness which will be discussed in detail in chapter 12.

10 Dynamic measurement of lateral tension in tissue equivalents

Previous chapters described the necessary considerations for measurement of biomechanical properties in tissue equivalents. The measurement idea (Figure 6-6) was briefly introduced in chapter 6 and will be subsequently discussed in detail here. The dynamic determination of lateral tension in thin film tissue equivalents offered the possibility to avoid problems related to the short supply of tissue constructs and difficulties in handling the setups proposed so far.

In the CellDrum concept, the inner side of the membrane was coated with a collagen gel seeded with living cells, making up an artificial tissue construct after gelation. Typically, 800 µl of cell culture medium were poured on top of the gel and monitored by media colour. The silicon membrane was removed before the measurement to avoid any effects of gel to silicon interactions. After exciting membrane oscillations with a sound pulse, resonance oscillations occurred. Amplitude and frequency were measured to calculate the lateral tension of the tissue construct. Oscillation was monitored as a function of time in a non-contact way with a laser-based sensor (LK-031, KEYENCE GmbH, Neu-lsenburg). For membrane displacement sampling a data acquisition device was used (DAQ 6020 E, National Instruments, Austin, USA) at a sampling rate of 1 kHz and a resolution of 1 µm. Data processing including Fast Fourier Transformation(Cooley & Tukey 1965) (FFT) applying Hanning Windows, for precise frequency weighting was accomplished using our own software based on Lab View VI (National Instruments, Austin, USA). Only the fundamental vibration mode of the oscillating membrane was considered. Analysing the response frequency spectrum by FFT algorithm, we ensured that the entire membrane moved in phase in the fundamental (0,1) mode (chapter 10.4). Any potential ablation or abnormal oscillation of the collagen matrix would cause significant changes in the frequency spectrum. In such cases the data were discarded.

10.1 Modeling of rectangular and circular membranes

Finite element analysis: For finite element analysis the MSC Patran 2001R3 and NastranV707 software (MSC.Software Corporation, Santa Ana, USA) were used. Two principal models were analysed: 1) an uniaxial stretched rectangular membrane resembling tissue constructs of other authors (Brown et al. 1998; Eastwood et al. 1994; Kolodney & Wysolmerski 1992) and 2) a planar, concentrically stretched circular membrane as used in this work. As for the membranes, an Elastic modulus of 2.5 MPa (as for comparison: 210 GPa for steel!) and a Poisson's ratio of 0.49 were assumed (Marquez et al. 2005). For calculations, a linear, elastic approach and a freely scalable

unit-force at the boundary nodes being either uniaxial or concentrical were applied. The resulting pseudo-colour images (Figure 10-1) indicate the levels of the von Mises stress (identical colours represent the same stress levels).

Finite element analysis (FEM) was carried out using an uniaxially mechanically loaded elastic, rectangular strip versus a circular, concentrically loaded membrane as used in the CellDrum. At the same load and otherwise same assumptions on the material properties, the relative von Mises stress distribution in the strip varied from $8*10^{-5}$ to $1.4*10^{-4}$. Thus, the relative von Mises stress varied by almost 75%. The circular membrane instead showed almost no variation all over its area. Variances along the circumferential border of the membrane model result from theoretical force transmission points which became visible because of the limited number of boundary points considered in our calculations.

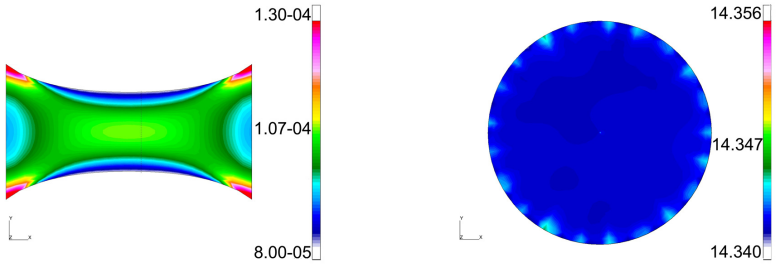

Figure 10-1 Color encoded von Mises stress distribution in a rectangular stretched membrane (left) as compared to a concentrically stretched circular membrane.

10.2 Cell orientation – isotropic/anisotropic behaviour

For adhesion on planar substrates, cultured cells usually adopt a flat morphology and cell traction is exerted onto the surface in a way that is essentially tangential. Therefore, the force vectors can be assumed to be two-dimensional in the plane of the substrate surface (Schwarz et al. 2002). An additional consideration regarding cell orientations allowing substantial simplification of the model should be taken into account. Since the deformation in thin cell seeded collagen film is biaxial the orientation of cells was homogeneously distributed (a tissue construct was called thin when its thickness was much smaller than the CellDrum`s diameter). This has already been proven to be true for 3D-Gels (chapter 9).

10.3 Theoretical considerations

In order to calculate the tension of the tissue construct we assumed a two-dimensional circular membrane oscillating at its fundamental frequency after excitation. This assumption appeared to be feasible since the tissue constructs were very thin. Furthermore, the tissue constructs can bend and fold easily and they have a low stiffness. Mechanically speaking they fulfill the requirements for real membranes. Thus, we assumed a stretched compound membrane (i.e. collagen matrix plus cellular construct) with a tension T in N/m and a density σ in kg/m^2. As preceding measurements showed, the damping ratio D in our system was typically between 0.02 and 0.07. Since this was <<1, the frequency shift due to damping was neglected.

10.4 Vibrational Modes of a Circular Membrane

There are two different kinds of vibrational mode shapes of a circular membrane. The nomenclature for labeling the modes is ***(m,n)*** where ***m*** is the number of nodal diameters and ***n*** is the number of nodal circles. Mode (0,1) in Figure 10-2 shows the fundamental mode shape of a vibrating circular membrane. The mode number is designated as **(0,1)** since there are no nodal diameters, but one circular node (the outside edge). The (0,1) mode, when the whole membrane moves in phase, is observed when the membrane is excited at its center. Since it radiates sound waves very well when vibrating in this manner, the membrane also transfers its vibrational energy effectively into sound energy and the vibration declines fast.

Asymmetric excitation induces vibrational mode shapes with nodal diameters (e.g. mode (1,1)) or superimposed shapes with circular and diameter nodes (e.g.mode(1,2)).

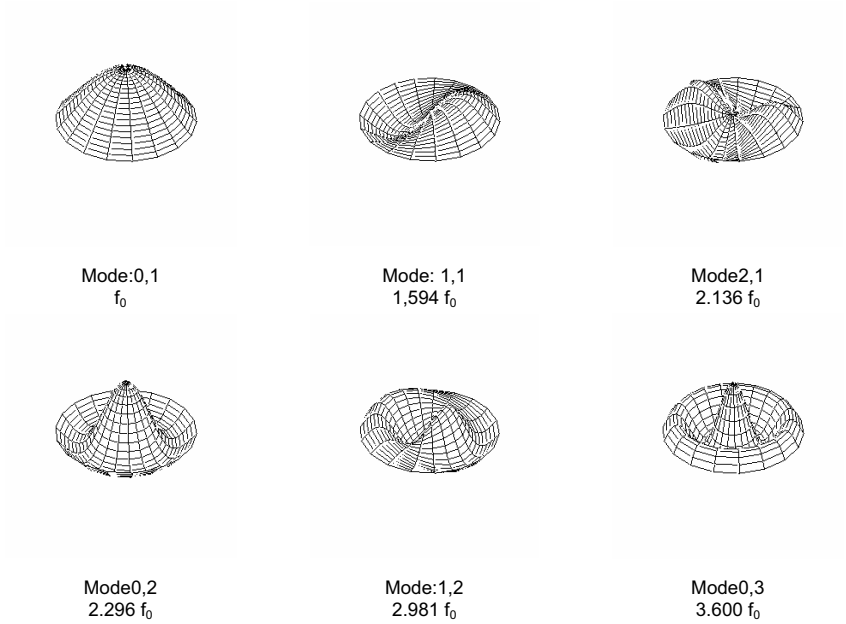

Figure 10-2 Typical vibration modes of an ideal membrane as published earlier (Rossing & Fletcher 1994). The mode designation (m,n) and the relative frequency are indicated below each figure.

Any variations of the vibration mode out of the fundamental or (0,1) mode respectively, would shift the membrane's oscillating frequency to higher values. Vibrational modes with nodal diameters (e.g. mode 1,1) typically are introduced by an asymmetric excitation of the membrane. To avoid any misinterpretation of the measured frequencies it was necessary to ensure that the membrane was properly excited and oscillated in the (0,1) mode. Proper excitation was investigated by the visualization of the pressure pulse. Figure 7-9 on page 39 demonstrates that there were no turbulences detected within the dynamic analysis system. Thus, it was reasonable to assume, that the membrane excitement led to an oscillation in the fundamental mode. Because of the importance of this particular point, further investigations were accomplished to ensure that the entire membrane moves in phase. Thus, we measured directly the membrane indentation after excitation along the membrane's diameter (data not shown). The measurements ensured that the membrane moved in

phase. As a kind of third check, FFT analysis, embedded in the measurement software, revealed that there was no second and higher order resonances observed.

10.5 Elastic membrane model

Already Rayleigh performed detailed work on small vibrations of elastic membranes (Strutt & Baron Rayleigh 1894). This study was based on books published later on (Nowacki 1972; Nowacki 1974; Graff 1975).The solutions lead to cylindrical functions (Bessel's equations), as described by Jahnke (Jahnke et al. 1966) and Abromowitz (Abromowitz & Stegun 1965).

The differential equation of a pre-stressed, homogeneous membrane of the thickness h and at the pressure p was

$$T\nabla^2 w + p = \rho h \ddot{w} \qquad \text{Formula 10-1}$$

where T was the pre-stress and w the central indentation.
In this equation, ρ represents the mass density and T a line force per length. With the Laplace-operator in polar coordinates r, θ

$$\nabla^2 = \frac{1}{r}\frac{\partial}{\partial r}\left(r\frac{\partial}{\partial r}\right)+\frac{1}{r^2}\frac{\partial^2}{\partial \theta^2} = \frac{\partial^2}{\partial r^2}+\frac{1}{r}\frac{\partial}{\partial r}+\frac{1}{r^2}\frac{\partial^2}{\partial \theta^2} \qquad \text{Formula 10-2}$$

we get

$$T\left(\frac{\partial^2 w}{\partial r^2}+\frac{1}{r}\frac{\partial w}{\partial r}+\frac{1}{r^2}\frac{\partial^2 w}{\partial \theta^2}\right)+p(r,\theta,t) = \rho h \frac{\partial^2 w(r,\theta,t)}{\partial t^2} \qquad \text{Formula 10-3}$$

Wave velocity: $c = \sqrt{T/\rho h}$ respectively $c^2 = T/(\rho h)$

Boundary condition: $w(r = r_a, \theta, t) = 0$

Free vibrations with $p(r,\theta,t) = 0$:

A product approach according to Bernoulli (with $i = \sqrt{-1}$)

$$w(r,\theta,t) = R(r)\Theta(\theta)Ae^{i\omega t} \qquad \text{Formula 10-4}$$

leads to

$$c^2\left[\left(\frac{\partial^2 R}{\partial r^2}+\frac{1}{r}\frac{\partial R}{\partial r}\right)\Theta+\frac{1}{r^2}\frac{\partial^2\Theta}{\partial\theta^2}R\right]Ae^{i\omega t} = -\omega^2 Ae^{i\omega t}$$

This partial differential equation is valid for all times, if (after cancelling with $R\Theta$)

$$\frac{1}{R}\left(\frac{\partial^2 R}{\partial r^2}+\frac{1}{r}\frac{\partial R}{\partial r}\right)+\left(\frac{\omega}{c}\right)^2 = -\frac{1}{\Theta}\frac{1}{r^2}\frac{\partial^2\Theta}{\partial\theta^2} \qquad \text{Formula 10-5}$$

is valid. Because the solution is in θ periodical, with $n \in N$ we can arrange $\Theta(\theta) = \alpha e^{in\theta}$, which results with $\frac{\partial^2\Theta}{\partial\theta^2} = -n^2\Theta$ for R in the common differential equation

$$\left(\frac{\partial^2 R}{\partial r^2}+\frac{1}{r}\frac{\partial R}{\partial r}\right)+\left[\left(\frac{\omega}{c}\right)^2-\left(\frac{n}{r}\right)^2\right]R = 0 \qquad \text{Formula 10-6}$$

This is a Bessel's equation of order n with the solution

$R(r) = BJ_n(\varpi r)+CY_n(\varpi r)$

with $\varpi = \frac{\omega}{c}$ and the cylindrical functions J_n, Y_n of first and second form. Because of $Y_n \to \infty$ for $r \to 0$ it has to be $C = 0$. W.l.o.g. it is set $\alpha = 1$.

From the boundary conditions, the frequency equation $R(r_a) = BJ_n(\varpi r_a) = 0$ follows. Next to the trivial solution $\varpi r_a = 0$ the following results appear:

$n = 0$: $\varpi_{01} r_a = 2.405$ $\varpi_{02} r_a = 5.520$ $\varpi_{03} r_a = 8.654$ $\varpi_{04} r_a = 11.792$ $\varpi_{05} r_a = 14.931$ …

$n = 1$: $\varpi_{11} r_a = 3.832$ $\varpi_{12} r_a = 7.016$ $\varpi_{13} r_a = 10.173$ $\varpi_{14} r_a = 13.324$ $\varpi_{15} r_a = 16.471$ …

$n = 2$: $\varpi_{21} r_a = 5.136$ $\varpi_{22} r_a = 8.417$ $\varpi_{23} r_a = 11.620$ $\varpi_{24} r_a = 14.796$ $\varpi_{25} r_a = 17.960$ …

$n = 3$: $\varpi_{31} r_a = 6.380$ $\varpi_{32} r_a = 9.761$ $\varpi_{33} r_a = 13.015$ $\varpi_{34} r_a = 16.223$ $\varpi_{35} r_a = 19.409$ …

Resonance frequencies:

$$f_{nm} = \frac{\omega_{nm}}{2\pi} = \frac{\varpi_{nm} r_a c}{2\pi r_a} = \frac{\varpi_{nm} r_a}{2\pi r_a}\sqrt{\frac{T}{\rho h}} \qquad \text{Formula 10-7}$$

Shapes of natural oscillations:

$$w_{nm}(r,\theta,t) = J_n(\varpi_{nm} r) e^{in\theta} A e^{i\omega t} \qquad \text{Formula 10-8}$$

In this equation n is the number of radial modes.

Fundamental frequency: $f_{01} = \frac{\varpi_{01} r_a}{2\pi r_a}\sqrt{\frac{T}{\rho h}} = \frac{2.405}{2\pi r_a}\sqrt{\frac{T}{\rho h}}$ Formula 10-9

Thus, the initial lateral tension *T* can be measured.

The effect of density variations due to matrix condensation

The density of the collagen matrix was considered constant ($\rho \approx 1$ g/cm^3 or cm^2 respectively; constant temperature). We also considered that even a shrinkage of the gel by 1000% which would be accompanied by an increased collagen concentration from typically 0.3% to 3% (1.003 g/ cm^3 to 1.03 g/ cm^3) would lead to a negligible change of the resonance frequency since $f \sim 1/\sqrt{\rho}$. A 10-fold shrinkage, however, would only appear in freely floating gels but not in circumferentially fixed ones, as it is the case in the CellDrum. Since the cell orientated mostly horizontally within the collagen matrix (chapter 9) our measurement showed only a typical shrinkage of about 10% of the total thickness during the cultivation period (Figure 12-6).

Further implementations

It is generally known that the resonance frequency for highly dampened oscillators correlates with the systems damping coefficient. Higher damping leads to reduced resonance frequency. Therefore, the damping in our system must be debated. Principally, we need to consider three damping mechanisms:

- Air damping: identical in all samples, can be neglected.
- Damping due to the water column on top of the gel, there was no water column during the measurements; the effect can be neglected
- Internal damping (viscous effects inside the collagen membrane): In our system with the materials used, there was definitely a damping observed. However, the damping ratio was very small (typically D= 0.02-0.07). Damping ratio factors being <<1 allows in a first approach the assumption of an undamped system. Furthermore, no damping values, received during the experiments could be related to the viscous-elastic properties of the investigated cell seed collagen membranes. The damping values did not vary significantly in correlation with the experimental treatment of the cell seeded matrices. It appeared reasonable to assume that the damping effect can be related to air damping alone. Membranes radiate sound very well when vibrating in the fundamental (0,1) mode. The membrane transfers its vibrational energy effectively into sound energy and the vibration declines.

10.6 Experimental protocol:

After the fibroblasts had been cultured for at least 24 h, the CellDrum was removed from the holder, rinsed with cell culture media containing 10% FCS and placed into the cell tension analyzer for tension measurements. Afterwards the CellDrum containing the tissue construct was submerged for at least 1h in fresh media containing stimulants or other chemicals described above at the desired concentrations. All experiments were performed at sterile conditions.

Experimental reagents

Cytochalasin D was dissolved in dimethylsulfoxide (DMSO) and stored at -20 °C. Before use the final concentration was adjusted with DMEM. Experiments with fetal calf serum (FCS) were carried out using one and the same aliquot of FCS throughout all experiments (Biochrom, Berlin, Germany).

Statistics:

Each individual measurement was repeated at least 10 times with a given sample. Numerical results were presented as means ± SD. A two-tailed Student t-test was used to determine statistical

significance of the difference between treated and untreated groups. Differences were considered statistically significant at $p < 0.01$.

10.7 Experimental results

Oscillating circular tissue constructs exhibited an almost ideal harmonic oscillation (Mode: 0,1) at a fundamental frequency (Figure 10-3). These oscillations with initial amplitudes of typically 100 µm showed a damping ratio D of about 0.03 (D<<1). Thus, it appeared reasonable to neglect a frequency shift due to damping. The fundamental oscillation frequencies depended on material properties of the gel and varied in between 20 to 50 Hz. Measurements performed right after pouring the gel, when it was still liquid-like, were possible. However, due to the partial onset of gelation the frequencies of subsequent measurements showed high variances. Acceptable data in terms of accuracy and variance could be first performed at about 0.5 h after pouring the fibroblasts-in-collagen solution into the CellDrum. Frequency data obtained from that time on became highly reproducible with a typical coefficient of variation between 0.01% and 1%.

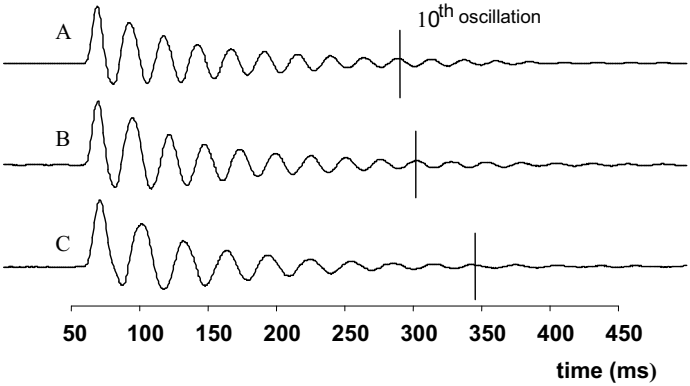

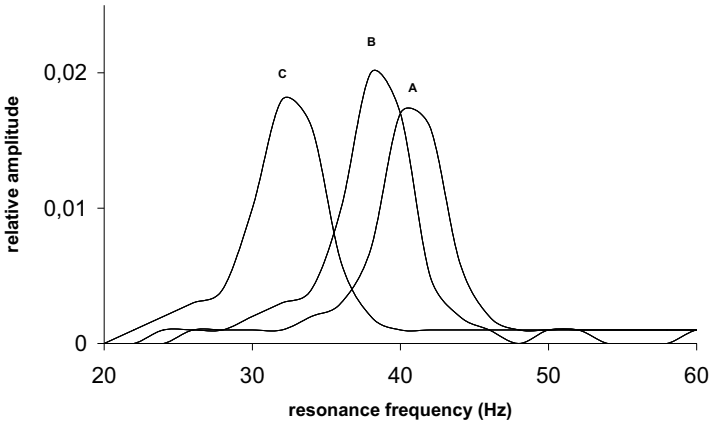

Figure 10-3 Top: Typical oscillations of a 1 mm thick collagen I gel seeded with 3T3 fibroblasts (seeding cell concentration $5x10^5$ cells/ml) at day 4 of culture. Curve A) represents a sample cultured with media containing 10% FCS. Curve B) same gel but exposed to media with no FCS, thus reducing cell contractility. This results in a shifting of the oscillation frequency to lower values. C) Same gel, however, no FCS and 1h of treatment with 10 μM cytochalasin destroying the cellular cytoskeletons. Oscillation frequencies were distinctly different. For direct comparison, the end of the 10th oscillation is marked in the figure. Bottom: Fast Fourier transformed signals of the same data. Clearly, the three major frequencies were identified.

Figure 10-3 shows plots of a 1 mm thick collagen I gel seeded with 3T3 fibroblasts at day 4 of culture. Curve A represents an untreated tissue construct (control) at 10% FCS. Subsequently, FCS was withdrawn from the sample for 60 min (curve B). A frequency shift to lower frequencies was observed due to the reduced stress fibroblasts imposed on the gel. After the cellular cytoskeletons have been destroyed by 10 μM cytochalasin D for 60 min (Curve C) stress was released further as indicated by the lowered frequency. After FFT analysis of the signals major frequency peaks were found at 40.9 Hz (curve A, control, 10% FCS), at 38.5 Hz (curve B, 60 min without FCS) and at 32.6 Hz (curve C, cytochalasin D treatment). The accuracy of frequency measurements based on FFT was at +/- 0.25 Hz.

Build up of lateral tension over time

To investigate the effects of proliferating fibroblasts on the build-up of lateral tension over a period of 13 days, a gel was seeded with 3T3 fibroblasts and stress measurements were taken at distinct time intervals (Figure 10-4).

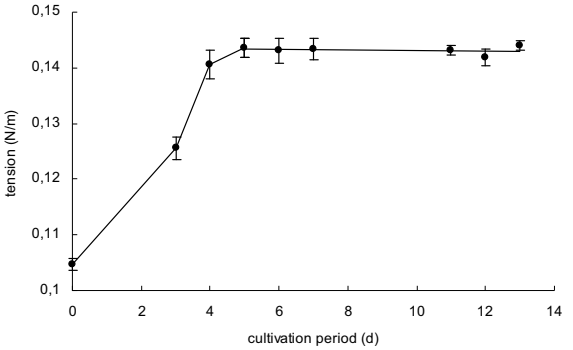

Figure 10-4 Lateral tension as a function of culture time of a 1 mm thick collagen I gel seeded with 3T3 fibroblasts at $5x10^5$ cells/ml. The tension increased within the first 4 days and reached a plateau afterwards.

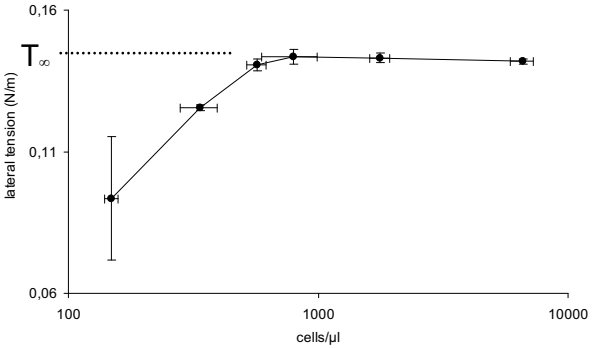

Figure 10-5 The cell number correlated almost linearly with the lateral tension of these gels below a cell concentration of 1000 cells/µl (day four). Remarkably, the tension remained almost constant although cell continued to proliferate.

During the first four days, the stress increased steadily and considerably, and then a plateau was reached. This build-up of stress correlated with the actual cell concentration in the gel. As can be seen in Figure 10-5, the stress increased until a cell concentration of 1000 cells/µl had been reached at day four. Afterwards, the cell concentration increased continuously. The stress, however, did not enhance further. This allows an interesting conclusion based on Figure 10-6. ECM rearrangement during culturing, the build up of the cells own ECM replacing and remodeling the Collagen I with time and increasing cell density lead to lower average tension per cell in the tissue construct. The curve in Figure 10-6 does not approximate zero tension, because all tissues have intrinsic residual tension even when they are not fixed at their rim (Fung 1993). It must approach a final value which is unknown so far, since the experiment had to be interrupted. Furthermore, the curve must have a maximum at very low cell densities. We assume that the collagen I gel forms a rather stiff substratum after gelation. After matrix remodeling this was changed and cells created their own natural environment.

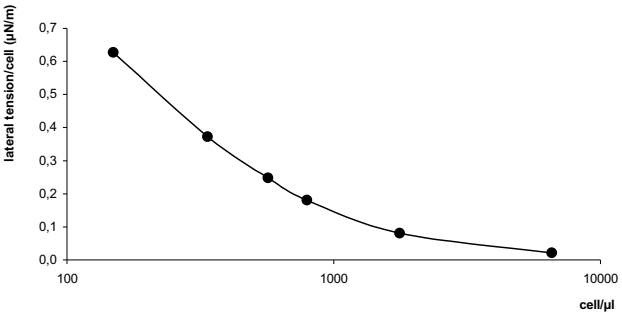

Figure 10-6 Average tension per cell as function of cell density (culture time). The dotted line represents the expected infinite average tension per cell.

Chemical stimulation of cellular tension

The CellDrum principle was applied for the detection of chemical effects on cell tension. Figure 10-7 represents lateral tension obtained at various subsequent treatments of a 1 mm thick collagen I gel cultured with 3T3 fibroblasts at 10% fetal calf serum (FCS) performed at day 4 and 5 of culture, respectively. Withdrawal of FCS led to a significant decrease of tension by 10.5%. After re-introducing media containing fresh FCS at 10% for 1h the lateral tension had increased by 8% relative to the control. Adding FCS at a final concentration of 20% for 1h, the membrane tension exceeded the control level by, in fact, 14%. After cytochalasin D was added, this tension was decreased by 32% as compared to the control level. After 24 h of cytochalasin D action, however, the tension reached 42% below control.

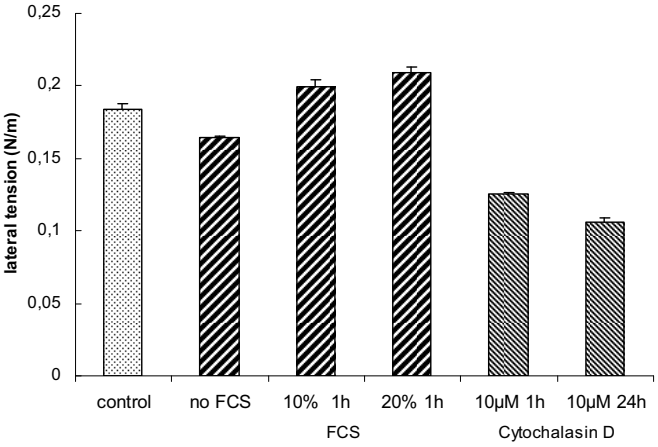

Figure 10-7 Typical lateral tension at various subsequent treatments of a 1 mm thick collagen I gel seeded with 3T3 fibroblasts at 10% fetal calf serum (FCS) performed at day 4 and 5 of culture, respectively. The measurements and drug exposures were performed at day 4 of culture only the measurement of 24 h incubation with cytochalsin D was preformed on the following day (day 5). Each column represents the average of 10 measurements. The subsequent treatments applied to the same gel as well as duration of the treatments are indicated in the figure.

Micro morphological evaluation

Micro-morphological studies were used to evaluate and compare experimentally received data concerning the mechanical properties of tissue constructs.

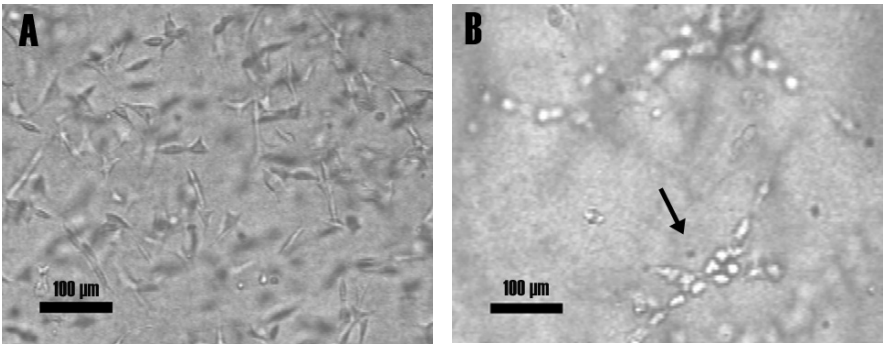

Figure 10-8 Microscopic images of 3T3 fibroblasts in a randomly chosen focal plane within a collagen matrix, at day four of culture. (A) Cells shown by arrow look healthy and well attached to the fibrous extracellular matrix. (B) The same gel after 24h of treatment with 10 µM cytochalasin D. Cells (arrows) aquire a round shape and most are dead. This explains the rapid loss of cell tension after cytochalasin.

The effect of cytochalasin D was visualized microscopically (Figure 10-8). At day four of culture the cells looked healthy and well attached to the fibrous extracellular matrix (Figure 10-8a). The cells appeared randomly distributed and seemed to assume orientations in parallel with the silicon membrane. After treating the same gel for 24 h with 10 µM cytochalasin D (Figure 10-8b) the cells auired a round shape. Dead cells and the ECM alone remained left, which still keep a considerable amount of residual tension.

10.8 Discussion

In this work we present a novel method for measuring lateral tensions in thin film tissue constructs (Figure 10-3). It is based on a drum like design where a thin circular collagen membrane seeded with fibroblast constitutes the tissue construct. Any change in the mechanical properties of this "compound membrane" made of proteins and cells translates into changes of the resonance frequency of the oscillating membrane.

Devices and methods reported previously were able to monitor mechanical properties of tissue constructs (Brown et al. 1998; Eastwood et al. 1994; Eschenhagen et al. 1997a; Kasugai et al. 1990; Kolodney & Wysolmerski 1992). Although the data reported might have been quite reproducible, they were of limited value. As our finite element models revealed, the tension distributions within uniaxially loaded tissue constructs varied by 75% of von Mises tensions within the same gel (see chapter 10.1).In contrary, the principle used here is based on uniform and homogeneous stress distributions within the tissue construct (chapter 9). Thus, it was reasonable to assume that during the sound pulse excitation cells within the tissue construct were exposed to almost identical stress levels in all over the membrane.

To seriously address this "mechanical boundary condition" is very important. This is not only important from a point of view of biomechanical engineers but also for biologists interested in protein and gene expressions studies (Huang et al. 2002; Langholz et al. 1995) of tissue constructs under mechanical load. The activity of a cell is regulated, in part, by changes in the mechanical environment in which it resides (Eastwood et al. 1998; Wakatsuki et al. 2000). A tension over culture-time plot of fibroblast in a collagen I gel is shown in Figure 10-4. During the first four to five days tension increased with time whereas it remained unchanged afterwards which is in good agreement with previous findings (Feng et al. 2003). At day five the tension had reached a plateau of approximately 0.143 N/m and the cell density was 750 cell/µl (Figure 10-5). At later times cells continued proliferating. At day twelve there were as much as 12600 cells/µl counted. This finding must be further explored. It might help in answering some questions on how fibroblasts interact with the extracellular matrix in wound contraction (Tejero-Trujeque 2001) and whether there is a threshold tension T_∞ at which fibroblasts stop proliferating.

Some of these results correlated well with various direct force measurements based on independent methods. It has been shown before that there was a linear elevation in the tension as generated by fibroblasts in stabilized, tethered collagen lattices which closely correlated with cell attachment and spreading (Delvoye et al. 1991; Eastwood et al. 1994; Kasugai et al. 1990; Kolodney & Wysolmerski 1992). Once this pre-stress was established, it was maintained at a relatively constant level over a long period of time (Tomasek et al. 2002). Fig 9-6 shows the average tension per single cell. Obviously cells during culturing do not only remodel the ECM surrounding them, they as well rearrange their micro-mechanical environment at which they can exist properly. In Figure 10-5 a threshold line T_∞ is indicated. This line would assign a lateral mechanical tension, which would be exerted inside a tissue construct cultured for much longer than the time chosen here. This value would mark the optimum mechanical tension per cells in a cultured tissue construct. Whether this

exists or not and how large it really is cannot yet be decided based on the measurements above. Much longer culture times are obviously needed to decide about this question. This kind of information, however, is very necessary in tissue engineering, as a mechanical parameter for tissue construct conditioning as for example in artificial skin culturing.

Thus, the usage of planar circular membranes for studying lateral tensions in flat tissue constructs, provides valuable insights in biomechanical aspects of tissue culturing.

Culture of fibroblasts within a three-dimensional type I collagen gel is generally considered as a model tissue construct and is widely used to study cellular responses to the extracellular matrix related conditions (Bell et al. 1979; Elsdale & Bard 1972b; Zigrino et al. 2001). In those studies, the ability of cultured fibroblasts to reorganize and contract three dimensional collagen I gels were regarded as an in vitro model for the reorganization of connective tissue during wound healing. Time course experiments were performed where the reduction of the diameter of the collagen lattice due to forces induced by embedded fibroblasts was used as one of the experimental parameters (Figure 9-1). However, such unstrained gels must be considered as mechanically completely different models to study mechanically regulated cellular processes. In a living organism almost all tissues are composed in a way that cell contraction will inevitably increase stress in the surrounding matrix. This feedback mechanical signal is missing in floating circumferentially unconstrained collagen lattices (Tomasek et al. 2002). Moreover, the fact that fibroblasts were allowed to freely contract the gel does not allow the conclusion that the tissue assumed a zero stress state - the actual stress in such contracted gels is simply unknown (Liu & Fung 1988; Fung 1986). As an alternative we kindly suggest the usage of mechanically defined gels as described here.

A series of experiments with collagen I - fibroblast gels have been conducted to test the reliability of the measurement principle. The effects of well investigated substances with an impact on the tension developing apparatus of fibroblasts like cytochalasin D and Fetal Calf Serum (FCS) were studied (Boswell et al. 1992; Eastwood et al. 1994; Wakatsuki et al. 2000). FCS, like most agonists for non-muscle or smooth muscle contraction, stimulates the generation of contractile force (Kolodney & Elson 1993). Adding FCS to the cell culture medium, the lateral tension in the gel was enhanced. The gel became stiffer and the resonance frequency was higher (Figure 10-3 and Figure 10-7). In this study, the contractile properties of FCS could be confirmed and the tension induced was measured with high accuracy.

The relaxation effect of cytochalasin D on the tissue construct is shown in Figure 10-7. The integrity of the actin cytoskeleton is essential for force generation and maintenance. Disruption of actin microfilaments due to cytochalasin D action results in rapid relaxation of forces reducing the

tension within the gels (Eastwood et al. 1994; Kolodney & Wysolmerski 1992). After adding 10 µM cytochalasin D, significant reductions of the resonance frequency (Figure 10-3) and the lateral tension (Figure 10-7), respectively, were observed. The effect was highly significant after 1 h of treatment. However, it was not as fast as published previously (Kolodney & Wysolmerski 1992). It decreased further during the following 24 h.

The thin tissue constructs used here can be looked through, allowing microscopic observations of cells in their native environment. Figure 10-8 shows fibroblasts assembling in a collagen I gel. The figures show the typical shape of fibroblasts stretching out throughout the gel. The tethers of the cells were oriented in parallel to the membrane surface, confirming a fact that has been observed elsewhere (Takakuda & Miyairi 1996). These structural motives completely disappeared after cytochalasin D had been added for 24 h (Figure 10-8).

Unlike most devices introduced before, the system established here can easily be scaled up towards a high-throughput system providing simultaneous data of large numbers of various kinds of tissue constructs. The device can easily be operated under sterile conditions since all its components are autoclavable. This method and its implicated data acquisition and data processing software offers the opportunity to analyze further mechanical properties of tissue constructs. Further studies will focus on other material properties as storage and loss modulo, which indicate the portions of energy required to deform the tissue construct (Wakatsuki et al. 2000). In summary, the device introduced here may become a powerful tool to determine tensions in tissue constructs as well as a wide variety of material properties of soft tissues, gels and polymers in general. The method may also help in solving biomechanical questions involved in diseases, as for example Dupuytren's disease, where tension in the palmar fascia has been proposed as a key factor causing it (Citron & Hearnden 2003; Thurston 2003).

The necessity to derive mechanical properties in tissue constructs is undoubted. However, the dynamic measurement described offered the opportunity to analyse the residual stress in multiple tissue constructs in a short time. This technical approach may lead to high throughput tests in the future. However, the method was limited in its absolute resolution. A major factor causing this was due to the determination of the resonance frequency with FFT analysis. In chapter 12 we will show another technical solution with higher accuracy but lower sample throughput.

11 Steady state measurements: Self exciting myocardical cell layers

The popular use of complete cardiomyocyte monolayer cultures, even when cultivated on flexible silicon matrices (Komuro et al. 1990) had a major drawback so far: the major function in the heart, namely loaded isometric contraction could not be measured. In this chapter, we will present a method allowing us to undertake these kind of measurements (Artmann 2005b; Artmann 2005c; Artmann 2005a).

Cardiomyocytes from neonatal Wistar rats (Institute of Biochemistry, University Leipzig) were grown in flexible, circular collagen film membranes or directly on a thin (1µm) silicon membranes and exposed to strain in two directions (radial and circumferentially). This biaxial load mimics in vivo strain experienced by cardiac myocytes in the heart (Eschenhagen et al. 1997b; Zimmermann et al. 2000). The system consists of the CellDrum and, different from earlier approaches, uses mesh like anchors at the culture well periphery for cell and matrix attachment as described in chapter 5. Circular cell populated collagen gels were poured into the CellDrum on top of a flexible membrane or directly cultivated on the fibronectin coated membrane (Figure 11-1). The standard experimental setup (Figure 6-5) was modified. The cardiomyocyte seeded collagen matrix was pressurized with air and the centre deflection as a function of applied pressure was measured by a laser-based deflection sensor. This feature allows presetting the stress level on the cell externally. This is helpful to simulate the situation in vivo and furthermore essential for investigations focusing on stretch induced phenotypic changes, like hypertrophy. The relevant forces of spontaneously contracting hybrid cardiomyocyte-collagen films or monolayers, respectively, were measured as oscillating differential pressure change (typical amplitude ~1µN/mm^2) between the pressurised measurement chamber and the surrounding environment.

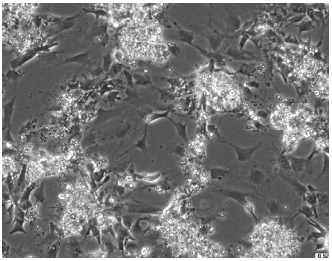

Figure 11-1 Neonatal rat cardiomyocytes grown at a subconfluent state

Experimental protocol:

Neonatal rat cardiomyocytes were seeded at a typical concentration of 2x10^6 cells/CellDrum in between two layers of collagen anchored with the CellDrum wall or directly onto the CellDrum membrane coated with fibronectin (30 µg/ml). The membrane deflection was actively defined and managed by the software controlled adjustment of the pressure inside the measurement chamber.

All experiments were performed under sterile conditions inside a humidified incubator at 37 °C and 5% CO_2. Prior to any measurements, the device was allowed to equilibrate any pressure differences introduced by temperature gradients due to the incubator opening and closing procedure.

Signal evaluation

When the cardiomyocytes start contracting, this intrinsic force leads to an oscillation of the pressurized membrane. Decreased volume due to cell contractions resulted in an increase of the pressure within the airtight measurement camber and visa versa. This differential pressure is measured to calculate the contractile forces in the tissue. The measured curves show an oscillating contraction signal superimposed with strong noise (Figure 11-3). This noise was filtered applying a Butterworth low pass filter. Calculations were performed using custom made software in Labview™ 7.1.

Theoretical considerations

The membranes used in the experiment are thin compared to their lateral dimensions or soft, fulfilling the requirements of negligible stiffness. A membrane is supported along its boundary and pre-stressed by the residual tension σ_0 introducing a homogenous stress distribution within the membrane.

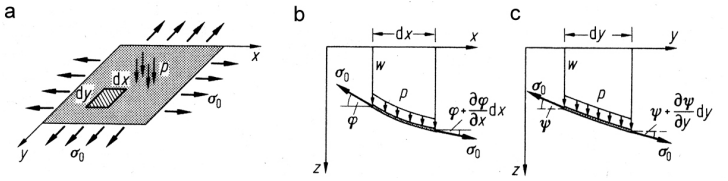

Figure 11-2 Schematic representation of a membrane under residual tension (a) and in its deflected position (b,c) from (Gross et al. 1995)

Any introduction of a perpendicular area load p(x,y) leads to an equilibrium in a deflected position. We assumed that the residual tension did not change due to the deflection and the membrane inclination is limited to small values. The sum of all forces in vertical direction can now be calculated:

$$\downarrow: \left(\sigma_0 t \frac{\partial \varphi}{\partial x} dx \right) dy + \left(\sigma_0 t \frac{\partial \psi}{\partial y} dy \right) dx + p\, dx\, dy = 0 \qquad \text{Formula 11-1}$$

Together with the angles $\varphi = \frac{\partial w}{\partial x}$ and $\psi = \frac{\partial w}{\partial y}$ we receive the Poisson's differential equation:

$$\sigma_0 t \left(\frac{\partial^2 w}{\partial x^2} + \frac{\partial^2 w}{\partial y^2} \right) = -p \qquad \text{Formula 11-2}$$

This equation can be solved for a circular membrane with the thickness *t* and radius *r* for its center deflection *w* in relation to the applied area load or pressure *p*.

$$p = \frac{4t\sigma_0}{r^2} w \qquad \text{Formula 11-3}$$

In this setup the laser sensor (resolution 1µm) could not detect any variations of the membrane deflection introduced by the contracting cardiomyocytes. Other parameters did not vary at the described experimental conditions and therefore it was reasonable to assume that any changes in the measured pressure *p* were directly related to the variation of residual tension introduced by the contracting myocytes.

$$\Delta\sigma_0 = \Delta p \qquad \text{Formula 11-4}$$

Experimental results

Figure 11-3 displays the differential pressure signal acquired from a spontaneously contracting cardiomyocytes monolayer grown on top of a fibronectin coated silicon CellDrum membrane. The signal was superimposed by electrical and mechanical noise due to the extreme sensitive signal acquisition setup, working at the maximum amplification and sensitivity level of the measurement device. The simultaneous contraction of the cardiomyocyte monolayer was detectable after data processing with a Butterworth low pass filter algorithm. The analysis of the filtered data indicates a variation of the residual tension within the cell monolayer of 1.62±0.17 µN/mm^2.

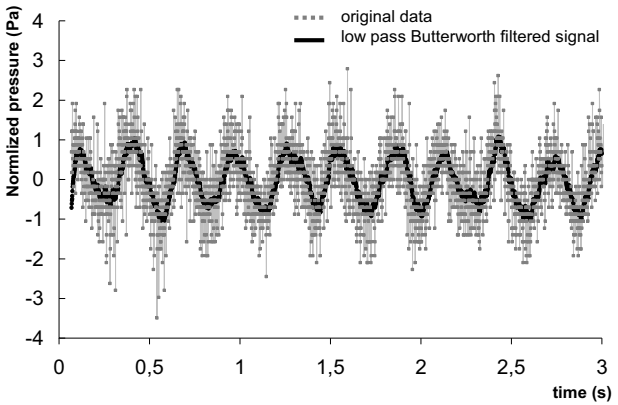

Figure 11-3 Rhythmic contraction of a cardiomyocyte monolayer

In principle, the cardiomyocyte based setup is extremely sensitive to any variation in its environment (temperature change, substrate stretching, etc.) resulting in contractile arrest and cell death when cell monolayers were used. The contraction of a collagen based tissue equivalent, however, could be analyzed in more detail due to the "shielding" effect of collagen based artificial ECM around the cells. The origin of the signal, resulting from the contraction of synchronously beating cardiomyocytes in a tissue equivalent setup was proven by the inhibition of the cellular contractions with a 10% Triton X-100 solution. A monolayer of cells was embedded in a collagen based tissue equivalent. In this setup a variation of the residual tension within the cell monolayer of 1.28±0.13 $\mu N/mm^2$ was detected and then Trition X was added to the cells. Figure 11-4 A shows the measured pressure curve before and after treating the cells with Triton X. Applying a Butterworth low pass filter (Figure 11-4B) allowed separating the contraction signal from the raw data. A FFT transformation (Figure 11-4 C) revealed the contraction frequency of the cells. For these calculations Labview™ 7.1 was used. The untreated cells had a major frequency at 3.3 Hz. After adding Triton X the cells died and the oscillation and this peak disappeared.

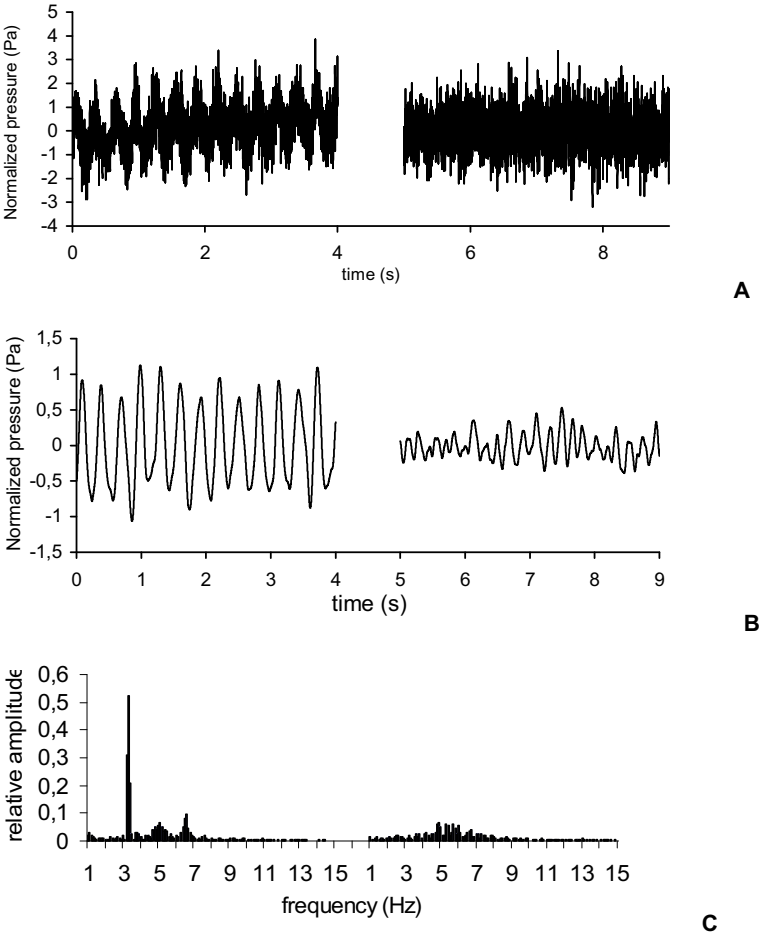

Figure 11-4: Pulsation characteristics of myocardial cells before and after treatment with 10% Triton X-100: A) measured pressure curve; B) the pressure curve filtered by a Butterworth filter kernel C) frequency domain

The effect of Noradrenalin and β blockers on the contraction frequency are shown in Figure 11-5. Initially, the cells were beating at 4.4 Hz. After ~ 6 min, 10^{-4} M noradrenalin was added. Immediate increase of the contraction frequency was observed reaching a peak after 4 min. The frequency increase was 11% above the initial level. Within the following 5.5 min the frequency dropped to 6%. Afterwards a linear decrease at 7.3 mHz/min was observed.

Thirty five minutes after the whole experiment was started 10^{-6} M β ½ blocker were added to the same tissue. The rate of frequency change due to the drug was 15.5 mHz/min. Finally, after ~ 60 min the frequency became constant over time at a level of 4.5% below the initial frequency at zero minutes.

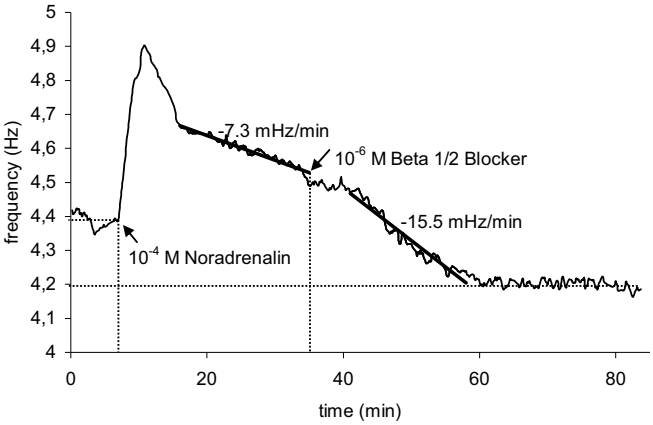

Figure 11-5 Effect of noradrenalin and Beta ½ blocker on contraction frequency of myocardial cells

Discussion and conclusion

So far cultured embryonic (or neonatal) cardiomyocyte did not allow measurements of their major function in the heart, the loaded contraction. Furthermore, there is still the need of a model for studying functional consequences of drug administration or genetic manipulation. In this study we present a system enabling such investigations. cardiomyocytes were grown in flexible, circular collagen film membranes (or directly on a 1µm thin silicon membrane) and exposed to strain in two directions (radially and circumferentially). This biaxial approach is more similar to in vivo strain conditions experienced by most cells than the commonly used uniaxially approach (Eschenhagen et al. 1997b; Zimmermann et al. 2000). The contraction rate of cardiomyocytes ranging between 2-4 Hz is typical for explanted cardiomyocytes cultivated in vitro (Jongsma et al. 1983; Yang et al. 2002). The inhibition of the signal followed by the application of appropriate chemical agents proved that the rhythmic contraction originated from synchronously beating cardiomyocytes. A direct force measurement was possible with both setups, the tissue equivalent and the monolayer.

The 20% decrease of contractile tension observed in the tissue equivalent approach in comparison to the cardiomyocyte monolayer might be addressed to the elastic properties of the collagen matrix of the tissue equivalent.

We analyzed the usability of the system for drug testing with typical drugs related to cardiac function (Figure 11-5).The cellular responses to the drugs in terms of frequency changes showed the correct functionality of the system. At this stage of the study the data were only analysed for frequency changes. The response of cardiac myocytes to Noradrenalin and beta blockers are well studied and published (Tirri & Lehto 1984; Cerbai et al. 2000), whereas nothing really reliable is known on the changes of contractile forces due to the lack of well functioning test systems.

Furthermore, the present study describes a culture system for the evaluation of active mechanical properties of cardiomyocyte monolayer preparations as well as for 3-dimensional collagen matrices seeded with cardiomyocytes. Single isolated neonatal rat heart cells beat slowly (in average beating interval duration ~ seconds) and irregularly (coefficient of variation higher than 40%). It was shown before that slowness and irregularity of the beating are intrinsic properties of these cells. They are not caused by dissociation damages or the lack of conditioning factors in the culture medium (Jongsma et al. 1983). When intracellular cell contacts are established either by cell growth or by plating the cells at high densities both interval duration and irregularity decrease. In contrast, confluent monolayers grown in the CellDrums or embedded in collagen, respectively, beat fast at intervals ranging from 200 to 400 ms which is close to the data published (Jongsma et al. 1983). We compared results obtained with monolayers versus 3D constructs. The 3-dimensional cell-collagen hybrid structure leads to more physiological intracellular contacts. These consist not only of end-to-end (intercalated discs) bonds but also side-to-side bonds (desmosomes, gap junctions and tight junctions). These cellular features resemble much better the architecture of the myocardium and appear to maintain a higher degree of cellular differentiation than the monolayer (Eschenhagen et al. 1997b). Mechanical load is an important growth regulator in the developing heart (Cooper 1987) and the orientation and alignment of neonatal rat cardiomyocytes is stress sensitive (Fink et al. 2000; Terracio et al. 1988) focused on these characteristics when we developed the CellDrum system with its well defined mechanical boundary conditions. As described previously (Trzewik et al. 2004b) the CellDrum system provides an isotropic stress distribution within the collagen matrix. The application of the described steady state method together with the CellDrum cultivation system will offer a wide variety of possibilities for in-vitro investigations of cardiac function in the future.

12 Residual stress and Elastic modulus of cell seeded thin film tissue constructs- a Load-deflection measurement

In this chapter we address another feature of the CellDrum system – the determination of residual stress and elastic modulus of cell seeded thin film tissue constructs based on load-deflection measurements. The popular use of uniaxially loaded collagen matrices for the evaluation of tissue properties had a major drawback. In living tissues a uniaxial tension distribution rarely exists. Additionally, using soft tissue, the uniaxial approach suffered from necking of collagen matrix which makes results difficult to obtain and to explain. Here we will present a method to extract the two independent tissue parameters, the residual stress σ_0 and the Elastic modulus E, in thin film CellDrum constructs at defined mechanical boundary conditions.

The described method was adapted for the biomechanical evaluation of tissue equivalents cultivated in CellDrum devices. But a preceding appraisement of the experimental setup using pure membrane suggests the use of the method for many other applications. The test method discussed in the subsequent chapter may be used in material test or quality control procedures for various thin film applications.

12.1 Experimental setup

In order to enable residual stress and elastic modulus measurements, CellDrums were mounted onto the airtight measurement chamber. The experimental setup is illustrated in Figure 6-5 (chapter 6.1). The CellDrum membrane is deflected under an applied uniform pressure differential. The deformation is a function of pressure and related to the mechanical properties of the cell seeded thin film membrane. An experimental setup was developed in which the fabricated Celldrums were pressurized with air delivered by a computer controlled syringe pump (Figure 6-4). The relative deflection d, corresponding to a certain stress level within the cell-membrane composite, and the appending pressure differential p (between both sides of the CellDrum) were recorded for each strain level. The deflection was measured by a laser based triangulation sensor or by custom made micrometer stage driven optical sensor (CMS), respectively. From p vs. d measurements, determination of the mechanical properties such as initial in-plane stress vs. strain behavior of the material was possible using models in which a relation is established among pressure, center deflection, geometry, and the mechanical properties of the film.

The films of interest must be thin compared to their lateral dimensions or being soft, fulfilling the requirements of negligible stiffness. This results in negligible bending stiffness and allows the films to deform largely under membrane (in-plane) stiffness action.

Theoretical considerations

The membrane stiffness is a function of geometrical change (Maseeh-Therani 1990). The initial stiffness of the film-cell composite is a function of the initial in-plane stress, caused by the CellDrum membrane fabrication and mounting process and initial in-plane stress generated by cells cultivated on top of the CellDrum membrane. For thin film cell seeded tissue constructs, the residual stress is introduced by cell mediated tissue condensation and contraction. Under an initial compressive stress, the film would not show stiffness until it has bulged enough to counter balance the compressive stress. Cabrera (Cabrera 1959) modified a theoretical model first developed by Beam to measure the intrinsic stress and the biaxial modulus of thin films (Beam 1959). In this model membranes were circular and large deformations were assumed. Similar to the CellDrum system, the membranes were deformed by air pressure. In later years, this theory was applied by others (Bromely et al. 1983).

The model was based on the following assumptions: The strains are assumed to be less than 5%; the material constitutive relation is governed by plane stress, and there was no time dependence of the stress and strain law. The membrane properties were isotropic. The material law was linear within the range of elasticity and the value of the determined modulus was taken as an average of the values in the nonlinear regime. The contribution of bending stiffness was assumed to be negligible compared to the membrane's stiffness, as it is the case for cell seeded collagen matrices. Finally, the deflected shape does not deviate from a spherical segment.

In this model, the states of strain distribution along the meridian and circumferential directions were constant. The stress σ using this model can be related to pressure gradient p across the membrane-composite, initial radius a, center deflection d, and film thickness t, as:

$$\sigma = p\, r^2 / (4td) \qquad \text{Formula 12-1}$$

$$\varepsilon = (2/3)\,(d/r)^2 \qquad \text{Formula 12-2}$$

$$\sigma = \sigma_0 + (2/3)\,(E/1\text{-}\nu)\,(d/r)^2 \qquad \text{Formula 12-3}$$

where σ_0 is the initial film stress, and ε is the resulting strain (without an initial strain component) under the applied pressure gradient. The equations (Beam 1959) can be combined to result in a model for deflection as a function of applied pressure gradient *p*.

$$p = \frac{4t\sigma_0}{r^2}d + \frac{8t}{3r^4}\frac{E}{1-\nu}d^3 \qquad \text{Formula 12-4}$$

or in a compendious form summarized as:

$$p(d) = c_1 d + c_2 d^3 \qquad \text{Formula 12-5}$$

with c_1 and c_2 as constants as calculated by the custom made experimental data analysis program. By measuring the bulge height *d* versus pressure *p* and fitting the data to a polynomial with first and third order terms the constants c_1 and c_2 can be easily determined. The Poisson's ratio ν may be evaluated in a different approach. The first order term of this equation is similar to the relation calculated for the steady state method (chapter 11).The tensile stress then is calculated using the known membrane thickness t and radius r, σ_0 and (E/1-ν). The tensile stress from this calculation is biaxial and the relation between the stress and strain results to the biaxial modulus (E/1-ν). The strain values from this formula, which assumes that strain is uniform over the surface of the cap, would result in a deflected shape that is less accurate than the generalized membrane model in which the strain varies from center to edge.

12.2 Data acquisition and fitting procedure

A custom made software was developed in Labview 6.0 to fit the function in Formula 12-6 to the load-deflection data. The residual tension σ_0 was determined by the first order term, while the third order term described the biaxial modulus (E/1-ν). Normally the fit obtained was excellent. However, this was only the case, when the tissue construct was fully anchored at its rim and there were no air bubbles between the membrane and the construct (Figure 12-1 left). If only one of theses preconditions was not fully satisfied, the experimental data did not fit to the model (Figure 12-1, right). This was such an obvious observation, that we decided to calculate the mean square error (MSE) between the fitted curve and the experimental data. As long as the MSE was smaller than two, we tolerated the data. When it was equal to two or higher, the data were rejected because of an artifact.

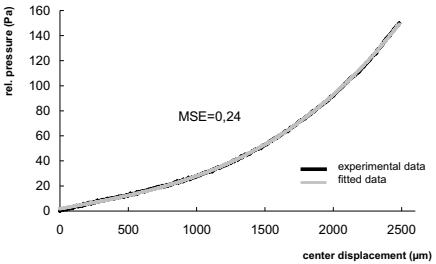

Figure 12-1 Typical deflection pressure relation for a one mm thick cell seeded collagen membrane.

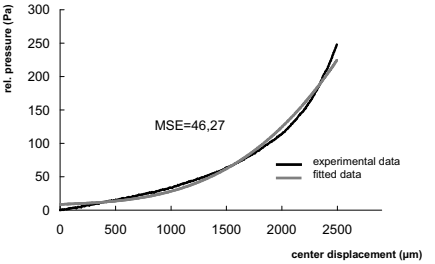

Figure 12-2 A similar sample but with a small air bubble in the intermediate layer between sensor membrane and tissue construct.

12.3 Evaluation study: Load-deflection relationship of pure CellDrum membranes

Experiments and Results

The approximate solution (Formula 12-7) provides the residual tension σ_0 and the biaxial modulus (E/1-ν) of membranes by measuring the height *d* versus pressure *p* and fitting the data to the polynomial.

As first application of this technical approach we investigated pure and untreated 1µm thick silicone membranes. The relationship between the centre deflection (bulk height) and the applied pressure

was studied in loading-unloading cycles. The effect of 1 % Tween 20 (polyoxyethylene sorbitan monolaurate), a surface-active wetting agent and detergent, widely used for surface tension lowering, was added subsequently to the CellDrum media at filling levels of 500 µl and 600 µl, respectively. Figure 12-3 shows loading-unloading pressure-deflection cycles for the same membrane. A variation from the typical CellDrum filling volume of 500µl cell culture medium to 600µl did not have an impact on the load-deflection curve. However, reduced surface tension (Tween 20, 1%) reduced the typical hysteresis of 0.44 Pa between the loading and unloading curves to 0.20 Pa in the 1% Tween 20 solution. It appeared reasonable to assume that the decreased hysteresis resulted from a reduced influence of CellDrum wall wetting effects (compare chapter 7.4). Nevertheless, more dominant and informative was the reduced slope in the Tween 20 treated solution data. The experimental data were obtained to acquire the slope related residual tension σ_0 and the biaxial modulus (E/1-ν) (Figure 12-4). The data derived were summarized in Table 3. There was no significant difference between the calculated biaxial modulus (E/1-ν) for all conditions. This is reasonable since Tween 20 is not known for changing the mechanical properties of the silicon membrane. However, the use of Tween 20 has an influence on the surface tension of liquids. Table 3 indicates that the total tension was reduced in the Tween 20 treated membrane by approximately 30% as compared to the untreated setup. It can be deduced from that, that the total tension σ_0 resulted from the surface tension $\sigma_{surface}$ of the liquid phase plus the tension $\sigma_{membrane}$. The difference between $\sigma_{surface}$(500µl and 600µl) and $\sigma_{surface}$ (1% Tween 20) was 0.03±0.01 N/m. A theoretical calculation with published data determines the same value. In this calculation, $\sigma_{membrane}$ was assumed to be constant and $\sigma_{surface}$ was derived from published data. In physics handbooks $\sigma_{surface}$(water) was 0.072 N/m at 20°C (Kuchling 1989) and $\sigma_{surface}$ published for a 1% Tween 20 solution was 0.036 N/m (Liu 1997)

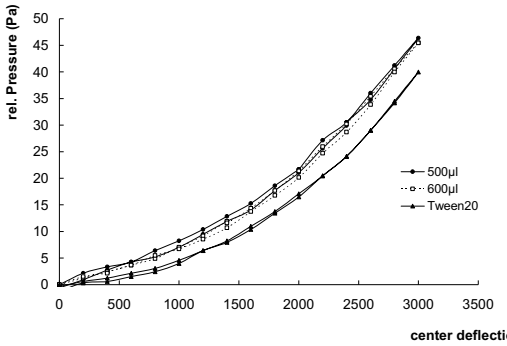

Figure 12-3 Loading-unloading cycles acquired with the CMS sensor at two different CellDrum filling volumes, 500 µl and 600µl, respectively. A 1% Tween 20 solution, known to lower the surface tension, visibly reduced the pressure needed to reach a given centre deflection. This experiment shows again the high sensitivity of the system.

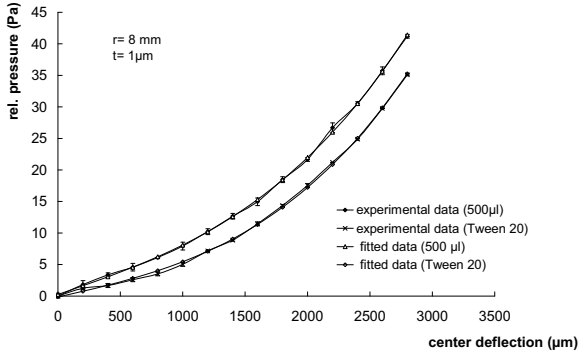

Figure 12-4 Averaged load-deflection curves at 500µl filling for a 1% Tween 20 solution as compared to their fitted curves.

Table 3 Experimental data for the same membrane at different experimental conditions

	σ_0 (µN/mm^2)	E/(1-ν) (MPa)	Typical fitting error (MSE)
CellDrum filling: 500µl	0.095	1.611	0.066
CellDrum filling: 600µl	0.107	1.695	0.032
CellDrum filling: 600µl + Tween 20	0.071	1.613	0.076

Conclusion

The experimental setup and the formula for residual tension σ_0 and biaxial modulus (E/1-ν) can be used for material testing in thin membranes. The variation of the surface tension did not alter the biaxial modulus (E/1-ν) calculated for the different experimental setups. The calculated residual tension fitted very well to data obtained with other methods published elsewhere. This was proven for the surface tension modification due to 1% Tween 20 solutions. Although in this chapter we only wanted to show the excellent accuracy of the method, theoretically it could be also used to measure surface tensions of liquids.
It can be summarized, that the method is very sensitive and should be useful for the determination of the mechanical properties of cells grown on top of the CellDrum membrane.

12.6 Mechanical properties of 3D tissue constructs

The laser based load-deflection setup allowed retrieving data on the residual stress and on the elastic-modulus of artificial tissues cultured on CellDrums. The strain rate chosen during the experiments was dε/dt=0.1%/min because loading curves for soft tissues are relatively insensitive in particular to slow strain rates (Wakatsuki et al. 2000). Soft tissues are hyperelastic materials deforming under load and recovering their initial shape after the load was turned off. In these materials, the loading-unloading curves show a hysteresis effect (Skalak et al. 1986). Except for the region of small strains, the determination of elastic moduli in such materials is difficult because of the lack of a well-defined linear region in the stress -strain curves (chapter 2.2). We used the Cabrera model (formula 9) limited to small strains below 5% for calculating the residual tension σ_0 and the biaxial modulus (E/1-ν) from the experimental load deflection curves.

Experimental Protocol:

Tissue constructs of 0.5 to 1mm thickness can induce rather high mechanical tension. This may lead to a disruption of the construct from its anchoring rim at the CellDrum. Thus, in this 3D approach the CellDrums were equipped with a circumferential rim of Velcro fibers to allow tight anchoring of the construct (chapter Figure 5-2). The CellDrums were coated with 500 µl of a collagen-3T3 fibroblast mixture at an initial concentration of 5 x 10^5 cells/ml and as described in detail in 14.2.2. The CellDrum containing the tissue construct was submerged for at least 1h in fresh media containing stimulants or other chemicals described above at the desired concentrations. All experiments were performed under sterile conditions.

Experimental reagents:

Cytochalasin D was dissolved in dimethylsulfoxide (DMSO) and stored at -20 °C. Before use, the final concentration was adjusted with DMEM. Experiments with fetal calve serum (FCS) were carried out using one and the same aliquot of FCS throughout all experiments (Biochrom, Berlin, Germany).

Results

We only analyzed the loading cycles for mechanical parameters, since during unloading we frequently observed that the tissue construct was losing contact with the silicon membrane. During unloading, the pressure inside the chamber had to be reduced. Because of the considerable mechanical tension inside the tissue construct and the relatively soft silicone membrane the two compartments detached from each other. This lead to false deflection data, because the deflection was taken between the sensor and the silicon membrane, which was always oriented towards the sensor. By principle, this problem cannot occur during the loading cycle since the silicon membrane is pressed against the tissue construct. The remodeling of the matrix by the cells strongly influences mechanical properties of the tissue construct.

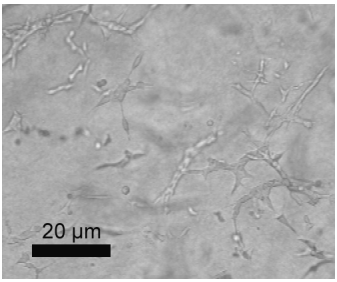

Figure 12-5 Brightfield microscopy of 3T3 Fibroblasts at one plane of focus within the gelated collagen matrix.

Standard brightfield microscopy showed, that after gelation and subsequent cultivation under cell culture conditions, the cells adhered to the collagen fibers and elongated preferably in the plain of strain, parallel to the CellDrum membrane within 60 minutes (Figure 12-5). Within that plane, cells were randomly distributed without any preferred orientation. Protrusions perpendicular to those planes rarely occurred (chapter 9). As a mechanical consequence, the gel did not change much in its thickness (Figure 12-6).

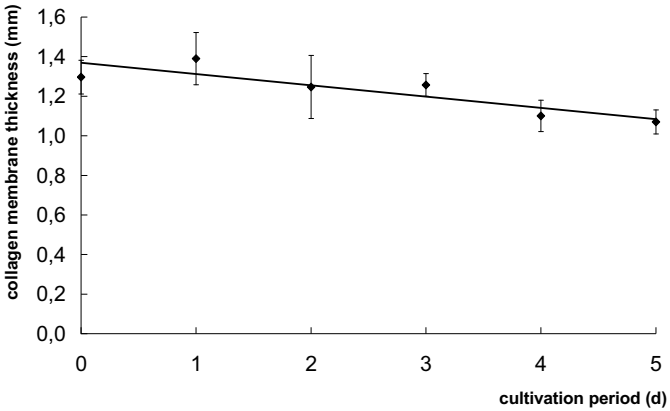

Figure 12-6 Thickness (z-axis) dependence of fibroblast seeded, circular fixed collagen matrices (n=5) on cultivation period. After gelation of the collagen and an initial swelling after 24h there is only little variation in collagen thickness due the fibroblast induced matrix remodelling.

For calculating the residual tension and the Elastic modulus, the constructs thickness was determined (chapter 9.3). The extracellular matrix and the cells were assumed to be nearly incompressible, with a Poisson's ratio of ν= 0.49 (Marquez et al. 2005). The residual stress increases with increasing cultivation time (Figure 10-4). One hour incubation resulted in a complete collagen gelation and cell spreading within this matrix. After 1h of incubation, the tension was 12μN/mm^2. After 2days of culturing the residual tension reached 54μN/mm^2, which was 42 μN/mm^2 higher than the initial tension. Data on the E-modulus after various subsequent treatments of a 1 mm thick collagen I gel seeded with 3T3 fibroblasts are shown in Figure 12-6. All measurements and drug exposures were started at day 4 of cultivation. The measurements after 24 h and 48 h incubation to 10 μM cytochalsin D, respectively, were preformed on day 5 and day 6. The exchange of the culture medium with medium without FCS (known to introduce contraction in fibroblasts), surprisingly, did not have an impact on the E-modulus. However, the application of cytochalasin D (known for decomposing actin fibers in the cytoskeleton) lowered the E-modulus by 35 % within the first 24 h. Further decomposition by cytochalasin action reduced the E-modulus additionally by 13 % within the next 24 h. Subsequent application of 0.1% collagenase I solution (dissociates major parts of collagen structures) reduced the E-modulus to 0.08 MPa. The E-modulus achieved after cytochalasin D application was associated with remaining collagen structures and the CellDrum membrane.

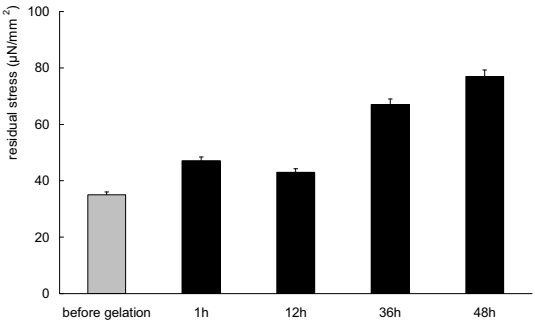

Figure 12-7 Lateral tension as a function of culture time of a 1 mm thick collagen I gel seeded with 3T3 fibroblasts at $5x10^5$ cells/ml. The tension increased within the first 48h due to cell proliferation and ECM remodelling.

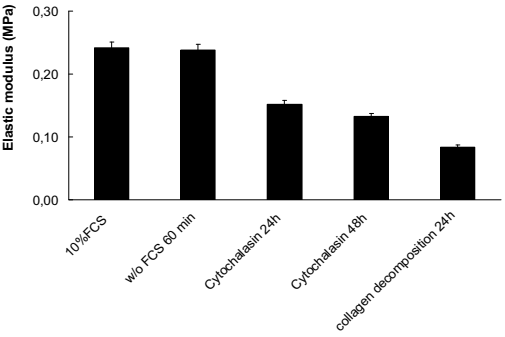

Figure 12-8 E-modulus after various subsequent treatments of a 1 mm thick collagen I gel seeded with 3T3 fibroblasts The measurements were started at day 4 of cultivation.

Discussion

We described a simple, flexible approach to measure the mechanical characteristics of reconstituted model tissue. In contrast to the common uniaxial stretching devices used for the determination of material properties in artificial tissues, the system described here uses biaxially fixed cell-seeded collagen matrices. Because of this boundary condition, the cells are isotropically distributed without a preferred direction of orientation. This was discussed in detail in chapter 9. This fact is important as the mechanical properties of tissues depend on the distribution and orientation of cells (Zahalak et al. 2000). In addition to the determination of the “residual tension” the method described here enables analysing the “Elastic modulus”. The specific degeneration of cellular components like f-

actin, a part of the cytoskeleton, had a direct impact on the E-modulus. The mechanical tension of the tissue construct must therefore be addressed to cytoskeletal components as well as to the cell surrounding extra cellular matrix. This matrix is mostly consisting of Collagen type I. The Elastic modulus determined in the experiments is about consistent with previously published data obtained with uniaxially stretched tissue constructs (Wakatsuki et al. 2000). Data from biaxially strained tissues were not available. It was interesting that the Elastic modulus of natural tissue is significantly higher than the one of artificial tissue. This raises the question of which other factors (mechanical, chemical, physical) are needed to finally form an artificial tissue showing mechanical properties like natural tissues. Our method was developed in order to study those effects in the future.

Type of tissue	**Elastic Modulus (MP)**	**Reference**
Tendo achilles	375	(Lewis & Shaw 1997)
Human knee menisci	73-151 (circumferential)	(Tissakht & Ahmed 1995)
Human knee menisci	30-60 (radial)	(Tissakht & Ahmed 1995)
Human brachial artery	4	(Bank et al. 1999)
Fibroblast-collagen matrix	0.06-1	(Chapuis & Agache 1992)
Fibroblast-collagen matrix	0.8	(Wakatsuki et al. 2000)
Fibroblast-collagen matrix	0.2-0.4	This work

Table 4 Comparison of E-modulus of different tissues obtained by other methods.

With the exception of work by Wakatsuki (Wakatsuki et al. 2000) and ours, the Elastic modulus was obtained before from the derivative of the stress strain relationship. The dependence on the strain rate was never characterized. Wakatzuki addressed the question of the existence of a "dynamic" Elastic modulus which he acquired from data obtained after a sinusoidal strain application at 0.5 Hz. It is well known that the E-modulus for soft tissues increases with the applied strain rate (Fung 1986). Therefore it is not surprising that data Wakatzuki obtained in his "dynamic method" were higher than ours achieved at static conditions. As a conclusion of our work, well defined boundary conditions and the possibility to measure the residual tension and the Elastic modulus simultaneously makes the CellDrum technique a unique tool for cell and tissue research. It can be applied at physiologically small strain levels which make our approach valuable and very promising.

13 Summary and future prospects

In this work we have shown that mechanical properties of tissue constructs can be analyzed with the CellDrum technology. The CellDrum can be used as either quasi-static or a dynamic setup which allows measuring the residual tension and the elastic modulus (static setup) in cell populated thin film tissue constructs.

The starting point of this work was a detailed analysis of previously existing devices and methods for the *in vitro* evaluation of mechanical properties of cell based constructs. Although most of these approaches were shown to be useful in evaluating mechanical properties of tissue constructs and individual cells, their value was significantly restricted by the fact that the mechanical boundary condition in all approaches did not mimic the in vivo situation of tissue. Furthermore, the methods used sophisticated experimental setups and overwhelmed with sterility and biocompatibility problems. High-Throughput approaches were impossible and long term cell cultivation experiments over weeks were almost impossible.

On the contrary, the approach described here was based on uniform and homogeneous 2D stress distribution within the tissue construct. This was shown theoretically by finite element methods and experimentally by *in vitro* studies of stress-induced cellular orientation. The biocompatibility of the CellDrum system was approved in different assays with a focus on the impact of CellDrum membrane coating. Different protein coatings were tested with the aim not only to enhance cell adhesion and cell proliferation but also to provide adequate force transduction between cell and CellDrum. These studies revealed significant differences in cellular responses when different protein coatings were used. For studying biocompatibility, specific apoptosis assays were performed which in all applications showed no apoptosis.

It is important to note that many of these events could be revealed and monitored only due to a novel custom made optical measurement system specially developed for stress-stain measurements on cell populated CellDrum membranes. These measurements were based on quantifying the membrane deflection compensated by a pressure gradient over the membrane. Obtained experimental values were further processed using a mathematical model developed and adapted for the evaluation of residual stress and elastic modulus in cell monolayers or tissue equivalents, respectively. Though the employed optical system did not allow direct acquisition of reliable data, the process parameters collected by it were extremely useful in further experiments, when the optical sensor had been replaced by a more sensitive triangulation based laser sensor. The data acquired under these experimental settings were similar to those published in the literature for uniaxially stretched cells seeded collagen constructs. But, in contrast to those data, the tissue

equivalents used in this work sensed a biaxial and homogenous stress field. This is an important feature of the CellDrum since the activity of a cell is regulated, in part, by the mechanical environment in which it resides.

The cellular activity defines the tissue's tensional homeostasis and this process, the increase of residual tension in relation to the tissue equivalents cultivation time could be detected using a stress-strain relationship, which is visa versa related to the tissue's mechanical properties. Furthermore, the impact of drugs on the mechanical properties could also be investigated. The application of the dynamic measurement method, analysing the resonance frequency of pressure step impulse excited CellDrums, revealed the same findings on the development of tension in the fibroblast seeded tissue constructs. Due to the benefit of that method, which is related to the ease and error-tolerant opportunity to analyse multiple samples over a long time of cultivation, even new details could be revealed. So it could be demonstrated that there was no further increase in tissue tension and a plateau level of tissue's tensional homeostasis was reached after a certain period of cultivation. The simultaneous evaluation of the cell proliferation inside the tissue constructs indicated that the impact of an individual cell was decreasing over the cultivation time.

The variation of tension by contracting cellular monolayer or cell-collagen composites was detected in a modified setup of the static method, when the centre deflection of a cell seeded CellDrum was kept constant at a desired strain level. The cardiomyocytes contracted synchronously on the CellDrum membrane in contrast to cardiomyocytes cultivated on stiff substrates. The contraction of synchronously beating cardiomyocytes was detected by pressure variations introduced by height variations of the cell seeded membrane. This approach offers the novel and unique possibility to cultivate synchronously beating cardiomyocytes and evaluate their contractile behaviour together with the monitored beating frequency.

Future perspectives (trends and expectations)

The major prospects for all described methods lie in a development toward a high throughput screening system. The use of circular samples constructs is becoming standard in many biotechnological screening assays where standard plates for 96 or 384 samples are common. In this regard, the CellDrum technology satisfies all necessary requirements to be embedded in an industry standard. Drug screening assays could be performed using either cell monolayers or collagen-based tissue equivalents. Both primary cell cultures and continuous cell lines can serve as a cell source for the experiments. Continuous cell lines may be used as a standard system, since they can be subcultivated without any further variations of their phenotype. For example, continuous

cardiomyocyte line HL-1 is constructed and is under evaluation at the moment. This may lead to a significant reduction in animal experiments together with an increased efficiency in sample handling and throughput. The use of a cardiomyocyte-based high throughput system is very promising but nevertheless it may need plenty of engineering time and resources. Many difficulties to advance the steady-state method towards a high throughput system would not occur if the dynamic method would be employed. The dynamic method is highly resistant to disturbances introduced through the systems environment, so that any noise or variation in the boundary conditions can easily be identified and filtered out by subsequent software analysis. Furthermore, the system provides sufficient number of measurements per time together with an efficient sample handling. The stress strain-analysis demands engineering recourses, but it may be worth while to apply it since it offers unique insights in important tissue parameters like residual tension and the tissue's elastic modulus. It can be easily up-scaled to larger sample sizes in sample geometry and may serve as a qualifying tool for skin tissue equivalents to be implanted to patients. The system can be also easily adapted to such an important medical application as the determination of mechanical properties of an amniotic sack, whose mechanical parameters are seemingly responsible for many premature birth cases. The system may also provide access to a deeper understanding of widespread diseases which are related to connective tissue dysfunction like hernia formation or female pelvic floor prolaps.

14 Documentation

14.1 Good laboratory practice

Bacteria and fungi free environment

Cell culture contamination by any microorganisms would have had a great impact on the investigated cell properties and behavior. All cell cultures were routinely checked for bacterial or fungal contamination using standard microscopic methods.

Micoplasma free environment

Mycoplasmas (0.2-2 µm in diameter) in cell cultures are extracellular parasites usually attached to the external surface of the cell membrane. Compared to the microbial infection, contamination with mycoplasmas represents a much bigger problem in terms of incidence, detectability, prevention and impact. It was estimated that between 5 and 35% of cell cultures in current use are infected with mycoplasmas (DSMZ 2004).

Since standard microscopic observation was not useful for mycoplasma detection, we proved the absence of that specific contamination by a very sensitive Polymerase Chain Reaction (PCR) amplification method. A commercially available VenorGeM® (BIOCHROM AG, Berlin, Germany) PCR detection kit was used for this purpose. Media from cell lines with a high passage number, which had been used intensively during most experiments, were analyzed. Results shown in Figure 14-1 indicate no mycoplasma contamination and therefore it is reasonable to assume that there was also no contamination in all previous cell passages. An untreated contamination during any cell proliferation process would have led to a contamination in all following steps of cultivation.

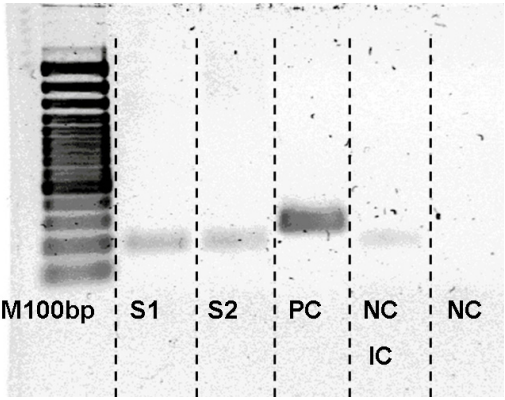

Figure 14-1 Agrose gel electrophoresis of PCR mycoplasma detection products. The first column (M100bp) shows a standard 100 bp DNA lader. The weak band at 192 bp in the Cell culture sample (S1,S2) indicates an effective PCR process, but absence of mycoplasma. The strong band at 270 bp in the positive control (PC) proves effective myocoplasma product amplification by the PCR process. Furthermore, negative controls with (NC IC) and without internal PCR amplification control were performed, proving the reliability of the procedure.

14.2 Cell culture methods

All reagents, unless otherwise specified, were purchased from Sigma-Aldrich Chemie (Taufkirchen, Germany).

Microscopic observations:

All samples were routinely checked with a bright-field objective (CP-Achromat 10 X/0.25 Zeiss, Oberkochen, Germany) mounted to an inverted microscope (Axiovert 25, Zeiss, Oberkochen, Germany). Images were taken using a digital camera (CF 8/1, Kappa GmbH, Gleichen, Germany). The initial thickness of the collagen lattice and the cell orientation after gelation, apoptosis and actin fibre development were measured with a confocal laser scanning microscope (LSM 510, Zeiss) typically using a 10x/0.3 objective lens (Plan-Neofluar, Zeiss). The image analysis was accomplished with integrated data processing software (LSM 3.0, Zeiss) in bright-field mode and fluorescence mode, respectively.

14.2.1 Cell lines BAEC, 3T3

Cell culture: 3T3 NIH fibroblasts (CLS Cellbank, Heidelberg, Germany) and BAEC-bovine aortic endothelia cells (primary culture) were cultured in Dulbecco's modified Eagle`s medium (DMEM) containing 10% fetal bovine serum, 50 U/ml penicillin, 50 µg/ml streptomycin und 2 mM L-glutamine in a humidified incubator at 37 °C and 5% CO_2. The culture medium was renewed every day in the CellDrum culture, otherwise twice a week.

Subculturing:

1. Remove and discard culture medium.
2. Rinse 3 times with HBSS (Hanks' balanced salt solution)
3. Briefly rinse the cell layer with 0.25% (w/v) trypsin- 0.53 mM EDTA solution to remove all traces of serum which contains trypsin inhibitor.
4. Add 2.0 to 3.0 ml of 0.25% trypsin-EDTA solution to flask and observe cells under an inverted microscope until cell layer is dispersed (usually within 5 to 15 minutes).
5. Add 6.0 to 8.0 ml of complete growth medium and aspirate cells by gently pipetting.
6. Add appropriate aliquots of the cell suspension to new culture vessels.
7. Incubate cultures at 37°C.

Medium renewal: Twice per week

Freeze

Typically, the content of an almost confluent T-75 flask were resuspended in 1.5 ml freeze medium and stored at -80°C in a Nunc-cryovial (Nunc,Wiesbaden) for 24 h. The recommended freezing rate was 1°C/min. The vial was afterward transferred into a liquid nitrogen storage container.
Freeze Medium: Complete growth medium supplemented with 10% (v/v) DMSO
Storage temperature: liquid nitrogen vapor phase

14.2.2 Tissue equivalent

Preparation of tissue constructs: 1 ml collagen gel aliquots were prepared by mixing 700 µl of cold unpolymerized acid-solubilized type-I collagen solution (0.5%) (Cellagen AC-5, ICN Biomedicals, Ohio), 100 µl 10X HEPES buffer, 100 µl 10X $NaHCO_3$ buffer and 100 µl 10X

DMEM solution so that a final mixture resulted in 0.35 mg/ml collagen and a physiological ionic strength of a normal DMEM solution. After preparing this mixture, 3T3 fibroblasts were added to a final concentration of typically 5 x 10^5 cells/ml. Before the onset of gelation, a 500 µl aliquot of this cell-collagen mixture was poured into the CellDrum. This amount results in a gel of approximately 1 mm in thickness after gelation. After adding culture medium, all samples were placed into a CellDrum holder (Cell & Tissue Technologies, Juelich, Germany) and incubated at 37 °C and 5% CO_2. Culture media were changed daily. In order to perform mechanical tension measurements, the CellDrum well was taken out of the incubator and placed into the Tissue Tension Analyser. The tissue constructs used in the load-deflection set were directly prepared in a CellDrum already placed inside the measurement device. The experiments were carried out at sterile conditions outside the incubator.

3D Cell counting method: Because of the three-dimensional cell proliferation in the collagen gel the conventional cell counting procedures were not applicable directly. The collagen gel had to be dissolved before. This was done in 2 ml 0.1% collagenase I solution. After approximately 15 minutes at room temperature there was no more visible tissue remaining. After centrifugation at ~120 g for 5 minutes the pellet was resuspended in the desired volume of PBS. The Cell concentration of this suspension was counted with a Neubauer Improved Counting Chamber. From this value the original concentration in the gel was calculated.

14.2.3 Cultured heart tissue equivalent

One day old neonatal Sprague Dawley rats were decapitated. The heart was transferred to cold PBS-PenStrep, arteries were removed and ventricles diced. Dices were trypsinized for cell preparation. Trypsination was performed 5-6 times by incubating ventricle dices for 15' at 37°C with a 0.02 % trypsin solution in HBSS. Dnase I at was added at 0.02 mg/ml if cell suspension became too viscous because of leaked DNA. After trituation with a plastic pipette, cells were collected in FCS to inhibit further proteolysis and remaining tissue dices were subjected to another round of trypsine digestion. Cells from the first round of digestion were discarded. After all tissue has been broken down, cells were washed in FCS: SM20-I culture medium (1:1) (Biochrom, Berlin) and finally resuspended in culture medium SM20-I. The number of viable cells was assessed by Trypan blue-staining and counting in a Neubauer counting chamber.

Collagen Gel: Cell drums were coated with 400µl of collagen gel made from Cellagen solution (AC-5; 0.5% Type I Collagen, pH3; MP Biomedicals) according to the tissue equivalent protocol using SM20-I medium instead of DMEM.

Cell culture: Cells were suspended in CO_2-independently buffered cell culture medium SM20-I supplemented with 8% FCS, penicillin (100 U/ml), streptomycin (100 µg/ml), hydrocortisol (1µg/ml), glutamine (2 mM) and $CaCl_2$ (1.3 mM) at a density of $2x10^6$ cells/cell drum. Cell drums were placed in petri dish and sealed with Parafilm to avoid influence of CO_2 on the medium. After 5 days of incubation at 37 °C cell drums were used for measurement.

14.2.4 Mito-capture™ Apotosis kit

For analyzing adherent cells on CellDrum membranes, the CellDrum with cells grown on the membrane were transferred on a coverslip and the entire procedure was performed directly on the coverslip.
The MitoCapture Reagent was diluted immediately prior to use: 1 µl MitoCapture was diluted to 1 ml pre-warmed Incubation Buffer for each assay and vortexed. Since the MitoCapture is poorly soluble in aqueous solutions the dye solution was centrifuged to remove particles for 1 minute at 5,000 x g. The adherent cells were incubated in 1 ml of the diluted MitoCapture solution at 37° C in a 5% CO_2 incubator for 15-20 min. The sample was resuspended afterward in 1 ml of the prewarmed Incubation Buffer
The cells were immediately observed under a fluorescence microscope (LSM 510, Zeiss, Oberkochen, Germany), 10x objective lens (LD-Achroplan, Zeiss) using a band-pass filter (detects fluorescein and rhodamine). MitoCapture that has aggregated in the mitochondria of healthy cells fluoresces red. In apoptotic cells, MitoCapture cannot accumulate in the mitochondria, it remains as monomers in the cytoplasm, and fluoresces green.

14.2.5 Determination of F-actin

In order to identify actin fibers in 3T3 fibroblast monolayers at different strain condition the LSM 510 (Zeiss, Oberkochem, Germany) was used. F-actin fibers were specifically stained with Alexa 488 phalloidin [Ex 495 nm/Em 518 nm] (Molecular Probes, Leiden, Netherlands) according to the following protocol:

- Wash cells twice with prewarmed (37°C) phosphate-buffered saline, pH 7.4 (PBS).

- Fix the sample in 3.7% formaldehyde solution in PBS for 10 minutes at room temperature.
- Wash the sample two or more times with PBS.
- Place each coverslip in a glass petri dish and extract it with 0.1% TRITON® X-100 in PBS for 3 to 5 minutes.
- Wash two or more times with PBS.
- When staining with any of the fluorescent phallotoxins, dilute 5 µl methanolic stock solution into 200 µl PBS for each cover slip to be stained. To reduce nonspecific background staining with these conjugates, add 1% bovine serum albumin (BSA) to the staining solution.

14.2.6 Fluorescence labeling of live cells for cell orientation studies

3T3 fibroblast were stained with fluorescent cytoplasmic dye Celltracker™ Green CMFDA [Ex 492 nm/Em 517 nm] (Molecular Probes, Leiden, Netherlands) prior to the preparation of collagen based tissue constructs. CMFDA is colorless and nonfluorescent until the acetate groups are cleaved by intracellular esterases; hydrolysis of the acetates yields a product with the indicated spectral properties. The cells remain fluorescent and viable for typically more than 3 days after staining.

Cell Preparation

- Dissolve the lyophilized product in high-quality DMSO to a final concentration of 10 mM. Dilute the stock solution to a final working concentration of 5 µM in serum-free medium. Avoid amine- and thiol containing buffers. Warm the working solution to 37°C.
- Remove the cell culture medium with the celltracker working solution and incubate the cells for 15-45 minutes inside the incubator at 37°.
- Replace the probe solution with fresh, prewarmed medium and incubate the cultures for another 30 minutes at 37°C. During this time, the chloromethyl group (and for some probes, the acetate group) of the dye undergo modification or are secreted from the cell.
- Wash the cells with PBS and start the trypsination process to suspend the cells for further handling.

14.2.7 Cell-Tak™

1. Prepare a neutral buffer solution. 0.1 M sodium bicarbonate, pH 8.0 is recommended when coating aseptically. Filter-sterilize the buffer.
2. Calculate amount of BD Cell-Tak required from the size and number of vessels to be coated, calculate total surface area. The best density of BD Cell-Tak depends on your specific application, or cell type. A preliminary dose-response experiment is recommended to determine optimal density. Otherwise, start at a density of 3.5 µg BD Cell-Tak/cm^2 of surface area. High densities will not necessarily improve performance, so the "minimum effective density" should be determined empirically.
3. Neutralize the BD Cell-Tak and dispense to the vessel. The exact volume of buffer will depend on whether the sides of vessels will be coated. Dilute the correct amount of BD Cell-Tak into the buffer, mix thoroughly, and dispense within 10 minutes.

NOTE: If the pH in the coating buffer is not between 6.5 - 8.0, Cell-Tak will not perform optimally. An aid to attaining this pH window is to use a volume of 1N NaOH equal to half the volume Cell-Tak solution used in combination with a neutral buffer. For example: Use 10 µl Cell-Tak, 285 µl sodium bicarbonate, pH 8.0 and 5 µl 1N NaOH (added immediately before coating) to make 300 µl Cell-Tak solution

4. Incubate for adsorption. A minimum incubation of twenty minutes is recommended, but longer times will not adversely affect adsorption, even if all the liquid evaporates. Pour off, or aspirate, the BD Cell-Tak and wash with sterile water to remove bicarbonate. If vessels are to be used later, they should be air-dried and stored at 2-8 °C up to two weeks or with dessicant up to 4 weeks.

14.2.8 Protein profile analysis

The protein composition of mechanically stressed vs. intact cells was detected and compared by one- and two-dimensional SDS-PAGE. After harvesting and washing, the suspensions were subjected to 3 freeze-thaw cycles in an extraction buffer (1D SDS PAGE: Tris-HCl pH7, 2% SDS, 5mM EDTA, 1mM PMSF; 2D SDS PAGE: 8M Urea, 2% CHAPS, 50mM DTT, 0.2% (w/v) BioLyte® ampholytes (BioRad). A two-step extraction method has been applied to improve the quality of 2D SDS PAGE resolution. The strong detergent ASB-14 in combination with tributylphosphine (TBP) was used in this approach, increasing the extraction power on the second stage of the extraction. Following the centrifugation at 11000 g to remove cell debris the SDS-PAGE at 10% (w/v) of the supernatant was carried out. Alternatively, for 2D-applications,

isoelectrofocusing on 7cm polyacrylamide strips with immobilized pH gradient was carried out before PAGE. The gels were stained with colloidal Coomassie brilliant blue stain (PageBlue™, Fermentas). Gels were scanned and densitometry profiles were obtained using image analysis. Respective molecular weights of the bands were estimated with the DIAdem software (version 8.0; National Instruments, Austin, USA) using molecular weight markers as standards.

15 Publications by J. Trzewik related to this and preceding work

Trzewik, J., Mallipattu, S. K., Artmann, G. M., Delano, F. A. & Schmid-Schonbein, G. W. 2001. Evidence for a second valve system in lymphatics: endothelial microvalves. *FASEB J.* 15: 1711-1717.

(this article was **cited** in **Science** June 2002, p.1883-1886)

Trzewik, J., Ates, M. & Artmann, G. M. 2002. A novel method to quantify mechanical tension in cell monolayers. *Biomed Tech (Berl)* 47 Suppl 1 Pt 1: 379-381.

Trzewik, J., Artmann-Temiz, A., Linder, P. T., Demirci, T., Digel, I. & Artmann, G. M. 2004. Evaluation of lateral mechanical tension in thin-film tissue constructs. *Ann.Biomed Eng* 32: 1243-1251.

Trzewik, J., Linder, P. T., Demirci, T. & Artmann, G. M. 2004. Three-dimensional analysis of cell orientation and location in thin film tissue constructs at various mechanical stress conditions. *Biomed Tech (Berl)* 49 Suppl 2 Pt 2: 1044-1045.

Demirci, T., **Trzewik, J.**, Linder, P. T., Digel, I., Artmann, G. M. & Artmann-Temiz, A. 2004. Mechanical Stimulation of 3T3 Fibroblasts activated Genes: ITGB5 and p53 responses as quantified on the mRNA level. *Biomed Tech (Berl)* 49 Suppl 2 Pt 2: 1030-1031.

Demirci, T., **Trzewik, J.**, Linder, P. T., Digel, I., Artmann, G. M. & Artmann-Temiz, A. 2004. Mechanical Stimulation of 3T3 Fibroblasts activated Genes: Real time PCR products and suppliers by comparison. *Biomed Tech (Berl)* 49 Suppl 2 Pt 2: 1047-1048.

Digel, I., **Trzewik, J.**, Demirci, T., Artmann-Temiz, A. & Artmann, G. M. 2004. Response of fibroblasts to cyclic mechanical stress: A proteome approach. *Biomed Tech (Berl)* 49 Suppl 2 Pt 2: 1042-1043.

Linder, P. T., Rueffer, M., **Trzewik, J.**, Porst, D. & Artmann-Temiz, A. 2005. Mechanical Tension in Spontaneously Contracting 3D-Myocard Tissue Constructs: A High Throughput Approach. *Int.J.Artif.Organs* 28: 319.

Trzewik, J., Linder, P. T., Porst, D. & Artmann, G. M. 2005. Determination of Residual Stress and Biaxial Modulus of Cell Seeded Thin Film Tissue Constructs. *Int.J.Artif.Organs* 28: 350.

Symphosium presentations:

Trzewik J., Artmann G., Schmid-Schoenbein G.W. Investigation on Lymphatic Endothelial Microvalves.
34. Jahrestagung Deutsche Gesellschaft f. Biomedizinische Technik, 28.-20. Sep. 2000, Lübeck

Schmid-Schoenbein G.W; Trzewik J. Evidence for a Primary Valve System in Initial Lymphatics.
Biomedical Engineering Society Annual Meeting October 12-14, 2000 Seattle, Washington USA

Trzewik J., Artmann G., Schmid-Schoenbein G.W. Investigation on Lymphatic Endothelial Microvalves.
Bio-X 2000, Nov. 11-14 2000, Shanghai, China

Trzewik J., Schmid-Schoenbein G.W. Evidence for a second valve system in Lymphatics: Endothelial Microvalves.
Experimental Biology 2001, March 31- April 4 2001, Orlando, FL, USA

Trzewik J., Schmid-Schoenbein G.W. Evidence for a second valve system in Lymphatics: Endothelial Microvalves.
Bioengineering Conference, June 27-July 1 2001, Snowbird, Utha, USA

Trzewik Jürgen, Sandeep. K. Mallipattu, Gerhard M. Artmann, Frank DeLano, Schmid-Schoenbein G.W. Mechanics of Lymph Transport: Evidence for a second valve system.
Annual Fall Meeting of the Biomedical Engineering Society October 4-7, 2001, Durham, USA

Schmid-Schonbein G.W., Trzewik J., DeLano F.A. The cellular basis for a second valve system in the initial lymphatics.
World congress on microcirculation, 2001, Sydney, Australia

Trzewik J, Ates M, Artmann GM A novel method to quantify mechanical tension in cell monolayers.
36. Jahrestagung der Deutschen Gesellschaft für Biomedizinische Technik 2002.Karlsruhe

Trzewik J., A. Artmann-Temiz, P.Linder und G.M. Artmann, Lateral Mechanical Tension in ultra flat fibroblast-Collagen Gels
World Congress on Medical Physics and Biomedical Engineering, August 24-29, 2003, Sidney, Australia,

Trzewik J., A. Artmann-Temiz, P.Linder und G.M. Artmann, Lateral Mechanical Tension in ultra flat fibroblast Collagen Gels, Biomedical Engineering Society, 2003, Orlando, USA

Fibroblast response to cyclic mechanical stress. Role of the adhesion substrate.
I. Digel, T. Demirci. J. Trzewik, P. Linder and A. Temiz Artmann International Conference on Biorheology, August 2004, Shanghai, China

Reference List

Abromowitz, M. & Stegun, I. A. 1965. Handbook of mathematical functions: with formulas, graphs, and mathematical tables. New York: Dover Publications.

Akiyama, S. K., Hasegawa, E., Hasegawa, T. & Yamada, K. M. 1985. The interaction of fibronectin fragments with fibroblastic cells. *J.Biol.Chem.* 260: 13256-13260.

Artmann, G. M. Keynote lecture; Contemporary Bioengineering and Cell Mechanics. A Major Challenge for Engineers. 2005a. 2nd World Congress on Regenerative Medicine, Leipzig, May 18-20, 2005, Germany.

Artmann, G. M. Keynote lecture; Mechanical tension in Cells and Tissues: An Experimental Approach. 2005b. 4th Annual Meeting of the European Tissue Engineering Society, Munich, 31 Aug - 3 Sept, 2005, Germany.

Artmann, G. M. Keynote lecture; Sensing Mechanical Forces. 2005c. 3rd International Symposium on Sensor Science (I3S 2005), Juelich, July 18 - 21, 2005, Germany.

Artmann, G. M., Kelemen, C., Porst, D., Buldt, G. & Chien, S. 1998. Temperature transitions of protein properties in human red blood cells. *Biophys.J.* 75: 3179-3183.

Balaban, N. Q., Schwarz, U. S., Riveline, D., Goichberg, P., Tzur, G., Sabanay, I., Mahalu, D., Safran, S., Bershadsky, A., Addadi, L. & Geiger, B. 2001. Force and focal adhesion assembly: a close relationship studied using elastic micropatterned substrates. *Nat.Cell Biol.* 3: 466-472.

Banes, A. J., Lee, G., Graff, R., Otey, C., Archambault, J., Tsuzaki, M., Elfervig, M. & Qi, J. 2001. Mechanical forces and signaling in connective tissue cells: cellular mechanisms of detection, transduction, and responses to mechanical deformation. *Current Opinions in Orthopaedics* 12: 389-396.

Bank, A. J., Kaiser, D. R., Rajala, S. & Cheng, A. 1999. In vivo human brachial artery elastic mechanics: effects of smooth muscle relaxation. *Circulation* 100: 41-47.

Bard, J. B. & Hay, E. D. 1975. The behavior of fibroblasts from the developing avian cornea. Morphology and movement in situ and in vitro. *J.Cell Biol.* 67: 400-418.

Beam, J. W. 1959. Structures and properties of thin films. New York: Wiley.

Bell, E., Ivarsson, B. & Merrill, C. 1979. Production of a tissue-like structure by contraction of collagen lattices by human fibroblasts of different proliferative potential in vitro. *Proc.Natl.Acad.Sci.U.S.A* 76: 1274-1278.

Benjamin, M. & Hillen, B. 2003. Mechanical influences on cells, tissues and organs - 'Mechanical Morphogenesis'. *Eur.J.Morphol.* 41: 3-7.

Bissell, M. J., Hall, H. G. & Parry, G. 1982. How does the extracellular matrix direct gene expression? *J.Theor.Biol.* 99: 31-68.

Bluhm, W. F., McCulloch, A. D. & Lew, W. Y. 1995. Active force in rabbit ventricular myocytes. *J.Biomech.* 28: 1119-1122.

Boswell, C. A., Majno, G., Joris, I. & Ostrom, K. A. 1992. Acute endothelial cell contraction in vitro: a comparison with vascular smooth muscle cells and fibroblasts. *Microvasc.Res.* 43: 178-191.

Brady, A. J. 1991. Mechanical properties of isolated cardiac myocytes. *Physiol Rev.* 71: 413-428.

Brady, A. J., Tan, S. T. & Ricchiuti, N. V. 1979. Contractile force measured in unskinned isolated adult rat heart fibres. *Nature* 282: 728-729.

Bray, D. 1979. Cytochalasin action. *Nature* 282: 671.

Bray, D. 1992. Cell movements. New York & London: Garland Publishing, INC.

Bromely, E. I., Randall, J. N., Flanders, D. C. & Mountain, R. W. A technique for the determination of stress in thin films. J.Vac.Sic.Tech. 1, 1364-1366. 1983.

Brown, R. A., Prajapati, R., McGrouther, D. A., Yannas, I. V. & Eastwood, M. 1998. Tensional homeostasis in dermal fibroblasts: mechanical responses to mechanical loading in three-dimensional substrates. *J.Cell Physiol* 175: 323-332.

Burton, K. & Taylor, D. L. 1997. Traction forces of cytokinesis measured with optically modified elastic substrata. *Nature* 385: 450-454.

Cabrera, S. quoted by Beams (1959). 1959.

Cavanaugh, M. 1957. Studies on the pharmacology of tissue cultures. I. The action of quinidine on cultures of dissociated chick embryo heart cells. *Arch.Int.Pharmacodyn.Ther.* 110: 43-55.

Cerbai, E., Sartiani, L., De Paoli, P. & Mugelli, A. 2000. Isolated cardiac cells for electropharmacological studies. *Pharmacol.Res.* 42: 1-8.

Chapuis, J. F. & Agache, P. 1992. A new technique to study the mechanical properties of collagen lattices. *J.Biomech.* 25: 115-120.

Chien, S., Sung, K. L., Skalak, R., Usami, S. & Tozeren, A. 1978. Theoretical and experimental studies on viscoelastic properties of erythrocyte membrane. *Biophys.J.* 24: 463-487.

Citron, N. & Hearnden, A. 2003. Skin tension in the aetiology of dupuytren's disease; a prospective trial. *J.Hand Surg.[Br.]* 28: 528-530.

Cohen, C. R., Mills, I., Du, W., Kamal, K. & Sumpio, B. E. 1997. Activation of the adenylyl cyclase/cyclic AMP/protein kinase A pathway in endothelial cells exposed to cyclic strain. *Exp.Cell Res.* 231: 184-189.

Cooley, J. W. & Tukey, J. W. 1965. An algorithm for the machine calculation of complex Fourier Series. *Mathematics Computation* 19: 297-301.

Cooper, G. 1987. Cardiocyte adaptation to chronically altered load. *Annu.Rev.Physiol* 49: 501-518.

Cotran, R. S., Kumar, V. & Collins, T. 1999. Robbins Pathologic Basis of Disease. Philadelphia: Saunders.

Deacon, M. P., Davis, S. S., Waite, J. H. & Harding, S. E. 1998. Structure and mucoadhesion of mussel glue protein in dilute solution. *Biochemistry* 37: 14108-14112.

Delvoye, P., Wiliquet, P., Leveque, J. L., Nusgens, B. V. & Lapiere, C. M. 1991. Measurement of mechanical forces generated by skin fibroblasts embedded in a three-dimensional collagen gel. *J.Invest Dermatol.* 97: 898-902.

Demirici, T., Trzewik, J., Linder, PT., Artmann, G. M. & Artmann-Temiz, A. 2004. Mechanical Stimulation of 3T3 Fibroblasts activated Genes: ITGB5 and p53 responses as quantified on the mRNA level. *Biomed Tech (Berl)* 49 Suppl 2: 1030-1031.

DSMZ . Deutsche Sammlung von Mikroorganismen und Zellkulturen. 2004.

Duval, J. L., Letort, M. & Sigot-Luizard, M. F. 1988. Comparative assessment of cell/substratum static adhesion using an in vitro organ culture method and computerized analysis system. *Biomaterials* 9: 155-161.

Eastwood, M., McGrouther, D. A. & Brown, R. A. 1994. A culture force monitor for measurement of contraction forces generated in human dermal fibroblast cultures: evidence for cell-matrix mechanical signalling. *Biochim.Biophys.Acta* 1201: 186-192.

Eastwood, M., McGrouther, D. A. & Brown, R. A. 1998. Fibroblast responses to mechanical forces. *Proc.Inst.Mech.Eng [H.]* 212: 85-92.

Eckl, K. & Gruler, H. 1988. Description of cell adhesion by the langmuir adsorption isotherm. *Z.Naturforsch.[C.]* 43: 769-776.

Elsdale, T. & Bard, J. 1972a. Collagen substrata for studies on cell behavior. *J.Cell Biol.* 54: 626-637.

Ernst, H. 1991. Einführung in die digitale Bildverarbeitung. München: Franzis.

Eschenhagen, T., Fink, C., Remmers, U., Scholz, H., Wattchow, J., Weil, J., Zimmermann, W., Dohmen, H. H., Schafer, H., Bishopric, N., Wakatsuki, T. & Elson, E. L. 1997. Three-dimensional reconstitution of embryonic cardiomyocytes in a collagen matrix: a new heart muscle model system. *FASEB J.* 11: 683-694.

Feng, Z., Matsumoto, T. & Nakamura, T. 2003. Measurements of the mechanical properties of contracted collagen gels populated with rat fibroblasts or cardiomyocytes. *J.Artif.Organs* 6: 192-196.

Fink, C., Ergun, S., Kralisch, D., Remmers, U., Weil, J. & Eschenhagen, T. 2000. Chronic stretch of engineered heart tissue induces hypertrophy and functional improvement. *FASEB J.* 14: 669-679.

Franke, R. P., Grafe, M., Schnittler, H., Seiffge, D., Mittermayer, C. & Drenckhahn, D. 1984. Induction of human vascular endothelial stress fibres by fluid shear stress. *Nature* 307: 648-649.

Fung, Y. C. 1967. Elasticity of soft tissues in simple elongation. *Am.J.Physiol* 213: 1532-1544.

Fung, Y. C. 1986. Mechanics of Soft Tissues. In Skalak, R. & Chien, S. (Eds) Handbook of Bioengineering New York: McGraw-Hill Book Company.

Fung, Y. C. 1993. Biomechanics. New York: Springer.

Galbraith, C. G. & Sheetz, M. P. 1997. A micromachined device provides a new bend on fibroblast traction forces. *Proc.Natl.Acad.Sci.U.S.A* 94: 9114-9118.

Gonzalez, R. & Woods, R. 1992. Digital Image Processing. Addison Wesley.

Gordon, V. D., Valentine, M. T., Gardel, M. L., Andor-Ardo, D., Dennison, S., Bogdanov, A. A., Weitz, D. A. & Deisboeck, T. S. 2003. Measuring the mechanical stress induced by an expanding multicellular tumor system: a case study. *Exp.Cell Res.* 289: 58-66.

Graff, K. F. 1975. Wave motion in elastic solids. Oxford: Clarendon Press.

Grinnell, F., Ho, C. H., Lin, Y. C. & Skuta, G. 1999. Differences in the regulation of fibroblast contraction of floating versus stressed collagen matrices. *J.Biol.Chem.* 274: 918-923.

Gross, D., Hauger, W., Schnell, W. & Wriggers, P. 1995. Technische Mechanik 4. Berlin Heidelberg New York: Springer Verlag.

Guckel, H., Randazo, T. & Burns, D. W. A simple methode for the determination of mechanical strain in thin films with application to polysilicon. J.Appl.Phys 57, 1671-1675. 1985.

Hamill, O. P., Marty, A., Neher, E., Sakmann, B. & Sigworth, F. J. 1981. Improved patch-clamp techniques for high-resolution current recording from cells and cell-free membrane patches. *Pflugers Arch.* 391: 85-100.

Harris, A. 1973. Behavior of cultured cells on substrata of variable adhesiveness. *Exp.Cell Res.* 77: 285-297.

Harris, A. K., Stopak, D. & Wild, P. 1981. Fibroblast traction as a mechanism for collagen morphogenesis. *Nature* 290: 249-251.

Harris, A. K., Wild, P. & Stopak, D. 1980. Silicone rubber substrata: a new wrinkle in the study of cell locomotion. *Science* 208: 177-179.

Haut, T. L., Hull, M. L. & Howell, S. M. 1998. A high-accuracy three-dimensional coordinate digitizing system for reconstructing the geometry of diarthrodial joints. *J.Biomech.* 31: 571-577.

Heath, J. P. & Dunn, G. A. 1978. Cell to substratum contacts of chick fibroblasts and their relation to the microfilament system. A correlated interference-reflexion and high-voltage electron-microscope study. *J.Cell Sci.* 29: 197-212.

Henderson, J. H. & Carter, D. R. 2002. Mechanical induction in limb morphogenesis: the role of growth-generated strains and pressures. *Bone* 31: 645-653.

Horbett, T. A. & Schway, M. B. 1988. Correlations between mouse 3T3 cell spreading and serum fibronectin adsorption on glass and hydroxyethylmethacrylate-ethylmethacrylate copolymers. *J.Biomed.Mater.Res.* 22: 763-793.

Huang, W., Sher, Y. P., Peck, K. & Fung, Y. C. 2002. Matching gene activity with physiological functions. *Proc.Natl.Acad.Sci.U.S.A* 99: 2603-2608.

Iijima, T., Yanagisawa, T. & Taira, N. 1984. Increase in the slow inward current by intracellularly applied nifedipine and nicardipine in single ventricular cells of the guinea-pig heart. *J.Mol.Cell Cardiol.* 16: 1173-1177.

Jahnke, Emde & Lösch 1966. Tafeln höherer Funktionen - Tables of Higher Functions. Stuttgart: Teubner.

Jiang, L., Jha, V., Dhanabal, M., Sukhatme, V. P. & Alper, S. L. 2001. Intracellular Ca(2+) signaling in endothelial cells by the angiogenesis inhibitors endostatin and angiostatin. *Am.J.Physiol Cell Physiol* 280: C1140-C1150.

Jongsma, H. J., Tsjernina, L. & de Bruijne, J. 1983. The establishment of regular beating in populations of pacemaker heart cells. A study with tissue-cultured rat heart cells. *J.Mol.Cell Cardiol.* 15: 123-133.

Kalkman, C. J. 1995. LabVIEW: a software system for data acquisition, data analysis, and instrument control. *J.Clin.Monit.* 11: 51-58.

Kasugai, S., Suzuki, S., Shibata, S., Yasui, S., Amano, H. & Ogura, H. 1990. Measurements of the isometric contractile forces generated by dog periodontal ligament fibroblasts in vitro. *Arch.Oral Biol.* 35: 597-601.

King, G. L. & Suzuma, K. 2000. Pigment-epithelium-derived factor--a key coordinator of retinal neuronal and vascular functions. *N.Engl.J.Med.* 342: 349-351.

Kolodney, M. S. & Elson, E. L. 1993. Correlation of myosin light chain phosphorylation with isometric contraction of fibroblasts. *J.Biol.Chem.* 268: 23850-23855.

Kolodney, M. S. & Wysolmerski, R. B. 1992. Isometric contraction by fibroblasts and endothelial cells in tissue culture: a quantitative study. *J.Cell Biol.* 117: 73-82.

Komuro, I., Kaida, T., Shibazaki, Y., Kurabayashi, M., Katoh, Y., Hoh, E., Takaku, F. & Yazaki, Y. 1990. Stretching cardiac myocytes stimulates protooncogene expression. *J.Biol.Chem.* 265: 3595-3598.

Korn, E. D., Carlier, M. F. & Pantaloni, D. 1987. Actin polymerization and ATP hydrolysis. *Science* 238: 638-644.

Kuchling, H. 1989. Taschenbuch der Physik. Thun und Frankfurt/Main: Verlag Harri Deutsch.

Langendorff, O. 1895. Untersuchungen am überlebenden Säugetierherzen. *Pügers Arch.ges.Physiologie,* 61: 291-332.

Langer, K. 1861. Zur Anatomie und Physiologie der Haut: I. Über die Spaltbarkeit der Cutis. *Sitzungsber.Akad.Wiss.Wien* 44: 19-46.

Langholz, O., Rockel, D., Mauch, C., Kozlowska, E., Bank, I., Krieg, T. & Eckes, B. 1995. Collagen and collagenase gene expression in three-dimensional collagen lattices are differentially regulated by alpha 1 beta 1 and alpha 2 beta 1 integrins. *J.Cell Biol.* 131: 1903-1915.

Lanir, Y. & Fung, Y. C. 1974a. Two-dimensional mechanical properties of rabbit skin. I. Experimental system. *J.Biomech.* 7: 29-34.

Lanza, R., Langer, R. & Vacanti, J. 2000. Principles of tissue engineering. San Diego: Academic press.

Lee, J., Leonard, M., Oliver, T., Ishihara, A. & Jacobson, K. 1994. Traction forces generated by locomoting keratocytes. *J.Cell Biol.* 127: 1957-1964.

Lewis, G. & Shaw, K. M. 1997. Tensile properties of human tendo Achillis: effect of donor age and strain rate. *J.Foot Ankle Surg.* 36: 435-445.

Lin, G., Palmer, R. E., Pister, K. S. & Roos, K. P. 2001a. Miniature heart cell force transducer system implemented in MEMS technology. *IEEE Trans.Biomed.Eng* 48: 996-1006.

Liu, M. 1997. Synchronized changing of transinterface pressure, bubble radius and surface tension: a unique feature of lung surfactant. *Chem.Phys.Lipids* 89: 55-65.

Liu, S. Q. & Fung, Y. C. 1988. Zero-stress states of arteries. *J.Biomech.Eng* 110: 82-84.

Loscalzo, J. 2003. Proteomics in cardiovascular biology and medicine. *Circulation* 108: 380-383.

Madou, M. 1997. Fundamentals of microfabrication. Boca Raton: CRC Press.

Marquez, J. P., Genin, G. M., Zahalak, G. I. & Elson, E. L. 2005. The relationship between cell and tissue strain in three-dimensional bio-artificial tissues. *Biophys.J.* 88: 778-789.

Maseeh-Therani, F. Chracterisation of Mechanical Proberties of Microelectronic Thin Film. 1990. Massachusetts Institute of Technology. Dissertation

McGregor, E. & Dunn, M. J. 2003. Proteomics of heart disease. *Hum.Mol.Genet.* 12 Spec No 2: R135-R144.

Miyazaki, H., Hasegawa, Y. & Hayashi, K. 2000. A newly designed tensile tester for cells and its application to fibroblasts. *J.Biomech.* 33: 97-104.

Morales, E., Cole, W. C., Remillard, C. V. & Leblane, N. 1996. Block of large conductance Ca(2+)-activated K+ channels in rabbit vascular myocytes by internal Mg2+ and Na+. *J.Physiol* 495 (Pt 3): 701-716.

Nowacki, W. 1972. Dynamika budowli. Warschau: Arkady-Verlag.

Nowacki, W. 1974. Baudynamik. Wien, New York: Springer-Verlag.

Oliver, T., Dembo, M. & Jacobson, K. 1999. Separation of propulsive and adhesive traction stresses in locomoting keratocytes. *J.Cell Biol.* 145: 589-604.

Palmer, R. E., Brady, A. J. & Roos, K. P. 1996. Mechanical measurements from isolated cardiac myocytes using a pipette attachment system. *Am.J.Physiol* 270: C697-C704.

Payumo, F. C., Kim, H. D., Sherling, M. A., Smith, L. P., Powell, C., Wang, X., Keeping, H. S., Valentini, R. F. & Vandenburgh, H. H. 2002. Tissue engineering skeletal muscle for orthopaedic applications. *Clin.Orthop.* S228-S242.

Pelham, R. J., Jr. & Wang, Y. 1997. Cell locomotion and focal adhesions are regulated by substrate flexibility. *Proc.Natl.Acad.Sci.U.S.A* 94: 13661-13665.

Pollard, T. D. 1986. Assembly and dynamics of the actin filament system in nonmuscle cells. *J.Cell Biochem.* 31: 87-95.

Rasmussen, R. E. 1984. In vitro systems for exposure of lung cells to NO2 and O3. *J.Toxicol.Environ.Health* 13: 397-411.

Ratner, B. D. 1992. Plasma deposition for biomedical applications: a brief review. *J.Biomater.Sci.Polym.Ed* 4: 3-11.

Ratner, B. D., Hoffmann, A. S., Schoen, F. J. & Lemons, J. E. 1996. Biomaterials Science. San Diego: Academic Press.

RONA, G., CHAPPEL, C. I., BALAZS, T. & GAUDRY, R. 1959. An infarct-like myocardial lesion and other toxic manifestations produced by isoproterenol in the rat. *AMA.Arch.Pathol.* 67: 443-455.

Rossing, T. D. & Fletcher, N. H. 1994. Principles of Vibration and Sound. New York: Springer.

Rotsch, C. & Radmacher, M. 2000. Drug-induced changes of cytoskeletal structure and mechanics in fibroblasts: an atomic force microscopy study. *Biophys.J.* 78: 520-535.

Sato, M., Levesque, M. J. & Nerem, R. M. 1987. An application of the micropipette technique to the measurement of the mechanical properties of cultured bovine aortic endothelial cells. *J.Biomech.Eng* 109: 27-34.

Schakenraad, J. M., Busscher, H. J., Wildevuur, C. R. & Arends, J. 1988. Thermodynamic aspects of cell spreading on solid substrata. *Cell Biophys.* 13: 75-91.

Schneider, G. Automatische Formbestimmung einzelner strömungskräftefreier Erythrozyten durch Auswertung von Intensitätsbildern defokussierter mikroskopischer Aufnahmen. 1996. TU Ilmenau. Dissertation

Schwarz, U. S., Balaban, N. Q., Riveline, D., Bershadsky, A., Geiger, B. & Safran, S. A. 2002. Calculation of forces at focal adhesions from elastic substrate data: the effect of localized force and the need for regularization. *Biophys.J.* 83: 1380-1394.

Skalak, R., Chien, S. & et al 1986. In Skalak, R. & Chien, S. (Eds) Handbook of Bioengineering New York: McGraw-Hill Book Company.

Strutt, J. W. & Baron Rayleigh 1894. The Theory of Sound. London: MacMillan.

Sutherland, F. J., Shattock, M. J., Baker, K. E. & Hearse, D. J. 2003. Mouse isolated perfused heart: characteristics and cautions. *Clin.Exp.Pharmacol.Physiol* 30: 867-878.

Takakuda, K. & Miyairi, H. 1996. Tensile behaviour of fibroblasts cultured in collagen gel. *Biomaterials* 17: 1393-1397.

Tarr, M., Trank, J. W., Leiffer, P. & Shepherd, N. 1979. Sarcomere length-resting tension relation in single frog atrial cardiac cells. *Circ.Res.* 45: 554-559.

Tasche, C., Meyhofer, E. & Brenner, B. 1999. A force transducer for measuring mechanical properties of single cardiac myocytes. *Am.J.Physiol* 277: H2400-H2408.

Tejero-Trujeque, R. 2001. How do fibroblasts interact with the extracellular matrix in wound contraction? *J.Wound.Care* 10: 237-242.

Terracio, L., Miller, B. & Borg, T. K. 1988. Effects of cyclic mechanical stimulation of the cellular components of the heart: in vitro. *In Vitro Cell Dev.Biol.* 24: 53-58.

Theret, D. P., Levesque, M. J., Sato, M., Nerem, R. M. & Wheeler, L. T. 1988. The application of a homogeneous half-space model in the analysis of endothelial cell micropipette measurements. *J.Biomech.Eng* 110: 190-199.

Thoumine, O., Ott, A. & Louvard, D. 1996. Critical centrifugal forces induce adhesion rupture or structural reorganization in cultured cells. *Cell Motil.Cytoskeleton* 33: 276-287.

Thurston, A. 2003. Dupuytren's disease or Cooper's contracture?: Kenneth Fitzpatrick Russell Memorial Lecture. *ANZ.J.Surg.* 73: 529-535.

Tirri, R. & Lehto, H. 1984. Alpha and beta adrenergic control of contraction force of perch heart (Perca fluviatilis) in vitro. *Comp Biochem.Physiol C.* 77: 301-304.

Tissakht, M. & Ahmed, A. M. 1995. Tensile stress-strain characteristics of the human meniscal material. *J.Biomech.* 28: 411-422.

Tomasek, J. J., Gabbiani, G., Hinz, B., Chaponnier, C. & Brown, R. A. 2002. Myofibroblasts and mechano-regulation of connective tissue remodelling. *Nat.Rev.Mol.Cell Biol.* 3: 349-363.

Trzewik, J., Linder, P., Demirici, T. & Artmann, G. M. 2004a. Three-dimensional analysis of cell orientation and location in thin film tissue constructs at various mechanical stress conditions. *Biomed Tech (Berl)* 49 Suppl 2 Pt 2: 1044-1045.

Trzewik, J., Artmann-Temiz, A., Linder, P. T., Demirci, T., Digel, I. & Artmann, G. M. 2004b. Evaluation of lateral mechanical tension in thin-film tissue constructs. *Ann.Biomed.Eng* 32: 1243-1251.

Vandenburgh, H. H. 1988. A computerized mechanical cell stimulator for tissue culture: effects on skeletal muscle organogenesis. *In Vitro Cell Dev.Biol.* 24: 609-619.

Vandenburgh, H. H. 1992. Mechanical forces and their second messengers in stimulating cell growth in vitro. *Am.J.Physiol* 262: R350-R355.

Vandenburgh, H. H. & Karlisch, P. 1989. Longitudinal growth of skeletal myotubes in vitro in a new horizontal mechanical cell stimulator. *In Vitro Cell Dev.Biol.* 25: 607-616.

Vawter, D. L., Fung, Y. C. & West, J. B. 1978. Elasticity of excised dog lung parenchyma. *J.Appl.Physiol* 45: 261-269.

Wakatsuki, T., Kolodney, M. S., Zahalak, G. I. & Elson, E. L. 2000. Cell mechanics studied by a reconstituted model tissue. *Biophys.J.* 79: 2353-2368.

Wierzbicka-Patynowski, I. & Schwarzbauer, J. E. 2003. The ins and outs of fibronectin matrix assembly. *J.Cell Sci.* 116: 3269-3276.

Yang, H. T., Tweedie, D., Wang, S., Guia, A., Vinogradova, T., Bogdanov, K., Allen, P. D., Stern, M. D., Lakatta, E. G. & Boheler, K. R. 2002. The ryanodine receptor modulates the spontaneous beating rate of cardiomyocytes during development. *Proc.Natl.Acad.Sci.U.S.A* 99: 9225-9230.

Zahalak, G. I., Wagenseil, J. E., Wakatsuki, T. & Elson, E. L. 2000. A cell-based constitutive relation for bio-artificial tissues. *Biophys.J.* 79: 2369-2381.

Zigrino, P., Drescher, C. & Mauch, C. 2001. Collagen-induced proMMP-2 activation by MT1-MMP in human dermal fibroblasts and the possible role of alpha2beta1 integrins. *Eur.J.Cell Biol.* 80: 68-77.

Zimmermann, W. H., Fink, C., Kralisch, D., Remmers, U., Weil, J. & Eschenhagen, T. 2000. Three-dimensional engineered heart tissue from neonatal rat cardiac myocytes. *Biotechnol.Bioeng.* 68: 106-114.

Symbols and abbreviations

γ	surface energy; general
γ_1	surface energy liquid
γ_2	surface energy substrate
γ_{12}	surface energy between liquid and substrate
γ_c	critical surface energy
ε	strain
$\Phi(r_i, r_o)$	wall function
λ	elongation of the test specimen
ν	poisson's ratio
σ	tension –general-
σ_0	residual tension
θ	contact angle
ρ	mass density
$\rho_0 W$	strain energy per unit initial volume
BAEC	bovine aortic endothelial cell
CMS	custom made optical sensor
°C	temperature in Celsius
CO_2	carbon dioxide
CS	control cells, soluble protein fraction
CU	control cells, hardly soluble protein fraction.
D	damping ratio
DMEM	Dulbecco's modified Eagle's medium
DMSO	dimethyl sulfoxide
DTT	dithiothreitol
$E_{i,j}$	Green's strain
E	elastic or young's modulus
ECM	extra cellular matrix
EDTA	ethylene-diamin-tetra-acid
f	fundamental frequency
FCM	fibroblast seeded collagen matrix
FCS	fetal calf serum
FFT	Fast Fourier Transformation
h	membrane thickness
HBSS	Hanks' balanced salt solution
L_s	equilibrium length
LSM	Scanning Electron Microscopic
HEPES	4-(2-hydroxyethyl)-1-piperazineethanesulfonic acid
MW	molecular weight marker
NO	nitrogen monoxide
Pa	Pascal
PBS	phosphate-buffered saline
PCR	polymerase Chain Reaction
r	inner radius of the CellDrum
r_i	inner pipette radius
r_o	outer pipette radius

p	pressure
RGD	arginine-glycine-aspartic acid sequence
PDMS	polydimethylsiloxane
PEDF	pigment epithelium derived factor
PMSF	phenyl methyl sulfonyl fluoride
SDS	sodium dodecylsulfate
SEM	Scanning Electron Microscope
$S_{i,j}$	Kirchhoff stress
t	Film thickness
T	line force per length
Tris	tris-(hydroxymethyl)-aminomethan
TS	cells mechanically stressed, soluble protein fraction
TU	cells mechanically stressed, hardly soluble proteins
VEGF	vascular endothelial growth factor

Acknowledgement

This thesis reports on the product of my collaboration with many individuals. It is a pleasant aspect that I have now the opportunity to express my gratitude for all of them.

I would like to express my gratefulness especially to my promoter Prof. Artmann. He provided an ideal environment to conduct this work. I would like to thank him for finding the time to advise me in spite of the tremendous amount of his other duties. I am convinced that this work could not have been accomplished without him.
Professor Henning offered me the chance to work on my PhD at his chair, for which I am very grateful.

My colleagues of the cellular engineering laboratory all gave me the feeling of being at home at work. A special thank to my colleague Peter Linder who contributed many hours supporting data acquisition programming and cell culture handling. I am also thankful to Dr. Ilya Digel who provided great help in the protein profile analysis. Darius Porst, Christina Maggakis-Kelemen, Peter Kaiser and Prof. Aysegül Temiz Artmann, many thanks for being your colleague. I want to thank Prof. Staat for his contribution to the theoretical, mechanical modeling section.

This work was supported by the “Assistenten-programm” grant from the Ministry of Science and Education in North Rhine Westfalia, Germany, I also would like to thank Willi Ziesmann at University Research Machine Shop for his excellent support. I’m also thankful to Markus Rüffer from the Biochemistry Institute at the University of Leipzig for his support during the evaluation of contracting cardiomyocytes.

I would like to thank my wife Sabine for her moral and emotional support when I was under dark clouds; she provided life, energy and the strength to march forward.

Finally, I owe much to my parents for getting to the point of undertaking this work.

16 Abstract

A person's health is determined by the biomechanical integrity and performance of tissue and organs. Widespread diseases like hernia formation or pelvic floor malfunction are directly related to a reduced biomechanical functionality of the concerned soft tissue. These exemplary diseases, but also dysfunction of the cardiovascular system are caused by processes, which are based on changes of biomechanical properties at the cellular level. Fundamental research in this topic on humans is limited for practical and ethical reasons, especially the evaluation of active substances. The systems for the in vitro evaluation of biomechanical material properties, as described in the literature, are adopted from standard material test methods mainly focusing on an uniaxial loading. But uniaxial loading is rarely seen in nature since most load cases are two or three dimensional. This work describes a new measurement principle, which allows the cultivation of cell monolayers or thin tissue composites under biaxial load conditions and mechanical evaluation at the same time.

A new cell cultivation module, termed CellDrum, was developed for that purpose. The Celldrum consists of a thin, biocompatible silicon membrane attached to a cylindrical well (∅ 16 mm). The CellDrum membrane can be populated with cells grown in monolayer structures or serves as a sealing boundary layer for thin film cell-matrix constructs anchored with the Cell Drum's wall. The CellDrum technology is a universal approach and can be used for almost any kind of material test on thin films. Investigations can be performed either under a dynamic or quasi-statical mode. Mechanical properties of cell populated CellDrum constructs were analyzed in the dynamic setup, after excitation via a pressure impulse and measuring the resonance frequency of vibrating tissue constructs anchored to the CellDrum. The quasi-statical mode allows evaluating the stress-strain behavior of test material (in this work: cell monolayer and thin tissue equivalents). Technologies were developed, adapted to the specific questions and experimental needs, ranging from flexible, µm-thin, biocompatible membranes over hard- and software solutions up to the biomechanical analyses for the extraction of adequate biomechanical parameters. This interdisciplinary effort between cell- and molecular biology, polymer chemistry, mechanics and other engineering fields, which had to be controlled in equal measure, was the major challenge of this work.

Optical monitoring during cell cultivation is vitally important for the development, standardization and optimization of cell-biological measurement protocols. The possibility of a continuous microscopic evaluation of the test specimen, at a minimal disturbance of the measurement environment, is a unique feature of the described apparatus. In combination with confocal laser microscopy it is also possible to identify cell density and orientation during the cultivation period. These values are important parameters for the correct interpretation of the derived measurement data.

Cell based systems can sense changes in their mechanical environment and promote alterations and adaptations in tissue structure and function, like metabolism, orientation, protein and gene expression. These factors were considered for the CellDrum development and carefully evaluated by accompanying experiments. The use of circular CellDrum constructs introduces a homogenous stress distribution within the sample construct, similar to the biaxial state found in most in vivo situations for soft tissues. The CellDrum system therefore supports a cell proliferation with random cell orientation in contrast to the initiation of parallel cell orientation found in common approaches with rectangular stretched cell seeded collagen cells. Furthermore, finite element method investigations proved the homogenous stress distribution for the circular CellDrum, compared to the strong variations of the van Mieses equivalent stress values in a rectangular stretched gel. Besides mentioned circumstances, further experiments had to be performed to evaluate the contributions of different membrane coatings on the cellular response to substrate strain variations. The cells reacted differently to the employed coating under strained and unstrained conditions.

The measurement system described in this work offers the opportunity to analyze the mechanical properties of cell constructs over a long period of time (weeks) under defined mechanical boundary conditions either in the dynamic or statistical setup. The relation between cell proliferation and residual tissue stress was exemplarily demonstrated. The studied cellular response, especially the plateau effect during the generation of tissue tension, provides further conclusions about mechanical homeostasis of soft tissue. The understanding of these phenomena may contribute to the understanding of the mechanics of wound healing and of scar formation.
The stimulation of tissue equivalents during cell cultivation and the variation of process parameters had a direct impact on the E-module and residual tension of the evaluated specimen. Both parameters were analyzed synchronously by the transfer and adequate adaptation of an analyzing method, which was originally developed for microsytem technologies.
Furthermore, described system is the first system which offers the novel and unique possibility to cultivate synchronously beating cardiomyocytes and evaluate the contractile behaviour together with the monitored beating frequency. A specific method was developed to obtain primary cardiomyocytes from 10 day old chicken embryos and later on transferred by a research partner on neonatal rat myocytes.
Complicated and error-prone experimental handling was a major concern in earlier methods, besides the unsatisfying situation of undefined mechanical boundary conditions. During pharmaceutical research activities, thousands of substances have to be evaluated for potential pharmaceutically efficacy by secondary screening. Unlike most devices introduced before, the system established here can easily be scaled up towards a high-throughput system providing simultaneous material data on large numbers of tissue constructs exposed to various chemical agents. This was exemplarily demonstrated for fibroblast-collagen composites.

17 Kurzfassung

Die biomechanische Integrität und Leistungsfähigkeit von Gewebe und Organen beeinflusst die Gesundheit des Menschen in extremer Weise. Weitverbreitete Erkrankungen wie Hernienbildung (Eingeweidebruch) und Beckenbodendefekte (jährlich alleine zehn Million Patientinnen in den USA) stehen mit einer verminderten biomechanischen Gewebefunktionalität in einem klaren Zusammenhang. Diese exemplarisch genannten Erkrankungen, aber auch Dysfunktionen des Herz-Kreislaufsystems sind auf biomechanische Veränderungen auf zellulärer Ebene zurückzuführen. Grundlagenforschung hierzu am Menschen ist aus ethischen und praktischen Gründen, insbesondere bei der Erprobung aktiver Substanzen problematisch. In der Literatur werden zur Evaluierung biologischer Materialeigenschaften in vitro Testsysteme vorgeschlagen, welche relativ unkritisch aus Methoden der konventionellen Materialprüfung abgeleitet worden sind. Dies betrifft insbesondere einachsiale Zugversuche. Die meisten Spannungssituationen in biologischen Systemen sind aber dreiachsial oder zweiachsial. Der einachsiale Spannungszustand tritt allenfalls in dünnen Sehnenstrukturen auf. In dieser Arbeit wurde ein Messprinzip entwickelt, welches es erlaubt, Zellmonolayer und dünne Gewebeschichten unter biaxialer Belastung zu züchten und mechanisch zu analysieren.

Ein grundlegender Bestandteil des Messverfahrens ist, das CellDrum genannte, Zellkultivierungsmodul. Die entwickelte CellDrum besteht aus einem biokompatiblen, Polycarbonatzylinder (∅ 16 mm), welcher mit einer ebenfalls biokompatiblen, dünnen (< 1 µm) und extrem flexiblen Siliconmembran einseitig verschlossen ist. Die Silikonmembran kann einerseits mit Zellmonolayern besiedelt werden oder dient als Halte- und Unterstützungschicht bei der Kultivierung von auf Zell-Kollagengel basierenden Gewebeäquivalenten.

Die CellDrum Technologie ist universell verwendbar für beinahe jede Art der Materialprüfung dünner Schichten. Untersuchungen können prinzipiell dynamisch und quasistatisch durchgeführt werden. Im dynamischen Ansatz wird die Resonanzfrequenz und somit die Eigenspannung des Gewebeverbundes analysiert, welcher durch einen Druckimpuls zum Schwingen angeregt wird. Der quasistatische Ansatz ermöglicht die Untersuchung des Spannungs-Dehnungsverhaltens der Testmaterialien (in dieser Arbeit: Zellmonolayer und Gewebeäquivalente). Den verschiedenen Fragestellungen und Testsituationen angepasst, wurden Technologien entwickelt, die von der Herstellung flexibler, biokompatibler Membranen mit Dicken im Mikrometerbereich über Hard- und Softwarelösungen bis hin zur biomechanischen Problemanalyse zur Ableitung geeigneter biomechanischer Parameter reichten. Es war diese extreme Interdisziplinarität zwischen Zell- und Molekularbiologie, Polymerchemie, Mechanik und anderen Ingenieurwissenschaften, die gleichermaßen gut beherrscht werden mussten, was die Herausforderung dieser Arbeit darstellte.

Zellbasierte Systeme reagieren hinsichtlich Orientierung, Morphologie, Stoffwechsel sowie Protein- und Genexpression auf Veränderungen ihrer mechanischen Umgebung. Diese Problematik wurde bei der CellDrumkonzeption bedacht, experimentell evaluiert sowie technisch und theoretisch realisiert. Neben den zuvor genannten Problemlösungen mussten Tests zur Eignung verschiedener Adhäsionsproteine durchgeführt werden. Ungeeignete Proteine zeigten im statischen Spannungszustand biokompatibles Verhalten; bei dynamischer Belastung initiierten dieselben Proteine ein Zellsterben. Ein anderes, nicht kleines Problem war die Verankerung des Randes der künstlichen Gewebeschicht an der Peripherie.

Das Zusammenspiel zwischen Gewebespannung, Zellproliferation und Zellkonzentration wurde in der Vergangenheit mit verschiedenen Verfahren experimentell analysiert. Die Neuheit des in dieser Arbeit beschriebenen Verfahrens besteht darin, die Zellverbände über lange Zeiten (Wochen) statisch oder dynamisch unter genau definierten mechanischen Randbedingungen kultivieren zu können und gleichzeitig die Möglichkeit zu haben, den mechanischen Spannungszustand des

gezüchteten Konstruktes zu beliebigen Zeiten zu messen. Es wurde hier der Zusammenhang zwischen Gewebespannung und Zellproliferation für mit Fibroblasten besiedelte Gewebeäquivalente exemplarisch dargestellt. Die gewonnenen Erkenntnisse, insbesondere Plateaueffekte bei der Gewebespannungsgeneration, lassen aufschlussreiche Rückschlüsse auf die Spannungshomeostase im Gewebe zu. Die Stimulierung von Gewebeäquivalenten durch Wirkstoffe und die Variation von Prozessparameteren während der Zellkultivierung bestimmen Eigenspannung und E-Modul des Messobjektes mit. Durch die Anpassung bestehender Verfahren der Mikrosystemtechnik konnte ein Verfahren in die biologische Materialprüfung transferiert werden. Dieses quasistatische Verfahren ermöglicht die Messung von Gewebeeigenspannung und E-Modul in nur einem Messdurchlauf.

Die Zellaktivität (Morphologie, Metabolik, Protein- und Genexpression) wird durch ihr mechanisches Umfeld determiniert. Viele in der Literatur beschriebene Messverfahren induzieren ein inhomogenes Spannungsfeld mit van Mieses Vergleichsspannungen, die im selben Gewebekonstrukt um mehr als 75% variieren. Die kreisrunde Geometrie der CellDrum erlaubt ein weitestgehend homogenes Spannungsfeld.

Zur Untersuchung von autolog und synchron schlagenden Kardiomyozyten (Herzmuskelzellen) wurden geeignete Zellkulturtechniken entwickelt, um diese als Monolayer oder Gewebeäquivalente mit der CellDrum Technik untersuchen zu können. Es wurde eine Methode entwickelt, um primäre Kardiomyozyten aus zehn Tage alten Embryos angebrüteter Hühnereier zu gewinnen. Die Methode wurde später mit einem Partner auf neonatale Rattenmyocyten transferiert.

Zur Entwicklung, Optimierung und Standardisierung zellbiologischer Messprotokolle ist insbesondere die Möglichkeit einer optischen Überwachung während der Kultivierungsphase von großer Bedeutung. Die Möglichkeit der kontinuierlichen mikroskopischen Evaluierung, bei gleichzeitig minimaler Störung der Messumgebung ist einmalig und in der beschriebenen Apparatur gewährleistet. In allen Anwendungen ist für die Interpretation von Meßdaten auch die Zelldichte ein entscheidender Parameter. In Verbindung mit einem invertierten konfokalen Lasermikroskop können Zelldichte und Orientierung während der Kultivierungsperiode ermittelt werden. Neben der weitgehend unbefriedigenden biomechanischen Situation früherer Methoden, war oft auch die Versuchsdurchführung kritisch, kompliziert und fehlerbehaftet. Zum Sekundärscreening potentieller therapeutischer Wirksubstanzen müssen zehntausende Substanzen funktionell getestet werden. Das CellDrum-Verfahren liefert als bisher einzige Technik die Grundlage für ein automatisierbares Hochdurchsatz-Screening-Konzept. Dies wurde an Fibroblasten-Kollagen Verbunden exemplarisch gezeigt.